High Capacity Radio over Fiber Transmission Links

Caballero Jambrina, Antonio

Publication date:
2011

Document Version
Publisher's PDF, also known as Version of record

High Capacity Radio over Fiber Transmission Links

Antonio Caballero Jambrina

Supervisors:
Professor Idelfonso Tafur Monroy,
Assistant Professor Darko Zibar and
Associate Professor Kresten Yvind

Delivery Date: 1st August 2011

DTU Fotonik
Department of Photonics Engineering
Technical University of Denmark
Building 343
2800 Kgs. Lyngby
DENMARK

DTU Fotonik
Institut for Fotonik

Abstract

This thesis expands the state-of-the-art on the detection of high speed wireless signals using optics. Signal detection at speeds over 1 Gbps at carrier Radio Frequency (RF) ranging from 5 GHz to 100 GHz have been achieved by applying novel concepts on optical digital coherent receivers. This achievement has satisfied the requirements on transmission robustness and high capacity of next generation hybrid optical fibre-wireless networks.

One important contribution of this thesis is the novel concept of photonic downconversion with free-running pulsed laser source for phase modulated Radio-over-Fiber (RoF) links. This scheme operates without high frequency electronics at the digital coherent receiver for the detection of high bitrate wireless signals. Based on this concept, I have experimentally demonstrated the recovery of up to 3.2 Gbps 16-QAM signal modulated at 40 GHz RF carrier. At that time, it was the highest bitrate reported of a wireless signal, with complex modulation format, detected using photonic means. I have developed an analytical model to support the experimental results and performed a linearity characterization to establish engineering design rules for this type of links. The results confirmed that this configuration provides high linear end-to-end transmission links and is capable of transparent transport of high spectral efficient modulation formats.

Furthermore, this thesis introduces a novel approach for the generation and detection of high speed wireless signals in mm-wave frequencies at carrier frequencies exceeding 60 GHz, using photonic baseband technologies. For signal generation, high spectral-efficient optical modulation technologies are used together with optical heterodyning. In the detection side, the mm-wave signal is modulated in the optical domain and received using digital coherent detection. The experimental demonstration tested the generation and detection in the 60 GHz and 75-110 GHz bands of signals with capacity up to 40 Gbps. Those results reported the highest bitrate at mm-wave frequencies for signal generation and detection using photonic

methods at the time of the writing of this thesis.

In conclusion, the results presented in this thesis demonstrate the feasibility of photonic technologies for the generation, distribution and detection of high speed wireless signals. Furthermore, it opens the prospects for next generation hybrid wireless-wired access networks providing ultra-high capacities.

Resumé

Denne afhandling højner stadet indenfor detektion af trådløse, højhastighedssignaler ved brug af optik. Signaldetektion ved datahastigheder over 1 Gbps på bærebølge radiofrekvenser mellem 5 GHz og 100 GHz er opnået ved at anvende nye principper for optiske, digitale og kohærente modtagere. Disse resultater tilfredsstiller krav om robust transmission med høj kapacitet i næste generations hybride, optiske fiber-trådløse netværk.

Et vigtigt bidrag i afhandlingen er det nye princip for fotonisk nedkonvertering til brug i fasemodulerede Radio-over-Fiber forbindelser ved hjælp af en fritløbende, pulseret laser. Denne metode til detektion af trådløse højhastighedssignaler f ungerer uden brug af højfrekvenselektronik i den digitale, kohærente modtager. Baseret på denne metode demonstreres eksperimentel gendannelsen af op til 3,2 Gbps 16-QAM sinaler, som er moduleret op på en 40 GHz RF bærebølge. På det pågældende tidspunkt var det den højeste, rapporterede datahastighed af et trådløst signal med avanceret modulationsformat, som blev detekteret ved brug af fotoniske midler. I afhandlingen præsenteres også en analytisk model til fortolkning af de eksperimentelle resultater, og der er udført en linearitetskarakterisering for derved at opstille ingeniørmæssige designregler for den pågældende type fiberforbindelse. Resulaterne bekræfter, at den nævnte konfiguration muliggør højlinearitets, ende-til-ende transmissionsforbindelser og således baner vej for transparent transmission af modulationsformater med høj spektral effektivitet.

Endvidere introducerer afhandlingen en ny tilgang til frembringelse og detektion af trådløse, højhastighedssignaler på mm-bølge bærebølgefrekvenser højere end 60 GHz ved brug af fotoniske, basisbåndsteknologier. Til frembringelsen bruges optiske modulationsmetoder med høj spektral effektivitet kombineret med optisk, heterodyn teknik. Til detektionen blev mm-bølgesignalet moduleret over i det optiske domæne og dernæst modtaget ved hjælp af digital, kohærent detektion. I den eksperimentelle demonstra-

tion blev afprøvet frembringelse og detektion i 60 GHz og 75-110 GHz frekvensbåndende af signaler med datahastigheder op til 40 Gbps. Disse resultater udgjorde den højeste datahastighed på mm-bølgefrekvenser for frembringelse og detektion ved hjælp af fotoniske metoder på det tidspunkt, da afhandlingen blev skrevet.

Sammenfattende dokumenterer afhandlingens resultater, at fotoniske metoder kan anvendes til frembringelse, distribution og detektion af trådløse højhastighedssignaler. Endvidere åbner resultaterne muligheder for næste generations hybride, trådløse-trådbundne abonnentnet med ultra-høj kapacitet.

Acknowledgements

First I would like to thank my supervisor, Professor Idelfonso Tafur Monroy, Assistant professor Darko Zibar and Associate professor Kresten Yvind. Idelfonso for believing in me since the first day I started my Master Thesis under his supervision. Also for being a reference on what hard work and dedication means. Darko, for all the time we have spent together in the lab and for teaching me that it is important to be methodic and organized at work. Kresten for instilling me the interest on the physics of what we work on and open my mind to different research topics during my Ph.D.

I would also like to thank all my colleagues at Metro-access group, Neil, Xianbin, Tim, Jesper, Kamau, Xu, Maisara, Robert, Xiaodan, Alexander, Thang, Bomin.... and also my colleagues in Fotonik department.

Thanks to my closest people in Denmark: Valeria, Roberto and Diana. Additionally, thanks to my salsa dancing friends. Thanks to the nice people I met during this years in Denmark, specially the Spanish invasion and Erasmus students. From my city, Zaragoza, to my closest friends, Daniel and Paula and the Teleco's troupe: Laura, Jorge, Paco, Felix and Sprint. Thanks to my friends all over Spain and rest of you that are now living in different parts of the world.

Finally, I would like to thank my family, for giving me support during this time; specially thanks to my parents, my sister and my grandparents for being there whenever I needed, supporting me in the distance.

Summary of Original Work

This thesis is based on the following original publications:

PAPER 1 A. Caballero, D. Zibar, C. G. Schäffer, and I. Tafur Monroy, "Photonic downconversion for coherent phase-modulated radio-over-fiber links using free-running local oscillator," *Optical Fiber Technology*, 17, pp. 263—266, 2011.

PAPER 2 A. Caballero, D. Zibar, and I. Tafur Monroy, "Digital coherent detection of multi-gigabit 16-QAM signals at 40 GHz carrier frequency using photonic downconversion," in *Proc. 35th European Conference on Optical Communication, ECOC'09*, Vienna, Austria, 2009, Post-Deadline Paper PDP3.4.

PAPER 3 A. Caballero, D. Zibar, and I. Tafur Monroy, "Digital coherent detection of multi-gigabit 40 GHz carrier frequency radio-over-fibre signals using photonic downconversion," *Electronics Letters*, vol. 46, no. 1, pp. 58–58, 2010.

PAPER 4 A. Caballero, D. Zibar, and I. Tafur Monroy, "Performance evaluation of digital coherent receivers for phase modulated radio-over-fiber links," *IEEE/OSA J. Lightw. Technol.*, accepted for publication, 2011.

PAPER 5 A. Caballero, N. Guerrero Gonzalez, F. Amaya, D. Zibar, and I. Tafur Monroy, "Long reach and enhanced power budget DWDM radio-over-fibre link supported by Raman amplification and coherent

detection," in *Proc. 35th European Conference on Optical Communication, ECOC'09*, Vienna, Austria, 2009, paper P6.09.

PAPER 6 A. Caballero, S. Wong, D. Zibar, L. G. Kazovsky and I. Tafur Monroy, "Distributed MIMO antenna architecture for wireless-over-fiber backhaul with multicarrier optical phase modulation," in *Proc. Optical Fiber Communication Conference and Exposition, OFC/NFOEC*, Los Angeles, CA, 2011, paper OWT8.

PAPER 7 N. Guerrero Gonzalez, A. Caballero, R. Borkowski, V. Arlunno, T. T. Pham, R. Rodes, X. Zhang, M. B. Othman, K. Prince, X. Yu, J. B. Jensen, D. Zibar, and I. Tafur Monroy, "Reconfigurable digital coherent receiver for metro-access networks supporting mixed modulation formats and bit-rates," in *Proc. Optical Fiber Communication Conference and Exposition, OFC/NFOEC*, Los Angeles, CA, 2011, paper OMW7.

PAPER 8 D. Zibar, R. Sambaraju, R. Alemany, A. Caballero, J. Herrera, and I. Tafur Monroy, "Radio-frequency transparent demodulation for broadband hybrid wireless-optical links," *IEEE Photon. Technol. Lett.*, vol. 22, no. 11, pp. 784–786, 2010.

PAPER 9 R. Sambaraju, D. Zibar, A. Caballero, I. Tafur Monroy, R. Alemany, and J. Herrera, "100-GHz wireless-over-fibre links with up to 16 Gb/s QPSK modulation using optical heterodyne generation and digital coherent detection," *IEEE Photon. Technol. Lett.*, vol. 22, no. 22, pp. 1650–1652, 2010.

PAPER 10 D. Zibar, R. Sambaraju, A. Caballero, J. Herrera, U. Westergren, A. Walber, J. B. Jensen, J. Marti, and I. Tafur Monroy, "High-capacity wireless signal generation and demodulation in 75- to 110-GHz band employing all-optical OFDM," *IEEE Photon. Technol. Lett.*, vol. 23, no. 12, pp. 810 –812, 2011.

PAPER 11 A. Caballero, D. Zibar, R. Sambaraju, J. Marti and I. Tafur Monroy, "High-capacity 60 GHz and 75-110 GHz band links employing all-optical OFDM generation and digital coherent detection,"

IEEE/OSA J. Lightw. Technol.. accepted for publication, 2011.

PAPER 12 A. Caballero, D. Zibar, R. Sambaraju, N. Guerrero Gonzalez and I. Tafur Monroy, "Engineering Rules for Optical Generation and Detection of High Speed Wireless Millimeter-wave Band Signals," in *Proc. 37th European Conference on Optical Communication, ECOC'11*, Geneva, Switzerland, 2011, paper We.10.P1.115.

Other scientific reports associated with the project:

[PAPER 13] D. Zibar, A. Caballero, N. Guerrero Gonzalez, and I. Tafur Monroy, "Hybrid optical/wireless link with software defined receiver for simultaneous baseband and wireless signal detection," in *Proc. 36th European Conference on Optical Communication, ECOC'10*, Torino, Italy, 2010, paper P6.09

[PAPER 14] D. Zibar, A. Caballero, N. Guerrero Gonzalez, C. Schaeffer, and I. Tafur Monroy, "Digital coherent receiver employing photonic downconversion for phase modulated radio-over-fibre links," in *Proc. IEEE International Microwave Symposium Digest, MTT'09*, Boston, MA, 2009, pp. 365–368.

[PAPER 15] A. Caballero, D. Zibar, and I. Tafur Monroy, "Digital coherent detection of multi-gigabit 40 GHz carrier frequency radio-over-fiber signals using photonic downconversion," in *Proc. 1. Annual Workshop on Photonic Technologies for Access and Interconnects*, Stanford, CA, 2010.

[PAPER 16] A. Caballero, I. Tafur Monroy, D. Zibar, J. A. Lazaro, J. Prat, C. Kazmierski, P. Chanclou, I. Tomkos, E. Tangdiongga, X. Qiu, A. Teixwira, R. Solila, P. Poggiolini, R. Sambaraju, K. Langer, D. Erasme, E. Kehayas, and H. Avramopoulos, "Subsystems for future access networks : Euro-fos project," in *Proc. 1. Annual Workshop on Photonic Technologies for Access and Interconnects*, Stanford, CA, 2010.

[PAPER 17] N. Guerrero Gonzalez, D. Zibar, A. Caballero, and I. Tafur Monroy, "Experimental 2.5 Gb/s QPSK WDM phase-modulated radio-over-fiber link with digital demodulation by a K-means algorithm," *IEEE Photon. Technol. Lett.*, vol. 22, no. 5, pp. 335–337, 2010.

[PAPER 18] K. Prince, J. B. Jensen, A. Caballero, X. Yu, T. B. Gibbon, D. Zibar, N. Guerrero Gonzalez, A. V. Osadchiy, and I. Tafur Monroy, "Converged wireline and wireless access over a 78-km deployed

fiber long-reach WDM PON," *IEEE Photon. Technol. Lett.*, vol. 21, no. 17, pp. 1274–1276, 2009.

[PAPER 19] R. Sambaraju, D. Zibar, A. Caballero, I. Tafur Monroy, R. Alemany, and J. Herrera, "GHz wireless on-off-keying link employing all photonic RF carrier generation and digital coherent detection," in *Proc. Access Networks and In-House Communications, ANIC'10*, Karlsruhe, Germany, 2010, paper ATHA4.

[PAPER 20] I. Tafur Monroy, N. Guerrero Gonzalez, A. Caballero, K. Prince, D. Zibar, T. B. Gibbon, X. Yu, and J. B. Jensen, "Convergencia de sistemas de comunicacion opticos e inalambricos (converged wireless and optical communication systems)," *Optica Pura y Aplicada, invited*, no. 2, pp. 83–90, 2009.

[PAPER 21] D. Zibar, R. Sambaraju, A. Caballero, I. Tafur Monroy, R. Alemany, and J. Herrera, "16 Gb/s QPSK wireless-over-fibre link in 75-110 GHz band with photonic generation and coherent detection," in *Proc. 36th European Conference on Optical Communication*, *ECOC'10*, Torino, Italy, 2010, paper Th.9.B.6.

[PAPER 22] R. Sambaraju, D. Zibar, A. Caballero, J. Herrera, I. Tafur Monroy, J. B. Jensen, A. Walber, U. Westergren, and J. Marti, "Up to 40 Gb/s wireless signal generation and demodulation in 75-110 GHz band using photonic techniques," in *Proc. Microwave Photonics, MWP'11*, Toronto, Canada, 2011, Post-deadline Paper PDP1.

Other scientific reports:

[C1] A. Caballero, R. Rodes, J. B. Jensen, and I. Tafur Monroy, "Impulse radio ultra wide-band over multi-mode fiber for in-home signal distribution," in *Proc. Microwave Photonics, MWP'09.*, Valencia, Spain, 2009, pp. 1–3.

[C2] A. Caballero, J. B. Jensen, X. Yu and I. T. Monroy,, "5 GHz 200 Mbit/s radio over polymer fibre link with envelope detection at 650 nm wavelength," *Electronic Letters*, vol. 44, no. 25, pp. 1479–1480, 2008.

[C3] T. B. Gibbon, X. Yu, R. Gamatham, N. Guerrero, R. Rodes, J. B. Jensen, A. Caballero, and I. Tafur Monroy, "3.125 Gb/s impulse radio ultra-wideband photonic generation and distribution over a 50 km fiber with wireless transmission," *IEEE Microw. and Wireless Comp. Lett.*, vol. 20, no. 2, pp. 127–129, 2010.

[C4] J. B. Jensen, R. Rodes, A. Caballero, X. Yu, T. B. Gibbon, and I. Tafur Monroy, "4 Gbps impulse radio (IR) ultra-wideband (UWB) transmission over 100 meters multi mode fiber with 4 meters wireless transmission," *Opt. Express*, vol. 17, no. 19, pp. 16 898–16 903, 2009.

[C5] R. Rodes, A. Caballero, X. Yu, T. B. Gibbon, J. B. Jensen, and I. Tafur Monroy, "A comparison of electrical and photonic pulse generation for IR-UWB on fiber links," *IEEE Photon. Technol. Lett.*, vol. 22, no. 5, pp. 263–265, 2010.

[C6] R. Rodes, X. Yu, A. Caballero, J. B. Jensen, T. B. Gibbon, N. Guerrero Gonzalez, and I. Tafur Monroy, "Range extension and channel capacity increase in impulse-radio ultra-wideband communications," *Tsinghua Science & Technology, Invited*, vol. 15, no. 2, pp. 169–173, 2010.

Contents

Chapter 1

Introduction

1.1 High capacity wireless links

The emerging services that end users are demanding, such as High-Definition video streaming, video-calls and cloud computing, have put severe pressure on the telecommunication network infrastructure to provide high capacity links, capable to support diverse service requirements, in different customer-premises environments and at a low cost. This demand has resulted in an evolution of short-range and wired access networks: from the copper-based transmission systems, with limited coverage and bandwidth, to the use of photonic technologies, achieving high capacity and long reach links [1, 2].

Regardless copper or optical fiber is used as a media for wired data transmission, delivery of data wirelessly to the end-user has advantages related to flexibility in the placement of transponders and broadcasting capabilities. However, opposed to wired media, wireless transmission commonly exhibits lower reach, caused by the high propagation losses of the signal through the air, and it is more prone to channel interferences during propagation. These characteristics result in a received signal after wireless transmission with strong time-varying properties. Wireless communication systems operating at low frequencies, below 5 GHz, have limited capacity, as there is scarce of RF spectrum available for broadband operation at such frequencies. Moreover, this RF spectrum needs to be shared with different services and users. For example, in the Global System for Mobile Communications (GSM) bands (900 MHz and 1.8 GHz) only 100 MHz of bandwidth is available. In order to achieve high capacity wireless links, one possibility is to move towards higher RF frequencies, where higher bandwidth is available. An example is the 5 GHz band, with about 500 MHz

of bandwidth available. For gigabit-per-second data links, mm-wave frequencies (above 60 GHz) can be used, as there are GHz of spectrum available [3, 4]. A different approach is to increase the bite rate over a given bandwidth, thus increasing the spectral efficiency. Spectral efficiencies over 2 $bit/s/Hz$ can be achieved by using complex modulation formats, such as Phase Shift Keying (PSK) or Quadrature Amplitude Modulation (QAM), as well as multiplexing schemes, such as subcarrier multiplexing or Orthogonal Frequency-Division Multiplexing (OFDM), as opposed to On-Off Keying (OOK) that achieves only 1 $bit/s/Hz$. However, at high RF carrier frequencies, the high capacity wireless link encounters high propagation losses. The stringent requirements of high modulation formats in terms of Signal-to-Noise Ratio (SNR) together with the propagation losses result in limited coverage. In spite of that, high capacity wireless links can be achieved, although over short distances.

The application of wireless link for access networks takes place in the last mile segment of the data transport, providing high capacity links to the end-user. One type of wireless signal distribution concerns cellular networks, where a certain geographical area needs wireless coverage, provided by a number of antenna Base Station (BS). For next generation cellular networks with increased capacity, the reach of the wireless link will be short, as a consequence of the higher RF carriers and the use higher modulation formats needed to achieve high capacity links. To provide proper coverage, the density of antennas per area needs to be increased, resulting in a large number of nodes to be distributed and controlled by the network. The new architecture shall support high number of BS, with possibly high number of antennas per BS, to support Multi-Input Multi-Output (MIMO). The transport of all the aggregated data, to/from the different antennas from/to a Central Station (CS), where the control is done, requires a high-capacity backhaul wired infrastructure, commonly optical fiber [26, 44]. As a CS can be placed some tens of kilometers away from the BSs, the fiber link is the most suitable connection between CS and BSs, benefiting from the high capacity and low attenuation of the optical fiber as a transmission media.

Traditionally in Radio-over-Fiber (RoF), the baseband to RF up and downconversion has been done at the BS, resulting in digital transport of the information through the fiber backhaul. By using optical fiber for the analogue transport of wireless signals, between BS and CS in a wireless-over-fiber architecture, it is possible to transport the wireless signal transparently through the fiber infrastructure, while providing the high capacity required for next generation wireless access networks [5, 6].

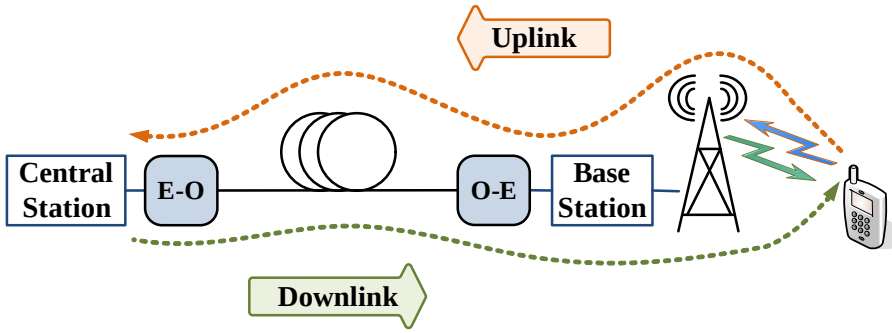

Figure 1.1: Schematic description of the two types of RoF link: uplink (from wireless user to BS to CS) and downlink (CS to BS to wireless user).

The basic diagram of a wireless-over-fiber architecture, where the wireless signal is transported transparently through the fiber infrastructure, is shown in Fig. 1.1. The detected wireless signal can be optically transported from the BS to the CS (uplink) or generated in the CS, transported to the BS, resulting in passive wireless generation in the BS (downlink) [5, 6]. The centralization of complex equipment at the CS, wireless demodulation, mixers, RF oscillators and network control, results in a simplified BS, with important cost savings and simple communication between the different cells. The requirements for downlink to uplink transmission links are different. For downlink transmission, the link should be able to generate a signal with low distortion, low noise and provide high RF power. On the other hand, the design of an uplink transmission systems has stringent requirements on dynamic range, as the users signals arrive to the BS after wireless transmission, with variable RF power caused by fading and potentially with high noise and interferences from the different users sharing the network.

1.2 Photonic technologies for wireless signal generation and detection

The generation and detection of wireless signals have been widely studied within the topic of Microwave Photonics (MWP). The generic microwave photonic link, called RoF, consists of the transport of an analogue signal through an optical fiber, by performing electrical to optical conversion at the transmitter and optical to electrical conversion at the receiver. Yet the term MWP goes beyond that, covering for example the photonic generation

and processing of microwave signals at high carrier frequencies, optically controlled phased array antennas and photonic Analogue-to-Digital Converter (A/D) conversion [5, 7–9].

1.2.1 Photonic generation techniques

The generation of wireless signal using optics has the advantage of the high bandwidth that photonic components can achieve [7, 10, 11], currently with over 100 GHz. An added advantage of photonics is the low attenuation and low non-linear distortion that optical fiber offers for signal propagation, as opposed to the electrical transport by using waveguide techniques. A common technique for the generation of a microwave signal is the beating at a Photodiode (PD) of two optical carriers, which are coherent and separated by the desired RF frequency. There are different ways to generate these optical carriers, mostly based on external electro-optical modulation via a reference RF frequency synthesizer [12–17]. By using these techniques it is possible to obtain RF carrier frequencies which are multiples of the one provided by the frequency synthesizer [12, 13]. Based on this approach, RF frequencies exceeding 100 GHz can be generated supporting bitrates over 20 Gbps [14–17].

A different approach is using optical heterodyning, with free running lasers, first proposed in [18], which can provide high bitrate wireless signals [10, 19]. A baseband signal is generated and optically combined with a second free running laser to create in a PD the electrical signal. This method avoids the need of an electrical RF source, but requires lasers with low phase noise and a robust receiver to compensate for the free running beating of the two optical sources.

To impose a modulation onto the wireless carrier, it is possible to use optical baseband modulation, instead of electrical waveform generation, as optics can provide high spectral-efficient modulation formats, such as Quadrature Phase Shift Keying (QPSK) or QAM. The use of all-Optical OFDM (O-OFDM) [20, 21] has been demonstrated to enable highly spectral-efficient optical channels, while decreasing the requirements of the baseband electronics.

This thesis reports on the generation of mm-wave frequency signals using optical heterodyning combined with digital coherent detection. In **PAPER 9**, up to 16 Gbps in W-band (75-110 GHz) was reported on a single carrier QPSK signal. For **PAPER 10**, O-OFDM baseband was used to generate and detect bitrates exceeding 20 Gbps in the 60 GHz and 75-110 GHz bands.

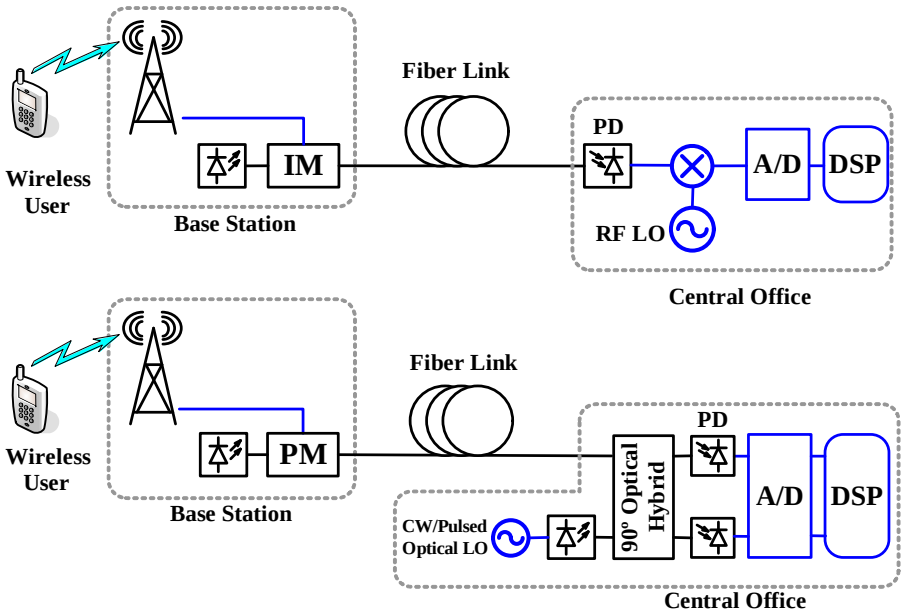

Figure 1.2: Schematic description of two different types of RoF link: Intensity-Modulated and Direct Detected (IM-DD) with external optical modulation (top) and Phase-Modulated assisted with digital Coherent detection (PM-Coh) (bottom).

1.2.2 Intensity modulated versus Phase modulated uplink radio-over-fiber links

Traditionally RoF links are based on Intensity Modulated with Direct Detection (IM-DD) links [8, 22], since they rely on already well established technology and can thereby provide low cost implementation. This kind of links have been studied in detail from the microwave design point of view and showed their capacity for the transport of broadband wireless signals, especially for the downlink. However, it might not be the best solution for the uplink, due to the stringent requirements in dynamic range. In Fig. 1.2 (top) a basic IM-DD link is illustrated, where the microwave signal modulates the intensity of an optical carrier. After fiber transmission the detection is performed using a single PD. In this case, an external modulator is used, typically a Mach-Zehnder Modulator (MZM) or Electro-Absorption Modulator (EAM), but also direct current modulation of the semiconductor light source is possible. After photodetection, the signal is translated to an Intermediate Frequency (IF) by performing RF mixing with an electrical Local Oscillator (LO). The IF signals falls within the

bandwidth of the A/D and it is demodulated in the digital domain using Digital Signal Processing (DSP) algorithms.

IM-DD RoF links require high received optical power in order to increase the link gain. The non-linear intrinsic response of the intensity modulators [23] results in a limited dynamic range. They also suffer from periodic RF power fading, due to chromatic dispersion after optical fiber propagation. More sophisticated variations of the IM-DD basic scheme have been proposed, such as Single-Side Band (SSB) or Double-Side Band (DSB) modulation, concatenated MZM, predistortion etc. [7, 24–26], in order to achieve better performance in terms of link gain and linearity, at the expense of a complex optical transmitter or receiver scheme or lower electro-optical efficiency.

As an alternative, optical phase modulated RoF links have been proposed and demonstrated to offer low distortion and higher linearity than unlinearized IM-DD links for the transport of high speed wireless signals [23, 27–33]. To recover the phase of the optical signal, several techniques have been proposed, such as phase-tracking receiver [23, 28, 30], interferometric detection [27, 29] or careful design of the link in terms of chromatic dispersion [31]. The use of these techniques has been proven to achieve better performance than IM-DD links in terms of dynamic range and linearity [23,27,34]. However, these improvements are typically over a limited bandwidth range and require low phase-noise optical sources [23, 27].

When moving to higher RF frequencies, it is interesting to explore photonic technologies, that allows the transports and detection of the RoF signal at a lower RF carrier frequency. The direct transport of the microwave signals in the optical domain might not be the best solution, due to the high bandwidth of the components, such as optical modulator, photodiodes and digitizers, needed at the receiver and the higher influence of chromatic dispersion. Also, electrical mixers presents high losses, limited bandwidth and low linearity at high RF frequencies. By using photonic technologies it is possible to perform downconversion in the optical domain, usually called Photonic Downconversion (PDC). The RoF signal is shifted to a lower RF frequency by using, for example, external modulators. An added advantage of PDC is that photonic sources can generate pulses with very high repetition rate, low jitter and high stability, something complex to be achieved in the electrical domain with the current technology [41]. Several schemes has been proposed [35–40], performing photonic downconversion of RF frequencies over 40 GHz RoF to IF below 5 GHz with low penalty.

1.2.3 Hybrid wireless-optical links for next generation access networks

Next generation broadband access networks will provide heterogeneous services, wired and wireless. The inclusion of wireless, in a form of RoF, into access networks needs to be compatible with existing access architectures and coexist with the baseband signals. The most promising architecture for optical access networks is Passive Optical Network (PON) because of low cost, simple maintenance and operation, and high-bandwidth provision [1, 54]. Several architectures has been proposed in order to include optical wireless signal distribution in PON, called hybrid PONs. Among the different multiplexing techniques for PON, WDM is the most promising solution for future broadband access networks, as it can accommodate exponential traffic growth, support different broadband services and allow fast network reconfiguration due to the flexibility in wavelength allocation [26, 54, 55, 58].

The use of PM-Coh links in hybrid PON can offer advantages over the traditional IM-DD based PON systems reported in the literature [24, 26, 44, 54, 55, 58], due to the higher linearity and superior receiver sensitivity. PM-Coh links provide also easy integration with Wavelength Division Multiplexing (WDM) PON networks, by the flexibility in wavelength selection given by coherent detection. In terms of cost, despite PM-Coh is a more complex architecture than IM-DD or other phase modulated RoF architectures, the centralization of the complex equipment in the CS and the absence of a bias control of PM to operate in the linear regime, as opposed to IM, makes it suitable for simple BS and allows future upgradeability.

1.3 Photonic digital coherent detection for wireless signals

The use of digital coherent detection for wireless links relies on the capability of digital signal processing for the compensation of the various link distortions occurring both in the wireless as well as in the wired link (optical or electrical signal impairments). The principle of coherent detection in optical fiber communications started in the 90s [42] allowing full reconstruction of the optical received field by beating it with a reference optical LO in a 90° optical hybrid. By detecting the In-phase (I) and Quadrature (Q) components with photodiodes, it is possible to recover the optical field of the detected signal, relative to the LO. This is done by digitizing the

photocurrents using fast A/D converters and performing signal demodulation in the digital domain. By using DSP it is possible to compensate the phase and frequency offset due to the free-running laser beating and other impairments, such as chromatic dispersion, imbalances in the transmitter and receiver, etc. Coherent detection thus allows great flexibility in the use of different modulation formats, as information can be recovered from the encoded amplitude, phase and polarization state of an optical carrier allowing high capacity optical links [64].

In this thesis, the capabilities of coherent receivers to recover the optical field has been studied in two different ways. First, in phase-modulated links, to recover the phase information of the optical source, where the wireless signal has been imposed. This is named Phase Modulated RoF link assisted with Coherent Detection (PM-Coh). Furthermore, for intensity modulated RoF links, by optical filtering one of the modulation side-bands, resulting in a baseband optical signal. In order to recover the in-phase and quadrature components, it is necessary to demodulate it using a reference signal, which is given by the LO in a coherent receiver. In this thesis, this architecture is named Intensity Modulated RoF link assisted with Coherent Detection (IM-Coh), as opposite to the PM-Coh.

1.3.1 Phase modulated radio-over-fiber links

The combination of digital coherent detection and phase modulated link for analogue transport was first reported in [43] using self homodyne detection from the same laser source as LO. It offers advantages in dynamic range and digital demodulation by recovering the optical field using a coherent receiver, thus the phase information. The detection of high RF frequencies, exceeding the bandwidth of the A/D converter, is possible by performing photonic downconversion with a second phase modulator and an RF acting as an electrical LO [32]. This architecture can be suitable for short links requiring high electrical gain and dynamic range, however it is not suitable for access networks, where the BS to CS link is implemented on a single optical fiber, with lengths of few kilometers.

The solution that is presented in this thesis for the integration of phase modulated link into next generation hybrid optical-wireless networks is based on intradyne coherent detection. The basic scheme is shown in Fig. 1.2 (bottom). The microwave signal modulates the phase of the optical carrier, using an optical phase modulator at BS, and transmitted through the fiber to the CS. In the detection side, an optical coherent receiver is used to recover the optical field. The implementation of the PM-Coh link

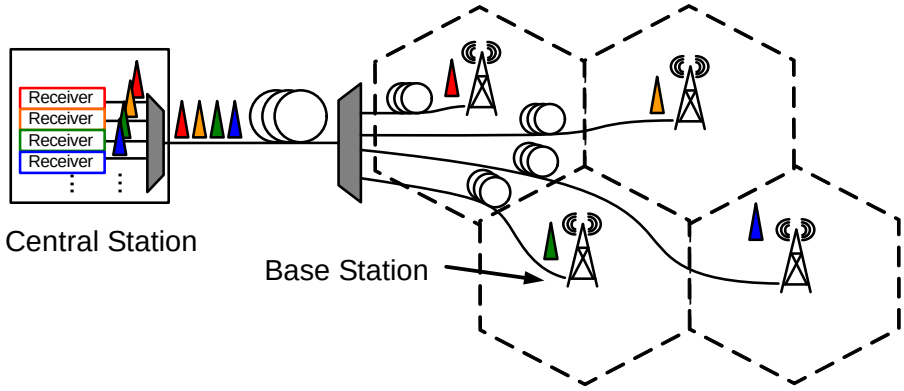

Figure 1.3: Hybrid Wireless-Optical Broadband-Access Network scenario consisting on point-to-multipoint RoF links with WDM.

uses two independent free-running lasers [33]. It avoids the use of a second fiber for the transport of the reference signal, by using a free running laser at the CS acting as LO. This architecture presents benefits for the deployment, centralizing the more complex LO lasers at the CS, leaving a simple antenna BS. The recovered signal is then processed in the digital domain using DSP algorithms, which can compensate transmission impairments, such as fiber chromatic dispersion or beating noise from the two laser sources. Furthermore, PDC can be applied in a more flexible way, by creating a pulsed optical LO source, independent from the fiber transmission link.

The report of the experimental linearity measurements of the PM-Coh link is included in **PAPER 1**. The experimental demonstration of high speed wireless detection is reported in **PAPER 2** and **PAPER 3**, for up to 3.2 Gbps at 40 GHz RF frequencies. A detailed theoretical description of the PM-Coh link with ultimate performance evaluation is reported in **PAPER 4**.

A proposed scenario for next generation hybrid wireless-optical networks, using PM-Coh for wireless transport, is shown in Fig. 1.3. A number of antennas that provides coverage to a given geographical area are connected to the CS through an optical fiber link. Each of the antennas has assigned a different wavelength for the optical transport. Thus, the control of the BS is centralized, offering high flexibility in terms of reconfiguration management. The integration with existing WDM access networks is direct, as the same optical infrastructure can also handle baseband and RF data. It also allows for higher RF frequency reuse within the same CS coverage, as multiplexation is done in the optical domain.

This thesis includes other networking scenarios where PM-Coh links can be applied. For example, **PAPER 5** describes a network architecture based on ring topology. The use of fiber distributed Raman amplification can compensate the losses from the fiber connections through the ring. The application of PM-Coh link for next generation cellular networks, such as Long Term Evolution (LTE), takes place when Distributed Antenna System (DAS) is used to give extended coverage, resulting in a increased number of wireless channels, shared frequency allocation and high capacity wireless links. **PAPER 6** presents an architecture, based on subcarrier multiplexing, for the transparent transport to the CO of all the detected signals from the same BS. The integration of PM link with next generation coherent access networks is reported in **PAPER 7**. Moreover, a single reconfigurable photonic receiver is proposed in this paper and demonstrated for multiple services. By using the same digital coherent receiver, it is possible to detect different type of signals, such as baseband (QPSK, Vertical-Cavity Surface-Emitting laser (VCSEL) based OOK) or wireless (Ultra-Wide Band (UWB), OFDM).

1.3.2 mm-wave intensity modulated radio-over-fiber links

The second approach for the use of digital coherent detection in RoF link reported in this thesis is for IM-Coh links, namely, for the detection of high speed microwave signals in the mm-wave frequency range, 60 GHz and 75-110 GHz. It is based on the use of optical re-modulation of the mm-wave wireless signals, using a high speed electro-optical modulator following SSB modulation. The generated SSB signal results in a baseband signal that can be detected using digital coherent detection.

For the generation, high spectral-efficient modulation formats can be achievable by optical modulators using baseband electronics and detected using digital coherent detection, such as QPSK, M-QAM or O-OFDM [20, 45, 46]. By using optical heterodyning generation and IM-Coh detection, it is possible to generate and detect a wireless signal using traditional optical baseband technologies. Based on the robustness of the receiver, it is possible to compensate for link impairments, such as laser beating from the optical heterodyning RF generation and coherent detection or non-ideal response of the electro-optical components.

The block diagram of a IM-Coh link with O-OFDM signal generation is shown in Fig. 1.4. For the generation of the high-speed wireless signal, at the Central Office (CO) are placed a multicarrier optical generator, an O-OFDM modulator consisting on independent I/Q optical modulators and

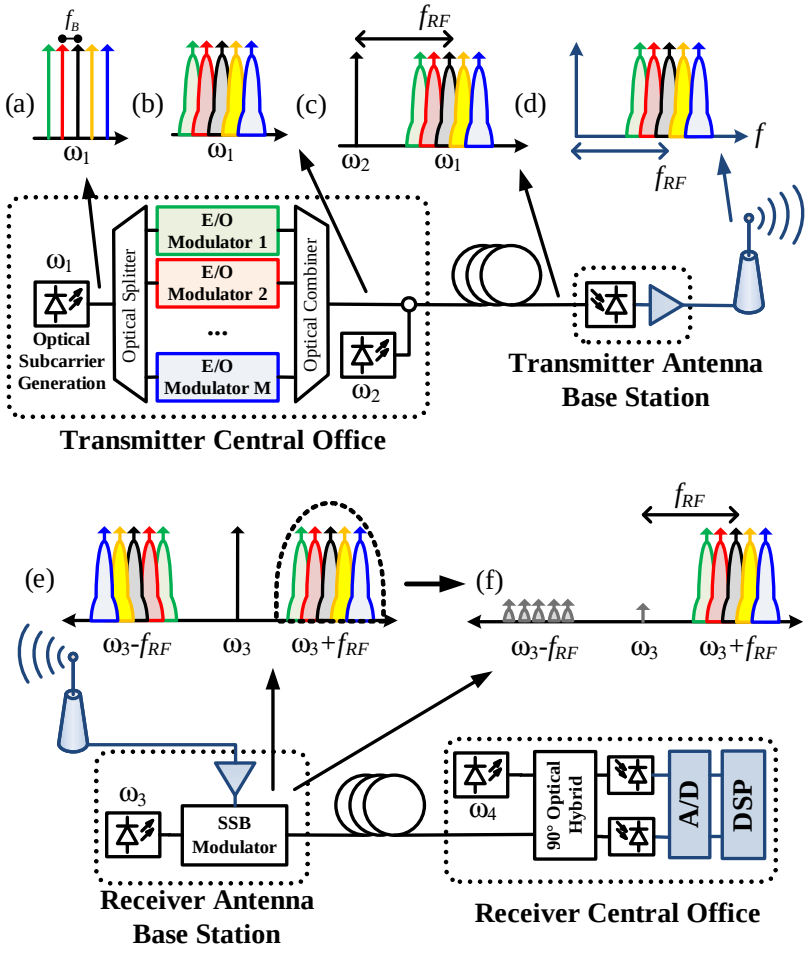

Figure 1.4: Block diagram for the generation and detection of mm-wave carrier frequency signals using Optical-OFDM (O-OFDM) baseband generation and optical reception using SSB modulation combined with digital coherent detection. (a) Multicarrier generation, (b) O-OFDM baseband signal, (c) Optical signals for RF optical heterodyning, (d) mm-wave RF signal generated, (e) Optical modulated received RF signal, (f) SSB baseband signal containing the transmitted O-OFDM signal.

the beating laser source. The optical signal is transported by optical fiber to the transmitter antenna base station, consisting on a high-speed PD and the transmitter antenna. For the detection of the wireless signal, at the receiver antenna base station is placed a SSB optical modulator, which impose the received wireless signal into an optical carrier and transported

to the CO. At the CO, there is an optical digital coherent receiver that performs optical signal detection and demodulation.

In this thesis, **PAPER 8** presents the principle of IM-Coh and demonstrates the detection and demodulation of 2.5 Gbps QPSK at 40 GHz. **PAPER 9** reports the generation and detection of 16 Gbaud QPSK in the W-band (75-110 GHz). Optical heterodyning is used for the generation and IM-Coh is performed for optical detection. **PAPER 10** reports the use of O-OFDM to increase the capacity using baseband optics, achieving over 20 Gbps in the 60 GHz and also in the 75-110 GHz. **PAPER 11** deals with the theoretical description of the link, photonic generation and detection, to establish the ultimate performance and the algorithms needed for the demodulation. **PAPER 12** analyzes the extension from QPSK to 16QAM baseband generation, towards 40 Gbps in a single RF carrier.

1.4 State-of-the-art

The efforts in the design of RoF links have been in obtaining high linear links, quantified in terms of Spurious-Free Dynamic Range (SFDR) with low noise figure. Conventional and most studied analogueue links are those based on IM-DD using a MZM modulator biased in the linear regime [9], which can achieve 110 $dB/Hz^{2/3}$ of SFDR. The performance of this configuration has some limitations, due to the intrinsic non-linear response of the MZM. Also the optical fiber chromatic dispersion tolerance is an issue when moving to high RF frequencies, causing periodic power fading at the output of the PD. Various linearization techniques has been proposed to improve these issues [7, 9, 22] based on concatenated MZMs and predistortion. Despite obtaining higher SFDR, up to 132 $dB/Hz^{2/3}$, they require a precise bias control and have narrow frequency band operation. All these technologies can achieve high performance at frequencies below 10 GHz [22, 47], but achieving those values over 10 GHz becomes a challenge for the architecture and component design. For high RF frequencies, a linearized IM-DD link at 18 GHz has been demonstrated [39], achieving an SFDR of 129 $dB/Hz^{2/3}$ and 114 $dB/Hz^{2/3}$ after PDC.

PM-DD links have been theoretically proven to offer higher linearity than un-linearized IM-DD links [23, 27], however they present challenges in the phase tracking in order to recover the phase information. The use of Optical Phase-Locked Loop (PLL) has been proposed for phase tracking in the receiver, capable to obtain high SFDR at low RF frequencies, with 134 $dB/Hz^{2/3}$ SFDR at 100 MHz [30] and 122 $dB/Hz^{2/3}$ at 300 MHz [48].

The use of DPLL can improve the tracking performance, due to the null loop delay. By using a digital coherent receiver and DPLL, 126.8 $dB/Hz^{2/3}$ was achieved at 900 MHz bandwidth [32]. PDC at 3 GHz and 10 GHz with 107 $dB/Hz^{2/3}$ of SFDR was also demonstrated. A different approach is the reception of the PM signal using interferometric detection [27, 29]. The theoretical analysis shows that it performs better than IM-DD links in terms of SFDR, noise figure and RF gain, but within a limited bandwidth [27]. Linearization using dual wavelength PM has been proven to achieve an SFDR of 127 $dB/Hz^{2/3}$ at 5 GHz. However, the approaches in [23, 27, 29, 30, 32, 48] result in complex and careful matched receivers with short fiber lengths (below 1 km), making it difficult to integrate in access networks. There are also efforts to increase the transmission length of analogueue links [34], with performance for distances of 40 km and over, proving that 100 km links up to 18 GHz are feasible with current technology, with SFDR values above 100 $dB/Hz^{2/3}$ and low noise figure (below 20 dB) but perhaps not simultaneously and neither over a broad band.

The second application presented in this thesis is the generation of wireless signals exceeding 10 Gbps using photonic technologies [49]. Bitrates over 30 Gbps in the 60 GHz band, within the 7 GHz of available bandwidth, can be achieved optically based on OFDM RF generation and photonic upconversion [50, 51]. Concerning the W-band, 75-110 GHz, OOK wireless systems has been demonstrated employing optical generation and electrical envelope detection at 10 Gbps [14] and 20 Gbps [17]. More spectral efficient links have been demonstrated using PSK modulation, up to 16 Gbps in the 70-80 GHz band [52] on a single chip all-electrical transceiver. A 1.25 Gbps link was achieved at 105 GHz RF frequency using IF optical upconversion [15]. The use of all-optical transmitter was reported in [16] using a DQPSK optical modulator, with up to 4.6 Gbps at 92 GHz RF frequency. For gigabit generation beyond 100 GHz, 8 Gbps was achieved at 250 GHz by optical heterodyning [10]. Recently, a 20 Gbps W-band wireless link has been demonstrated based on baseband generation and frequency quadrupling [53]. The reception was done using a broadband electrical mixer rather than with photonic technologies. The reported wireless transmission of only 3 cm (reactive near-field zone) demonstrates the feasibility of wireless transmission but reveals that several challenges need to be overcome to reach longer transmission distances [3].

With regard to the application of RoF to access networks, several scenarios has been proposed to combine PON and distribution of wireless signals using optical fibers. WDM PON has been the preference due to the

high capacity and flexibility in wavelength allocation [26, 54, 55]. The integration into access networks of hybrid wireless and baseband data delivery, called wireless-optical broadband-access network (WOBAN) scenario, as a way to extend the reach of existing PON [56, 57] is a promising architecture that can save on deployment cost as fibers are not required to reach each end-user. Moreover, it can be integrated into existing Time Division Multiplexing (TDM) and WDM PON architectures.

The inclusion of RoF for future hybrid optical-access networks has been mostly based on IM-DD links using MZM, and revealing that chromatic dispersion is the major source of performance degradation of such fiber radio links [24,44]. The use of SSB and DSB modulation can avoid chromatic dispersion fading, thus allowing longer fiber lengths. 155 Mbps data at 35 GHz carrier frequency distribution was reported using these techniques [13]. Wavelength reuse has been proposed, by using Reflective Semiconductor Optical Amplifier (RSOA), for bi-directional links to keep BS simple by avoiding the need of a local optical source [44, 55, 58]. The combination of IM-DD links and wavelength regeneration allows bi-directional transport for high capacity signals, for instance, up to 2.5 Gbps at 40 GHz [44] and 1.25 Gbps baseband and wireless data at 60 GHz [58]. The application of RoF links in future LTE networks, to support distributed antenna systems, has been analyzed, using IF signal transport [6, 59], or combined with gigabit wireless in the 60 GHz band, to create multiservice distribution for in-building environments [60]. The first demonstration of PM-Coh applied to WDM access networks was reported in [33]. 50 Mbaud BPSK and QPSK signals at 5 GHz were detected, using a PM-Coh link with 3 WDM channels spaced 12.5 GHz; however, no BER performance was reported. The demonstration of a converged wireless-optical access networks, supporting the deliver of different wired and wireless services, was experimentally demonstrated in [61]. A combined signal transport over a 78.8 km field-installed fiber of multiple baseband and wireless signal was reported [61]: differential quadrature phase shift keying (DQPSK) baseband access at 21.4 Gbps per channel, 250 Mbps OFDM PM-Coh at 5 GHz, impulse-radio UWB at 3.2 Gbps and a 256QAM WiMAX signal at 12 MBaud.

At the start of this Ph.D. project, there were few application of digital coherent receivers for RoF link: analogue applications (radar) using PM links [43] and [33], which is the first experimental demonstration of wireless signal transport using PM-Coh link, at a low bitrate. Despite the described advantage of a PM link for analogue optical transport [33], it was also the only work on this topic to the author knowledge. Further-

Table 1.1: Main experimental contributions to the state-of-the-art reported in this thesis.

	Bitrate	Mod. format	Carrier freq.	Fiber link
PAPER 1	50 Mbps	BPSK	5 GHz	40 km
PAPER 5	250 Mbps	BPSK	5 GHz	60 km
PAPER 13	2.5 Gbps	16QAM	6 GHz	B2B
PAPER 17	2.5 Gbps	QPSK	5 GHz	79 km
PAPER 2	4 Gbps	16QAM	40 GHz	40 km
PAPER 6	4.8 Gbps	16QAM	3 GHz	20 km
PAPER 8	2.5 Gbps	QPSK	35 GHz	26 km
PAPER 9	16 Gbps	QPSK	100 GHz	B2B
PAPER 10	40 Gbps	O-OFDM QPSK	60-100 GHz	B2B

more, there was no reported detailed analysis of the photonic components requirements, such as linewidth, optical power, modulation index, etc. for transport of high capacity wireless signals. Neither there was experimental demonstration of wireless detection of signal at bitrates exceeding 1 Gbps. The application of PM link for hybrid access networks was not reported either, as so far was focus on IM links [13, 44, 54–58]. The use of PDC had been studied for IM analogue links and also applied to various scenarios of access networks [35–37, 39]; for PM had only been reported for analogue links [38, 40]. However, no work was reported on the application of PDC in PM links for access networks. Neither the combination of PDC and digital coherent receivers for RoF link as a way to overcome the bandwidth limitation of A/D converters.

1.5 Beyond state-of-the-art

The work presented in this thesis has significantly extended the state-of-the-art in the area of detection of wireless signal using photonic technologies, by using novel techniques based on the use of digital coherent receivers and PDC with independent free-running optical LO. Table 1.1 gathers the main experimental results achieved during this Ph.D. project, financed by

the Danish Research Agency for Technology and Production (FTP) project **OPSCODER**, OPtically Sampled COherent DEtection Receiver. It shows the achieved bitrates, modulation format, RF carrier frequencies and fiber transmission length. The research performed during my Ph.D. has led to the demonstration of IM and PM links assisted with digital coherent detection achieving bitrates and in operating RF carrier frequencies that are part of today's state-of-the-art.

In the area of PM-Coh links, my work extended previous results [33,43] from ∼Mbps at 5 GHz with BPSK to 4 Gbps at 40 GHz using 16QAM. These achievements are presented in **PAPER 2** and **PAPER 3**. Regarding mm-wave photonic generation and detection, this project first reported the use of IM-Coh in **PAPER 8**, achieving 2.5 Gbps at 40 GHz. Furthermore, this project increased the previously reported performance to over 20 Gbps at 100 GHz using all-optical OFDM, **PAPER 10**.

I have extended the stat-of-the-art of PM RoF links assisted with coherent detection, expanding previous work towards high bitrates and high frequencies and providing designing engineering rules. I have also introduced the use of PDC for the detection of high RF frequencies signals, without the need of high speed electronics at the receiver, thus avoiding electrical downconversion. The first experimental demonstration of PM-Coh with PDC in the framework of this Ph.D. project is reported in **PAPER 1**, consisting of a 50 Mbit/s BPSK received signal, downconverted from 5 GHz to 300 MHz, including linearity measurements. Through this process, the PM-Coh link was evaluated for its application in different scenarios for next generation broadband access networks. **PAPER 5** reports the use of WDM Ring architecture with fiber distributed Raman amplification for RoF transport at 250 Mbps and 5 GHz. In collaboration with Stanford university, we reported in **PAPER 6** the use of PM-Coh for high capacity IF over fiber for next generation cellular network backhaul using distributed antenna systems, for total aggregated bitrate of 4.8 Gbps. Higher bitrates, 2.5 Gbps QPSK at 5 GHz, presented in PAPER 18, were detected using k-means clustering method. The most advanced PM-Coh link was reported in **PAPER 2** and **PAPER 3**, in which up to 3.2 Gbps in 40 GHz RF of 16-QAM modulated PM-Coh link was achieved. Another relevant application of PM-Coh was reported in **PAPER 7**, where up to 500 Mbps OFDM modulated at 5 GHz was transmitted through 78 km of installed fiber, in an heterogeneous hybrid wireless-wired access network, using a single reconfigurable digital coherent receiver. Finally, I developed a theoretical model of the PM-Coh link, presented in **PAPER 4**, and compared the experimental

results with computer simulations to define the engineering rules.

Elaborating further on the application of digital coherent receivers to RoF links, I collaborated under the framework of the EuroFos project of the European Commission, towards generation and detection of bitrates over 10 Gbps in mm-wave frequencies using intensity modulated links. The application of digital coherent detection for intensity modulated links, IM-Coh, is presented in **PAPER 8**. The key technology employed was the conversion of an intensity modulated RoF signal into baseband by optical filtering. Thus, with standard baseband coherent detection, it was possible to demodulate the resulting signal. A link exceeding 10 Gbps is reported in **PAPER 9** for QPSK modulation format, with up to 16 Gbps generation and detection in the 75-110 GHz band. Furthermore, an extension of the work is presented in **PAPER 10** using O-OFDM generation, achieving up to 24 Gbps and capable of working in 60 GHz and 75-110 GHz bands. Based on the experimental results, I performed theoretical analysis and computer simulation, presented in **PAPER 11**, to determine the ultimate requirements of this type of links on laser linewidth, amplifiers linearity and DSP algorithms. In **PAPER 12** I extended the analysis on the requirements of the electrical and optical components to achieve 40 Gbps at 100 GHz RF frequencies using optical baseband 16-QAM modulation. The overall scientific results and technical achievements presented in this Ph.D. thesis have significantly contributed to current state-of-the-art.

1.6 Main contribution and outline of the thesis

The main contributions of this thesis are in the area of the detection of high speed wireless signals using optics and digital coherent receivers.

First, this thesis proposes, studies and experimentally demonstrates the use of PM-Coh links combined with photonic downconversion to allow the detection and demodulation of high speed wireless signals with low speed electrical components. Detection of 3.2 Gbps at 40 GHz are reported with a A/D receiver bandwidth of only 3 GHz. Secondly, it contributes on the mm-wave signal detection using photonic technologies, with a transparent architecture in terms of carrier frequency, allowing the detection of high bitrate signals, over 20 Gbps, at RF frequencies from 60 GHz to 100 GHz, which could not be demodulated before using previous photonic technologies.

This thesis is structured as follows: Chapter 1 introduces the context of the main research papers included. It provides a short overview on the

topic of wireless signal generation and detection using photonic technologies and the impact that digital coherent receivers to extend the performance to analogue optical fiber links. Chapter 2 describes the novelty of the main contributions of the thesis. To conclude, chapter 3 summarizes the main achievements of this thesis and provides an outlook on the prospects of photonics technologies for the generation, distribution and detection of high speed wireless signals.

Chapter 2

Description of papers

This thesis is based on a set of articles already published or submitted for publication in peer-reviewed journals and conference proceedings. These articles present the results obtained during the course of my doctoral studies on the detection of high speed wireless signals using photonic methods, combining theoretical analysis, simulation and experimental results. The papers are grouped in two categories, dealing with the use of digital coherent receivers for phase modulated or intensity modulated radio-over-fiber links. Phase Modulated RoF link assisted with Coherent Detection (PM-Coh) links are studied and demonstrated experimentally in **PAPER 1** to **PAPER 7**. **PAPER 8** to **PAPER 12** present the theoretical analysis and experimental results for mm-wave generation and detection using Intensity Modulated RoF link assisted with Coherent Detection (IM-Coh) links.

2.1 Phase modulated radio-over-fiber links assisted with coherent detection

I present in **PAPER 1** the first reported experimental results for Photonic Downconversion (PDC) applied to PM-Coh links. The main novelty of this paper is the use of a pulsed and free-running laser source as Local Oscillator (LO) to realize PDC for a PM-Coh link. **PAPER 1** includes evaluation of the linearity of the link, in terms of Spurious-Free Dynamic Range (SFDR), for high RF carrier frequencies (5 GHz) with Continuous Wave (CW) operation and with PDC. As a proof of concept, a 50 Mbit/s BPSK signal at 5 GHz RF carrier frequency was phase modulated and

transmitted through 40 km of Single Mode Fibre (SMF). In the detection side, PDC was employed at the coherent receiver to transfer the signal down to 300 MHz, employing an A/D converter with a bandwidth of only 1 GHz.

PAPER 2 presents the first demonstration of the detection of a high bitrate wireless signals, with complex modulation formats, using digital photonic receivers. By using a PM-Coh link with PDC, up to 3.2 Gbps 16QAM at 40 GHz could be demodulated after 40 km of SMF transmission. This was the highest RoF uplink experimental demonstration reported to that date. This achievement is relevant because of the high bitrates and RF carrier frequencies employed and the fact that the lasers employed were not locked to each other. This free running behaviour was compensated afterwards using Digital Signal Processing (DSP) algorithms. **PAPER 2** was accepted as a post-deadline contribution in the 35^{th} European Conference on Optical Communication (ECOC'09). A more detail presentation of these results is reported in **PAPER 3**.

PAPER 4 presents a theoretical model and computer simulation results for a PM-Coh link with CW and PDC. The ultimate performance is evaluated for the transport of wireless links with capacities in the order of hundreds of Mbps. The analysis proves that PM-Coh link can provide low end-to-end distortion for the transport of high capacity wireless signals through a fiber link. It concludes that laser linewidth and modulation index are the key factors in the link design. By using commercially available lasers, with linewidth values in the 100 kHz range and low V_π modulators, below 7 V, it is possible to transport 1 Gbaud 16QAM signal with an induced Error Vector Magnitude (EVM) of only 7%. It also includes the experimental results from **PAPER 3** and **PAPER 6**, compared with the computer simulation results, showing a good agreement between the model and the experimental results.

PAPER 5 presents a novel networking architecture for hybrid wireless-optical networks, consisting of a fiber ring assisted with distributed Raman amplification for detection and transport of high speed wireless signals from multiple BS to a single CO. Raman amplification for wireless access scenarios is a novel approach for extended optical fiber reach and high capacity networks. 5 channels at 250 Mbps and 5 GHz carrier frequency were optically transported through 60 km of fiber with Wavelength Division Multi-

plexing (WDM) channels spaced only 12.5 GHz In the system a 2 m wireless link was also included.

PAPER 6 presents a networking architecture for transparent transport of multiple wireless channels employing a single laser source for Multi-Input Multi-Output (MIMO)-Distributed Antenna System (DAS). It is capable to support multiple users with high individual bandwidth requirements, making this architecture suitable for next generation cellular networks. This paper includes computer simulation and experimental demonstration of a cellular coverage of 12 x 400 Mbit/s (3 cells x 4 antennas, 100 Mbaud 16QAM) and 6 x 800 Mbit/s (3 cells x 2 antennas, 200 Mbaud 16QAM) on a single optical carrier, proving the potential integration of the proposed architecture into the next generation cellular networks.

PAPER 7 reports on the application of a reconfigurable digital coherent receiver for unified heterogeneous metro-access networks. 4 signals from different optical access technologies were WDM multiplexed onto the same optical fiber, transported through 78 km of installed optical fiber and detected using a single reconfigurable digital coherent receiver. The heterogeneous metro access network was composed of the following subsystems: 1) 5 Gbps directly modulated Vertical-Cavity Surface-Emitting laser (VCSEL). 2) Baseband 20 Gbps non return-to-zero (NRZ)-Quadrature Phase Shift Keying (QPSK). 3) Optically phase-modulated 2 Gbps Impulse Radio (IR) Ultra-Wide Band (UWB) and 4) PM-Coh link with 500 Mbps OFDM at 5 GHz RF frequency.

2.2 mm-wave photonic signal generation and detection

PAPER 8 proposes and experimentally demonstrates the use of IM-Coh link for for the detection of high speed wireless signals. A QPSK at 2.5 Gbps and 40 GHz was modulated in the optical domain using a MZM. The RF signal is converted to baseband in the optical domain by optically filtering one of the side-lobes, which is called Single-Side Band (SSB). After that, standard digital coherent detection was used for demodulation.

PAPER 9 presents a novel technique for all-photonic millimeter-wave wireless signal generation and digital coherent detection. For signal generation, direct conversion of an optical baseband QPSK signal to a millimeter-wave wireless signal using optical heterodyning was used. An optical baseband QPSK signal was mixed in a photodiode with a free-running unmodulated laser separated 100 GHz in frequency, generating a high capacity RF electrical signal. For demodulation, the technique presented in **PAPER 8** was used. 5 Gb/s amplitude-shift keying and up to a 16 Gb/s QPSK wireless signal in the band of 75–110 GHz was generated and successfully demodulated.

PAPER 10 presents an extension of **PAPER 9** by the use of all-Optical OFDM (O-OFDM) for increased spectral efficiency. Up to 3 orthogonal subcarriers were generated to create an all-optical OFDM up to 40 Gbps, with only 10 Gbps electronics. In order to demonstrate the RF frequency scalability and bit-rate transparency, the system was tested in the 60 GHz and 75-110 GHz bands at the baud rates of 5 and 10 Gbaud. The proposed system was experimentally tested up to 40 Gb/s. Additionally, a novel digital carrier phase/frequency recovery structure was employed to enable robust phase and frequency tracking between the beating lasers.

PAPER 11 presents theoretical and simulation results of the generation and detection of mm-wave wireless signals using baseband optics. The technique analyzed in **PAPER 11** is the same presented in **PAPER 8**, **PAPER 9** and **PAPER 10**. **PAPER 11** identifies the main signal impairments in the link, electrical and optical, and assesses their impact in the overall link performance. From this analysis, we draw engineering rules for the link design. The algorithms needed for the demodulation are proposed and studied by computer simulations and validated with experimental data.

PAPER 12 evaluates the requirements of the electrical and optical components for the generation and detection of microwave signals with bitrates approaching 40 Gbps. The performance for the case of 10 Gbaud QPSK links at 100 GHz was studied and proposed the extension steps towards a more complex modulation format, optically generated 16QAM, identifying the requirements for this modulation format. The conclusion is that a matched RF passband design of the electro-optical components, to have a linear response in the 100 GHz band, is required to move from QPSK to 16QAM links, as 16QAM modulation format has stringent requirements in the linearity and requires higher SNR than QPSK.

Chapter 3

Conclusion

3.1 Conclusions

This thesis addresses the design and performance evaluation of high speed wireless signals generation and detection using optics. The focus of the thesis is on the use of photonic digital coherent receivers as a technique for wireless signal detection and compensation for transmission impairments by using Digital Signal Processing (DSP) algorithms. The research results presented in this thesis are pioneering in two main areas: firstly, in the distribution and detection of high-speed wireless signals using Phase Modulated RoF link assisted with Coherent Detection (PM-Coh) architectures, combined with Photonic Downconversion (PDC). Detection of up to 3.2 Gbps at 40 GHz was experimentally demonstrated using this approach. Secondly, in the generation and detection of over 20 Gbps wireless signals in the mm-wave bands (60 GHz and 75-100 GHz), using baseband photonic for wireless generation and Intensity Modulated RoF link assisted with Coherent Detection (IM-Coh) links for the detection. These achievements fulfilled the requirements on transmission robustness and high capacity of next generation hybrid optical fibre-wireless networks.

3.1.1 Phase modulated RoF links assisted with coherent detection

PM-Coh links are shown in this thesis to be a prospective alterative to traditional Intensity Modulated with Direct Detection (IM-DD) links for the transport of wireless signals over the fiber infrastructure. The results in **PAPER 2**, **PAPER 3** and **PAPER 6** provide experimental demon-

stration of the capabilities of PM-Coh link for the transport high bitrate signals, at high RF frequencies and with low end-to-end distortion. The presented technology can be used with PDC to enable detection of high RF signals exceeding the Analogue-to-Digital Converter (A/D) bandwidth, while maintaining the linearity of the link. This conclusion is based on the results shown in **PAPER 1**, reporting experimental measurements of the linearity in terms of Spurious-Free Dynamic Range (SFDR), and also in **PAPER 2** and **PAPER 3**, for the case of high bitrate signal detection.

The integration of PM-Coh link into different scenarios of next generation optical access networks, was reported in **PAPER 5** ,**PAPER 6** and **PAPER 7**. The integration of PM-Coh RoF links with baseband access networks was also demonstrated in **PAPER 1**, **PAPER 5**, **PAPER 7** and PAPER 13 to be inherent due to the use of digital coherent receiver.

3.1.2 mm-wave photonic signal generation and detection

The use of photonic digital coherent receivers for the detection of wireless signals open new possibilities for novel networking architectures in high capacity hybrid wired-wireless access links. The use of photonics enables the transport and detection of wireless signal. It also allows the centralization of complex signal processing for the compensation of impairments caused by wireless and fiber transmission. A method for optical transport and detection of wireless signals using digital coherent receivers is presented in **PAPER 8** using Single-Side Band (SSB) modulation and IM-Coh link. Combining the transparency of direct electro-optical transmission and detection, given by IM-Coh, with the capabilities of the DSP to support high bitrates and to compensate impairments, it is possible to use high RF frequencies, in the mm-wave range, to realize high capacity wireless signals. The new possibilities that optics brings to create high spectral efficient modulation formats, by using IQ optical modulation, are used to generate high capacity wireless signals by optical heterodyning. **PAPER 9** reports the generation of 16 Gbps capacity link at 100 GHz carrier frequency. To achieve higher spectral efficiency, all-optical Orthogonal Frequency-Division Multiplexing (OFDM) was used in **PAPER 10**. The system was tested at bitrates up to 40 Gbps at 60 GHz and 100 GHz RF frequencies.

3.2 Future work

In this section I would like to provide a view of the future work that could be pursued for the generation and detection of high speed wireless signals using the optical technologies presented in this thesis, from the system architecture to the devices. Additionally, I would like to consider a more concrete target, 100 Gbps wireless transmission and envision on the application scenarios.

3.2.1 Technologies for ultra high capacity RoF links

New photonic devices with extended operation bandwidth and matched RF design will allow the implementation of higher capacity links beyond the work presented in this thesis. For wireless signal modulation in the optical domain, high bandwidth modulators have been reported in the literature, with bandwidths over 100 GHz in the form of Mach-Zehnder Modulator (MZM) and Electro-Absorption Modulator (EAM) [22, 62]. However, they are mostly design for broadband operation; a passband design on the frequency band of interest will results in improved efficiency. For the photonic generation, high speed photodetectors, with 300 GHz bandwidth have also been reported [11]. The generation of high repetition rate signals can be performed using pulsed optical light sources, such as mode-locked lasers [11,41,63], with repetition rates over 100 GHz, offering high stability and low jitter. The combination of pulsed sources with frequency doubling or quadrupling techniques [14,17] will allow the generation of subterahertz RF sources without the need of a high frequency electrical reference source or RF mixer. With regard to digital coherent receivers, current challenges are related to the A/D convertors limited bandwidth and effective number of bits and the real time implementation of DSP algorithms at the receiver [64].

3.2.2 Towards 100 Gbps wireless communication links

The high bitrates that fiber optics can provide is creating an imbalance between wired and wireless data delivery. Single carrier optical transmitters and receivers exceeding 100 Gbps are commercially available [64], however wireless links are still limited to some Gbps. The application scenarios for 100 Gbps wireless links are numerous. For instance, the delivery of the new High-Definition 3D video systems, including multi-view systems, requires high bitrate in order to support uncompressed video transmission so as to

avoid latency and decrease codec power consumption. High data rates will be needed for cloud computing, enabling the highly hardware processing to be moved out from the end-user to the network provider. In order to provide real time access to a large number of cloud services, high speed wireless connection will be needed.

To rise to the same level the capacities of optical fiber and wireless links, it is necessary to move to high RF carriers, beyond 100 GHz [3, 4]. The use of photonic generation and detection, as proposed in this thesis, can provide high capacity links at high RF carriers. Links exceeding 100 Gbps could be achieved with RF carrier frequencies in the low Terahertz (THz) region, from 100 GHz to 2000 GHz. For example, there is a THz transmission window with a center frequency around 240 GHz that offers about 100 GHz of bandwidth [3].

The challenges for wireless generation and detection at these high frequencies are many. The need of high power THz RF sources is a critical issue due to the high attenuation and low efficiency of a broadband RF range of operation. A careful design of components in the THz bandwidth will be needed to obtain maximum efficiency. Simple On-Off Keying (OOK) modulation might not be sufficient to achieve 100 Gbps due to the difficulty in broadband design of the components and the frequency dependent wireless channel properties. A more efficient use of the RF spectrum, by using advanced modulation formats, will decrease the requirements of the components for broadband operation, yet increase in terms of linearity. The capability of generating advanced modulation formats, in order to achieve spectral efficient wireless links, is an added challenge for the THz component design to provide also sufficient linearity.

Paper 1: Photonic downconversion for coherent phase-modulated radio-over-fiber links using free-running local oscillator

A. Caballero, D. Zibar, C. G. Schäffer, and I. Tafur Monroy, "Photonic downconversion for coherent phase-modulated radio-over-fiber links using free-running local oscillator," *Optical Fiber Technology*, 17, pp. 263—266, 2011.

Optical Fiber Technology 17 (2011) 263–266

Contents lists available at ScienceDirect

Optical Fiber Technology

www.elsevier.com/locate/yofte

Photonic downconversion for coherent phase-modulated radio-over-fiber links using free-running local oscillator

Antonio Caballero [a,*], Darko Zibar [a], Christian G. Schäffer [b], Idelfonso Tafur Monroy [a]

[a] DTU Fotonik, Technical University of Denmark, Oersteds Plads, Building 345v, DK-2800 Kgs-Lyngby, Denmark
[b] Helmut Schmidt University Hamburg, Holstenhofweg 85, 22043 Hamburg, Germany

ARTICLE INFO

Article history:
Received 24 August 2010
Revised 14 February 2011
Available online 29 April 2011

Keywords:
Phase-modulation
Radio-over-fiber
Coherent detection

ABSTRACT

A digital coherent receiver employing photonic downconversion is presented and experimentally demonstrated for phase-modulated radio-over-fiber optical links. Photonic downconversion adds additional advantages to optical phase modulated links by allowing demodulation of signals with RF carrier frequencies exceeding the bandwidth of electrical analog-to-digital converter. High spurious-free dynamic range is observed for RF carriers at 5 GHz photonically downconverted to 1 GHz.

1. Introduction

Radio-over-fiber (RoF) is a promising technology capable to provide simple antenna front ends, increased capacity and increased wireless access coverage [1]. RoF system has relied on already well established technology for baseband signals, based on intensity modulated and direct detection links, which can provide a very low cost of implementation [2]. However, baseband optical communication is moving towards coherent detection with digital signal processing (DSP), thus allowing for advanced modulation formats to be used [3]. A similar trend may follow for RoF systems. The use of coherent detection will enable the information to be carried either in amplitude, phase or in different states of the polarization of the optical field. Additionally, the selectivity of coherent receivers is very well suited for wavelength division multiplexing (WDM) access networks, where no optical filters are then needed in the receiver.

The proposed scenario is shown in Fig. 1, where a group of antennas, base stations (BS), providing coverage to a given geographical area, are connected to the central station (CS) through an optical fiber link, each of them using a different wavelength. Thus, the control of the BS is centralized, offering high flexibility in terms of reconfiguration. Furthermore, the same infrastructure can also handle baseband and RF data. It also allows of frequency reuse within the same CS coverage, as multiplexation is done in the optical domain.

Recently, there has been a lot of effort on coherent radio-over-fiber optical links using either analog or digital demodulation techniques [4–8]. Both analog and digital demodulation techniques have their advantages and disadvantages, however, when it comes to flexibility, implementation of different functionalities and impairment compensation, digital demodulation schemes are advantageous [8], for the use of phase modulation offers the mandatory high linearity needed for the transparent transport of high speed wireless signals at high carrier frequencies and complex modulation formats [4,5]. Optical phase modulated links assisted with coherent detection (PM-Coh) combine the advantageous features of both technologies to realize a transparent transport of wireless signal through the optical fiber link.

One of the challenges associated with digital demodulation techniques are the high sampling rates and bandwidth limitations of analog-to-digital (A/D) converters, which limits the operating range of coherent receivers using digital demodulation techniques up to few GHz [9,10].

One way to extend the frequency range of digital coherent receivers beyond few GHz in RoF systems is using photonic downconversion (PDC) [9–12]. In the electrical domain, downconversion is commonly done by using high frequency mixers, which presents high losses, limited bandwidth and low linearity at high RF frequencies. In contrast, PDC, by performing the downconversion in the optical domain, has been shown to offer low distortion while keeping required electronic to baudrate operation speed [7,9]. PDC is performed in the optical receiver front by employing a pulsed optical local oscillator (LO). With today technology, optical pulses can be generated with very high repetition rate, low jitter and high stability, making a universal optical front-end very

* Corresponding author. Address: Oersteds Plads B. 343 R.211, 2800 Kgs. Lyngby, Denmark.
E-mail address: acaj@fotonik.dtu.dk (A. Caballero).

1068-5200/$ - see front matter © 2011 Elsevier Inc. All rights reserved.
doi:10.1016/j.yofte.2011.03.001

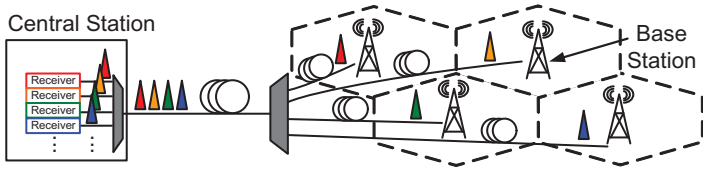

Fig. 1. Proposed scenario for RoF link with photonic downconversion. The base stations (BS) are connected to the central station (CS) through optical fiber, each of them using different wavelengths.

suitable for PDC [8]. These advantageous performance metrics are difficult to be achieved in the electrical domain with the current technology.

As it is shown in Fig. 2, the LO in the receiver is a pulse source with a repetition rate F_{LO}. After the coherent receiver, the RF signal, with a carrier frequency F_{RF}, is transferred to an intermediate frequency (IF), F_{IF}. The sum of the maximum estimated frequency deviation of the LO from the signal wavelength (F_{offset}) and the IF is designed to fall within the operating range of A/D converters. The demonstration of PDC in combination with digital coherent demodulation for phase modulated RoF links has been reported in [10], using homodyne detection with a single laser source. However, by taking advantage of digital signal processing, it is possible to use an independent and free-running laser in the receiver side and compensate the frequency offset beating from the two lasers by using a Digital Phase-Locked Loop (DPLL)[8].

In this paper, we propose and experimentally demonstrate the use of PM-Coh combined with PDC for high speed wireless transport over fiber. The main novelty of our approach is the use of a free running pulsed laser source as LO to realize PDC, instead of high speed electrical downconversion. We evaluate the performance of the system in terms of linearity of the PM-Coh link with and without PDC for high RF carrier frequencies (5 GHz) by realizing two-tone measurements. Thereafter, PM-Coh with PDC is employed in order to transfer a 50 Mbit/s BPSK signal at 5 GHz RF carrier frequency down to 300 MHz with A/D converter BW of only 1 GHz. We report on successful signal demodulation and data recovery for back-to-back and after 40 km of Single Mode Fiber (SMF) transmission. In the system presented in this paper, transmitter and LO laser are free-running, i.e. intradyne system. This means that the system is fairly simple since it does not require complex analog phase-locked loop for laser synchronization. Laser synchronization is performed in software as explained later.

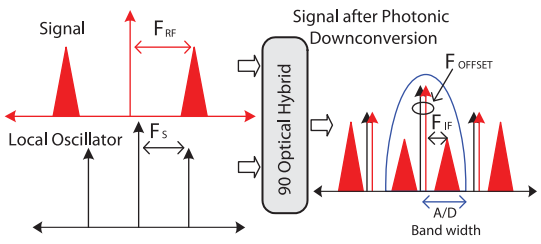

Fig. 2. Schematic description of photonic downconversion. The frequency of the RF signal (F_{RF}) is transferred to an intermediate frequency (F_{IF}) due to the repetition rate of the local oscillator (F_{LO}). The value of the IF is equal to the difference of the incoming RF and LO repetition rate. As the light sources are not frequency locked, there is still a remaining frequency offset (F_{offset}) that is removed at the DSP receiver.

2. Setup description

A schematic of the experimental setup is shown in Fig. 3. Two independent tones, with common reference clock, are generated and added to drive the Phase Modulator (ΦM). The frequencies are set to 5 GHz and 5.01 GHz. The two RF paths are isolated to ensure that any spurious intermodulation products are suppressed by >70 dB. The optical source (λ_0) is a distributed feedback laser (DFB) with ~1 MHz of linewidth at a wavelength of 1550 nm. The pulsed optical LO is composed of a tunable laser source, ~1 MHz linewidth, followed by an electro absorption modulator (EAM) driven by a +15 dBm RF power sinusoidal signal at 4 GHz. This results in an optical comb with a duty cycle of approximately 30%. The resultant optical LO signal is amplified using an erbium doped fiber amplifier (EDFA) and a 1 nm optical band-pass filter is used to reject out of band ASE noise. The wavelength of the LO (λ_{LO}) is tuned to be close to λ_0, leading to a typical frequency mismatch of ~300 MHz. In the receiver side, the incoming optical signal and LO are passed through polarization beam splitters (PBS) to assure detection of the same linear polarization. In a more practical approach, a polarization tracking system could be used to follow the polarization drifts of the received signal.

The coherent receiver is a 90° optical hybrid that has integrated balanced photodiodes with a 3 dB cut-off frequency of 7.5 GHz. The input optical power level is −2 dBm for the signal and −8 dBm for the LO. The LO average power is low to avoid saturating the photodiodes, due to high peak power of sampling pulses. The detected in-phase (I) and quadrature (Q) photocurrents are stored using a digital sampling oscilloscope (DSO) performing A/D conversion at 40 GSamples/s for offline (DSP).

For the validation of data transmission, a 50 Mbps BPSK signal at 5 GHz drives the ΦM with 8 dBm input power. The local oscillator frequency is set to 4.7 GHz. The incoming optical signal power is −18 dBm after 40 km of SMF transmission. The post-processing of the digitized signals consists of carrier-recovery DPLL, linear signal demodulation and RF demodulation (residual frequency estimation unit, RF carrier phase recovery and matched filtering) [8]. The carrier-recovery DPLL is used to remove optical frequency and phase difference between the transmitter and LO laser.

3. Results

In this section, we investigate the linearity of our RoF link operating at 5 GHz. Two-tone measurements have been done to assess the SFDR with respect to the third order distortion (TOD), which are the first order intermodulation components laying within the signal bandwidth. Fig. 4 shows the measured results for continuous wave operation and photonic downconversion (PDC) with an optical sampling frequency of 4 GHz. Similarly, the spectra of the recovered two tones for 9 dBm at CW and 12 dBm at PDC are also included in each graph. The noise level of both schemes can be determined by the minimum distinguishable third order distortion (TOD) from the resulting spectrum. The number of quantification

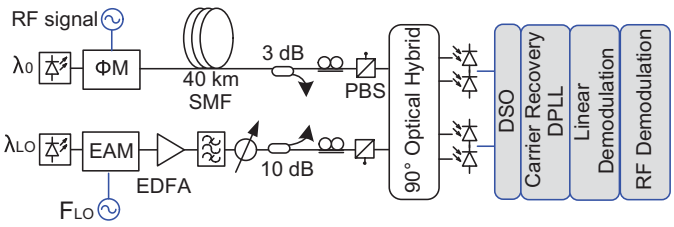

Fig. 3. Experimental setup. The laser source at λ_0 is modulated with an RF signal (F_{RF}) using a phase modulator (ΦM) and send through a single-mode fiber (SMF). On the receiver side, the local oscillator (λ_{LO}) is pulsed using an electro absorption modulator (EAM) with an RF frequency F_{LO}. Polarization beam splitters (PBS) are placed before the coherent receiver (90° Hybrid). The photodetected signals are digitalized using a digital sampling oscilloscope (DSO).

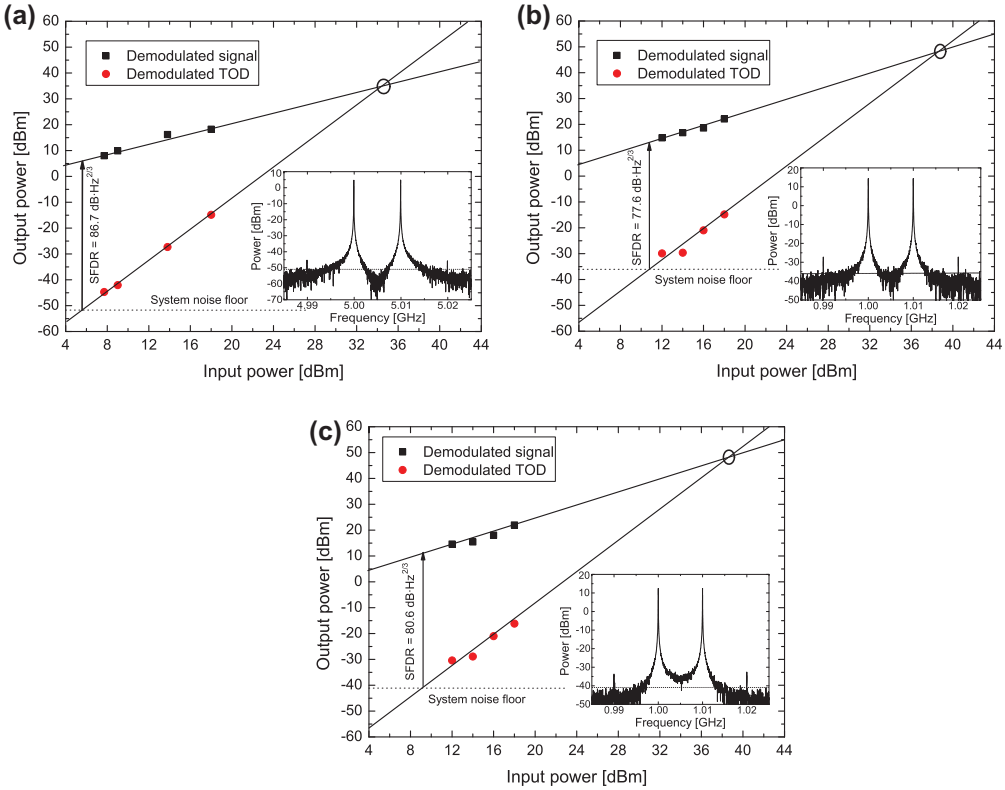

Fig. 4. Spurious-free dynamic range (SFDR) for different system configuration. (a) 5 GHz RF with continuous wave operation, including the spectrum of 9 dBm input power. (b) 5 GHz downconverted to 1 GHz with the spectrum of 12 dBm input power. (c) 10 GHz downconverted to 1 GHz with the spectrum of 12 dBm input power (20 kHz resolution bandwidth).

bits determined by the scope is 8, however the maximum effective bits at the experiment frequencies is 7, which gives a signal-to-noise ratio of 43.9 dB.

The measured value of the SFDR, shown in Fig. 4a, for our system is 86.7 dB $Hz^{2/3}$ with CW operation. With PDC at 1 GHz, Fig. 4b shows and SFDR of 77.6 dB $Hz^{2/3}$, resulting on a penalty of 9.1 dB. For 10 GHz operation, downconverted to 1 GHz (Fig. 4c), we have obtained 80.6 dB $Hz^{2/3}$ of SFDR. No comparison with CW operation at 10 GHz could be done, due to receiver limited bandwidth. The measured downconversion penalty is associated mainly to the difference on power between the principal and the first side lobe of the LO. This first lobe causes the replica of the signal information falls within the receiver bandwidth, thus decreasing the signal power. There is also a power penalty due to the higher harmonics that do not contribute to the resultant downconversion process.

The results are clearly limited by the noise due to the resolution of the A/D converter, which we believe can be decreased further more by increasing the bit resolution. We also would like to stress that no compensation for the non-linearities resulting from the photodiodes nor I/Q imbalance in the 90° optical hybrid has been included in the post-processing, which could potentially, improve the overall performance.

Finally, our proposed photonic downconversion scheme was tested in a RoF scenario, measuring the bit-error-rate (BER) as a function of the optical signal-to-noise ratio (OSNR) as shown in

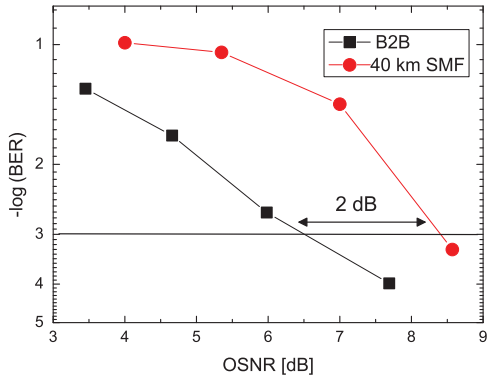

Fig. 5. Bit error rate (BER) measurements as a function of the optical signal to noise ratio (OSNR) with 0.1 nm resolution bandwidth. A penalty of 2 dB is observed from back-to-back (B2B) to transmission through 40 km of fiber.

Fig. 5. The RoF signal was successfully demodulated with ODC at a LO sampling frequency of 4.7 GHz. For the BER computation, we have considered 10,000 bits. BER values below 10^{-3} are achieved for back-to-back (B2B) and after 40 km of transmission, at which forward error correction can be used to maintain data quality. However, after 40 km of fiber transmission a penalty of about 2 dB is observed at a BER of 10^{-3}. We stress that we did not use any equalization algorithm, which could potentially improve the signal transmission by reducing the amount of intersymbol interference due to chromatic dispersion.

Our proposed system allows for detection on low power level incoming RoF signals, due to the inherent amplification provided by the LO in the coherent detection receivers, which is attractive for converged wireless and wireline signal transport over passive optical fiber access networks.

4. Conclusion

In this paper we have experimentally demonstrated the performance of PDC for detection of high frequency PM-Coh links. Since very high repetition rate and low jitter of an external pulsed LO can be easily achievable with current technology, the system can operate at high RF carrier frequencies, exceeding the A/D convertor bandwidth, decreasing significantly the requirements for coherent receivers assisted by DSP. The performance is mainly limited by the noise floor due to A/D converter dynamic range. However, DSP allows post-compensation of opto-electrical mismatches and non-linearities which makes this type of system beneficial. The requirement for the linewidth of the two lasers is low and no control loop for the wavelength difference of the two lasers is necessary. Our experimental results show the potential of high performance PDC receivers for future RoF systems with advance modulation formats that require high linearity and advanced demodulation algorithms.

Acknowledgment

This work was supported in part by the Danish Research Council under grant OPSCODER.

References

[1] J. Capmany, D. Novak, Microwave photonics combines two worlds, Nat. Photon. 1 (2007) 319–330.
[2] C.H. Cox III, E.I. Ackerman, G.E. Betts, J.L. Prince, Limits on the performance of RF-over-fiber links and their impact on device design, IEEE Trans. Microw. Theory Tech. 54 (2006) 906–920.
[3] T. Pfau, S. Hoffmann, O. Adamtzyk, R. Peveling, V. Herath, M. Pormann, R. Noe, Coherent optical communication: towards real time systems at 40 Gb/s and beyond, Opt. Exp. 16 (2008) 866–872.
[4] T.R. Clark, M.L. Dennis, Coherent optical phase-modulation link, IEEE Photon. Technol. Lett. 19 (2007) 1206–1208.
[5] H.F. Chou, A. Ramaswamy, D. Zibar, L.A. Johansson, J.E. Bowers, M. Rodwell, L.A. Coldren, High-linearity coherent receiver with feedback, IEEE Photon. Technol. Lett. 19 (2007) 940–942.
[6] Y. Li, D. Yoo, P. Herczfeld, A. Rosen, A. Madjar, S. Goldwasser, Receiver for coherent fiber-optic link with high dynamic range and low noise figure, in: Proc. Int. Topical Meeting Microw. Photon. Tech. Dig., Seoul, South Korea, 2005, pp. 273–276.
[7] D. Zibar, L.A. Johansson, H.-F. Chou, A. Ramaswamy, M. Rodwell, J.E. Bowers, Phase-locked coherent demodulator with feedback and sampling for optically phase modulated microwave links, J. Lightw. Technol. 26 (2008) 2460–2475.
[8] D. Zibar, X. Yu, C. Peucheret, P. Jeppesen, I. Tafur Monroy, Digital coherent receiver for phase-modulated radio-over-fiber optical links, IEEE Photon. Technol. Lett. 21 (2009) 155–157.
[9] M. Park, J.-W. Kim, F. Kaertner, M. Perrott, An optical–electrical sub-sampling receiver employing continues-time ΔΣ modulation, in: Proc. of the 32nd European Solid-State Circuits Conference, Montreux, Switzerland, 2006, pp. 182–185.
[10] T.R. Clark, M.L. Dennis, Photonics downconversion and linearization of an X-band fiber optic link using optical I/Q modulation, in: Conf. on Lasers and Electro-Optics, Baltimore, USA, 2007, paper CTuAA2.
[11] A. Ramaswamy, L.A. Johansson, J. Klamkin, D. Zibar, L.A. Coldren, M. Rodwell, J.E. Bowers, Optical phase demodulation of a 10 GHz RF signal using optical sampling, in: Proceedings of Conference on Coherent Optical Technologies, Boston, USA, 2008.
[12] I. Kim, C. Kim, G. Li, Requirements for the sampling source in coherent linear sampling, Opt. Exp. 12 (2004) 2723–2730.

Paper 2: Digital coherent detection of multi-gigabit 16-QAM signals at 40 GHz carrier frequency using photonic downconversion

A. Caballero, D. Zibar, and I. Tafur Monroy, "Digital coherent detection of multi-gigabit 16-QAM signals at 40 GHz carrier frequency using photonic downconversion," in *Proc. 35th European Conference on Optical Communication, ECOC'09*, Vienna, Austria, 2009, Post-Deadline Paper PDP3.4.

Digital Coherent Detection of Multi-Gigabit 16-QAM signals at 40 GHz Carrier Frequency using Photonic Downconversion

A. Caballero[(1)], D. Zibar[(1)], I. Tafur Monroy[(1)]

[(1)] DTU Fotonik, Department of Photonics Engineering, Technical University of Denmark, Kgs. Lyngby, Denmark, acaj@fotonik.dtu.dk

Abstract *We experimentally demonstrate detection of multi-gigabit 16-QAM modulated signals, of up to 4 Gb/s, at a 40 GHz carrier frequency by combining photonic downconversion and low bandwidth electronics.*

Introduction

Currently, there is a rapid increase and interest in new radio-over-fibre (RoF) technologies capable of enabling high capacity wireless access links[1,2]. The current trend is moving towards mm-wave frequencies, where complex modulation formats (QPSK, QAM[2,3]) and multiplexing schemes such as OFDM can be used in order to reach multi-gigabit capacities. Most of the reported works so far, focus on the photonic generation of multi-gigabit mm-wave signals[1-3], i.e downstream channel. However, the demodulation of signals at mm-wave frequencies still posses many technical challenges since it requires very high-speed and linear radio-frequency (RF) electronics[1-3]. It is therefore important to overcome the limitations of detection electronics and smoothly extend the operating frequency range of RoF links to mm-wave frequencies. Additionally, the uplink direction (from the antenna base-station towards the central office) presents a challenge in order to make it robust, flexible and yet with low complexity, while providing full bidirectionality and high bandwidth operation.

In this contribution, we demonstrate an uplink channel approach for detection of multi-gigabit mm-wave radio-over-fibre signal without the need for high frequency electronics. To the best of our knowledge, this is the first report on the use of photonic downconversion for detection of 16-QAM modulation format at 40 GHz carrier frequency, with up to 4 Gbit/s data signal bit-rates and digital coherent detection. Using the photonic downconversion (PDC), the mm-wave signal is downconverted to approximately 1.6 GHz bandwidth, where signal digitization is performed, followed by off-line digital signal processing.

Uplink approach with photonic downconversion

Although complex modulation formats allow for better bandwidth utilization, they require high RF power levels and a high-degree of linearity[1-3]. We therefore use an optical phase modulator at the antenna base station, see Figure 1, for transport of the multi-gigabit mm-wave signal from the antenna base station to the central office. This approach results in a simple and robust configuration as the system benefits from the inherent linearity of optical phase modulation and absence of bias voltage[4]. Optically phase modulated RoF systems require, though, a linear coherent receiver. Even though it is more complex than a conventional direct detection scheme, it offers several advantageous features such as modulation format transparent optical receiver font end, linear demodulation and linear impairment compensation by postdetection digital signal processing.

Experimental set-up

The experimental set-up for a phase modulated radio-over-fibre optical link employing PDC is shown in Fig. 1. The transmitter consists of a tuneable external cavity laser (ECL) at 1550 nm with an average output power of +10 dBm and <400 kHz linewidth. A 16-QAM signal is generated using a 15-bit arbitrary waveform generator (AWG) at 1.25 GSa/s, generating in-phase (I) and quadrature (Q) signal components. A vector signal generator (VSG) is used to perform up conversion to 40 GHz RF carrier frequency, with an output power of +16 dBm (4 V_{pp}). The VSG is used to drive an optical phase modulator (PM), with a V_{π} of 14 V at 40 GHz frequency. The optically phase modulated signal is transmitted through 40 km of standard single mode fiber (SMF) and detected using a coherent receiver, consisting of a 90° optical hybrid and two pairs of balanced photodiodes. The pulsed local oscillator (LO) is generated by gating light from a LO Continuous Wave (CW) laser source (linewidth ~100 kHz) and by applying a sinusoidal RF signal to an Electro-Absorption Modulator (EAM). The

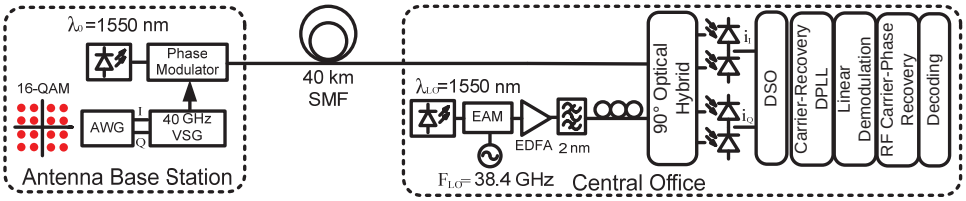

Fig. 1: Experimental set-up

wavelength of the LO CW laser source is set to 1550 nm and tuned to match the transmitter wavelength. The frequency of the applied RF signal is F_{LO}=38.4 GHz, with 18 dBm RF power and a bias voltage of 2 V in order to obtain the highest extinction ratio of the pulses. The generated optical pulses are subsequently amplified by an EDFA and thereafter filtered in order to remove amplified spontaneous emission which lies outside the signal bandwidth. The average output power of the optical pulse train is set to 0 dBm, in order to operate within the linear regime of the photodiodes of the coherent receiver. Due to the mixing process in the coherent receiver, the original data signal at 40 GHz RF carrier frequency will be downconverted to an IF frequency: $F_{IF}=F_{RF}-F_{LO}$=1.6 GHz. The output signals of the balanced photodiodes are then digitized using an 8 bits real time sampling-scope with 3 GHz analog bandwidth. The demodulation algorithms consist of carrier recovery digital PLL, linear demodulation, RF carrier phase recovery and symbol decision[4]. The frequency difference between the transmitter and LO laser, measured to be up to 1 GHz, can be successfully removed by the carrier-recovery digital PLL.

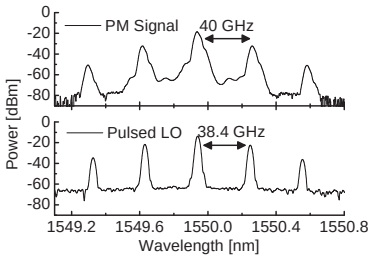

Fig. 2: Spectra of the phase-modulated (PM) signal at 40 GHz with 1 Gbit/s 16-QAM and pulsed local oscillator (LO) at 38.4 GHz.

Results

The optical spectra of the data signal and pulsed LO are shown in Figure 2. The peaks of the spectra are separated at 40 GHz for the optical data signal, and 38.4 GHz for the LO, so the resulting downconverted frequency component is at approximately 1.6 GHz. Figure 3 shows the bit-error-rate (BER) as a function of the optical signal-to-noise ratio (OSNR) for back-to-back (B2B) and after 40 km of transmission over SMF. The resulting bit-rate of the 16-QAM signal is 1 Gb/s. After fiber transmission of 40 km, we observe an ONSR penalty of only ~0.5 dB after using digital dispersion compensation. In figure 3, we also include as an inset an example of the constellation of the demodulated 16-QAM signal for 30 dB OSNR. The constellation points look clear and well separated.

In order to test the performance of the detection scheme for bitrates up to 4 Gb/s the 15-bits 1.25 GSa/s AWG is replaced with 12 GSa/s AWG

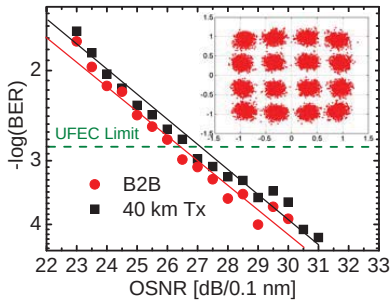

Fig. 3: BER as a function of the OSNR for back-to-back and transmission over 40 km of SMF. Top-right: Constellation of demodulated 1 Gbit/s 16-QAM at 30 dB OSNR

with 8-bits resolution. Figure 4 shows the results for the BER as a function of the increasing bitrate. For the bitrates of up to 3.2 Gbit/s, we are able to demodulate the signals with error rate below the threshold for forward error correcting coding (FEC). For the bitrates above 3.2 Gb/s, we are still able to perform signal demodulation, however, the BER is above the FEC limit, mainly due to the limited bandwidth and linearity of the I and Q mixer of the used VSG. We believe that for 1 Gbaud the signal error rate below the FEC limit could be obtained by using equalization algorithms.

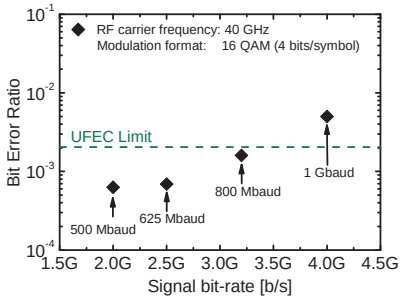

Fig. 4: BER as a function of generated bit-rate for 16-QAM modulation format at 40 GHz RF carrier frequency

Conclusions

Considering the UFEC limit of $2{\cdot}10^{-3}$, error free detection of 16-QAM signals with 40 GHz RF carrier frequency, for the total bit-rates up to 3.2 Gb/s is demonstrated. To the best of our knowledge, this is the first report on demodulation of advanced modulation formats at 40 GHz RF carrier frequency where no highly linear and complex RF electronic components are needed.

References

1 C. Lim et al., J. Opt. Netw. **8**, 201 (2009)
2 C. Weng et al., J. Lightwave Technol. **26**, 643 (2008)
3 C. Lin et al., Proc. CLEO'09, CPDA8 (2009).
4 D. Zibar et al., MTT'09, TUPF-3 (2009)

Paper 3: Digital coherent detection of multi-gigabit 40 GHz carrier frequency radio-over-fibre signals using photonic downconversion

A. Caballero, D. Zibar, and I. Tafur Monroy, "Digital coherent detection of multi-gigabit 40 GHz carrier frequency radio-over-fibre signals using photonic downconversion," *Electronics Letters*, vol. 46, no. 1, pp. 58–58, 2010.

Digital coherent detection of multi-gigabit 40 GHz carrier frequency radio-over-fibre signals using photonic downconversion

A. Caballero, D. Zibar and I. Tafur Monroy

Detection of high-speed radio signals is a challenge for next generation radio-over-fibre links, requiring high bandwidth and linearity in the receiver. By using photonic downconversion in a coherent receiver, detection of high bit-rate 16-QAM signals, up to 4 Gbit/s, at a 40 GHz carrier frequency using low bandwidth electronics, has been experimentally demonstrated.

Introduction: Currently, there is a rapid increase and interest in new radio-over-fibre (RoF) technologies capable of enabling high capacity wireless access links [1, 2]. The current trend is moving towards millimetre (mm)-wave frequencies, where complex modulation formats (QPSK, QAM [2, 3]) and multiplexing schemes such as OFDM can be used in order to reach multi-gigabit capacities. Most of the reported works so far focus on the photonic generation of multi-gigabit mm-wave signals [1–3], i.e downstream channel. However, the demodulation of signals at mm-wave frequencies still posseses many technical challenges since it requires very high-speed and linear radio-frequency (RF) electronics [1–3]. It is therefore important to overcome the limitations of detection electronics and smoothly extend the operating frequency range of RoF links to mm-wave frequencies. Additionally, the uplink direction (from the antenna base station towards the central office) presents a challenge in order to make it robust, flexible and yet with low complexity, while providing full bidirectionality and high bandwidth operation.

In this Letter, we demonstrate an uplink channel approach for detection of a multi-gigabit mm-wave radio-over-fibre signal without the need for high frequency electronics. To the best of our knowledge, this is the first report on the use of photonic downconversion for detection of 16-QAM modulation format at 40 GHz carrier frequency, with up to 4 Gbit/s data signal bit rates and digital coherent detection. Using photonic downconversion (PDC), the mm-wave signal is downconverted to approximately 1.6 GHz bandwidth, where signal digitisation is performed, followed by off-line digital signal processing.

Uplink approach with photonic downconversion: Although complex modulation formats allow for better bandwidth utilisation, they require high RF power levels and a high degree of linearity [1–3]. We therefore use an optical phase modulator at the antenna base station (see Fig. 1) for transport of the multi-gigabit mm-wave signal from the antenna base station to the central office. This approach results in a simple and robust configuration since the system benefits from the inherent linearity of optical phase modulation and absence of bias voltage [4]. Optically phase-modulated RoF systems require, though, a linear coherent receiver. Even though it is more complex than a conventional direct detection scheme, it offers several advantageous features such as a modulation format transparent optical receiver front end, linear demodulation and linear impairment compensation by post-detection digital signal processing.

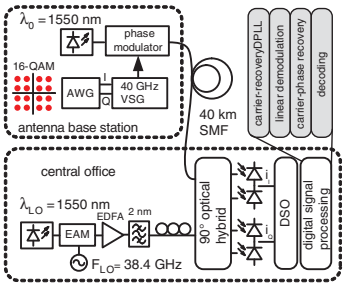

Fig. 1 *Experimental setup*

Experimental setup: The experimental setup for a phase-modulated radio-over-fibre optical link employing PDC is shown in Fig. 1. The transmitter consists of a tunable external cavity laser (ECL) at 1550 nm with average output power of +10 dBm and <250 kHz linewidth. A 16-QAM signal is generated using a 15-bit arbitrary waveform generator (AWG) at 1.25 GSa/s, generating in-phase (I) and quadrature (Q) signal components. A vector signal generator (VSG) is used to perform upconversion to 40 GHz RF carrier frequency, with output power of +16 dBm (4 Vpp). The VSG is used to drive an optical phase modulator (PM), with a $V\pi$ of 14 V at 40 GHz frequency. The optically phase-modulated signal is transmitted through 40 km of standard singlemode fibre (SMF) and detected using a coherent receiver, consisting of a 90° optical hybrid and two pairs of balanced photodiodes. The pulsed local oscillator (LO) is generated by gating light from a LO continuous-wave (CW) laser source (linewidth ~100 kHz) and by applying a sinusoidal RF signal to an electroabsorption modulator (EAM). The wavelength of the LO CW laser source is set to 1550 nm and tuned to match the transmitter wavelength. The frequency of the applied RF signal is FLO = 38.4 GHz, with 18 dBm RF power and a bias voltage of 2 V in order to obtain the highest extinction ratio of the pulses. The generated optical pulses are subsequently amplified by an EDFA and thereafter filtered to remove amplified spontaneous emission which lies outside the signal bandwidth. The average output power of the optical pulse train is set to 0 dBm, in order to operate within the linear regime of the photodiodes of the coherent receiver. Because of the mixing process in the coherent receiver, the original data signal at 40 GHz RF carrier frequency will be downconverted to an IF frequency: FIF = FRF − FLO = 1.6 GHz. The output signals of the balanced photodiodes are then digitised using an 8 bit real-time sampling-scope with 3 GHz analogue bandwidth. The demodulation algorithms consist of a carrier recovery digital PLL, linear demodulation, RF carrier phase recovery and symbol decision [4]. The frequency difference between the transmitter and LO laser, measured to be up to 1 GHz, can be successfully removed by the carrier-recovery digital PLL.

Results: The optical spectra of the data signal and pulsed LO are shown in Fig. 2. The peaks of the spectra are separated at 40 GHz for the optical data signal, and 38.4 GHz for the LO, so the resulting downconverted frequency component is at approximately 1.6 GHz. Fig. 3 shows the bit error rate (BER) against optical signal-to-noise ratio (OSNR) for back-to-back (B2B) and after 40 km of transmission over SMF. The resulting bit rate of the 16-QAM signal is 1 Gbit/s. After fibre transmission of 40 km, we observe an ONSR penalty of only 0.5 dB after using digital dispersion compensation. In Fig. 3, we also include as an inset an example of the constellation of the demodulated 16-QAM signal for 30 dB OSNR. The constellation points look clear and well separated.

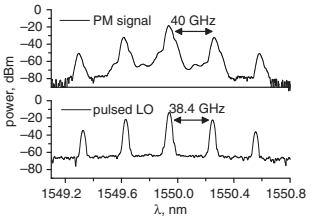

Fig. 2 *Spectra of phase-modulated (PM) signal at 40 GHz with 1 Gbit/s 16-QAM and pulsed local oscillator (LO) at 38.4 GHz*

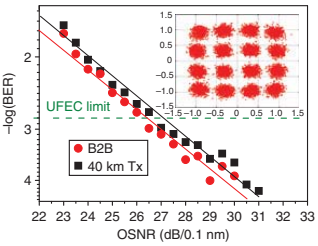

Fig. 3 *BER against OSNR for back-to-back and transmission over 40 km of SMF*

Inset: Constellation of demodulated 1 Gbit/s 16-QAM at 30 dB OSNR

To test the performance of the detection scheme for bit rates up to 4 Gbit/s the 15-bits 1.25 GSa/s AWG is replaced with a 12 GSa/s AWG with 8-bits resolution. Fig. 4 shows the results for BER against increasing bit rate. For bit rates of up to 3.2 Gbit/s, we are able to demodulate the signals with error rate below the threshold for forward error correcting coding (FEC). For bit rates above 3.2 Gbit/s, we are still able to perform signal demodulation; however, the BER is above the FEC limit, mainly due to the limited bandwidth and linearity of the I and Q mixer of the used VSG. We believe that for 1 Gbaud the signal error rate below the FEC limit could be obtained by using equalisation algorithms.

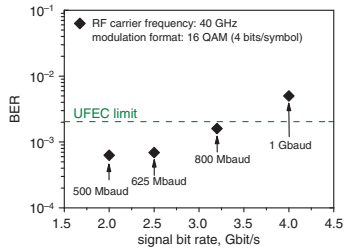

Fig. 4 *BER against generated bit rate for 16-QAM modulation format at 40 GHz RF carrier frequency*

Conclusion: Considering the UFEC limit of 2×10^{-3}, error-free detection of 16-QAM signals with 40 GHz RF carrier frequency, for total bit rates up to 3.2 Gbit/s, is demonstrated. To the best of our knowledge, this is the first report on demodulation of advanced modulation formats at 40 GHz RF carrier frequency where no highly linear and complex RF electronic components are needed.

Acknowledgments: The authors thank Yenista Optics, Tektronix and T. Jul of Nortelco Electronics, Denmark, for allowing the use of their equipment for this experiment.

8 October 2009
doi: 10.1049/el.2010.2827
One or more of the Figures in this Letter are available in colour online.

A. Caballero, D. Zibar and I. Tafur Monroy (*DTU Fotonik, Department of Photonics Engineering, Technical University of Denmark, Kgs. Lyngby, Denmark*)

E-mail: acaj@fotonik.dtu.dk

References

1 Lim, C., Nirmalathas, A., Bakaul, M., Lee, K.-L., Novak, D., and Waterhouse, R.: 'Mitigation strategy for transmission impairments in millimeter-wave radio-over-fibre networks', *J. Opt. Netw.*, 2009, **8**, pp. 201–214
2 Weng, C.-K., Lin, Y.-M., and Way, W.: 'Radio-over-fiber 16-QAM, 100-km transmission at 5 Gb/s using DSB-SC transmitter and remote heterodyne detection', *J. Lightwave Technol.*, 2008, **26**, pp. 643–653
3 Lin, C.-T., Wong, E.-Z., Jiang, W.-J., Shin, P.-T., Chen, J., and Chi, S.: '28-Gb/s 16-QAM OFDM radio-over-fibre system within 7-GHz license-free band at 60 GHz employing all-optical up-conversion'. Conf. on Lasers and Electro-Optics/Int. Quantum Electronics Conf., OSA Tech. Dig. (CD), (Optical Society of America, 2009), Baltimore, Maryland, USA, paper CPDA8
4 Zibar, D., Caballero, A., Gonzalez, N., Schaeffer, C., and Tafur Monroy, I.: 'Digital coherent receiver employing photonic downconversion for phase modulated radio-over-fibre links'. Microwave Symposium Digest, 2009. MTT '09. IEEE MTT-S Intern. Microw. Symp. Dig., Hong Kong, China, 2009, pp. 365–368

Paper 4: Performance evaluation of digital coherent receivers for phase modulated radio-over-fiber links

A. Caballero, D. Zibar, and I. Tafur Monroy, "Performance evaluation of digital coherent receivers for phase modulated radio-over-fiber links," *IEEE/OSA J. Lightw. Technol.*, accepted for publication, 2011.

Performance Evaluation of Digital Coherent Receivers for Phase Modulated Radio-over-Fiber Links

Antonio Caballero, Darko Zibar, and Idelfonso Tafur Monroy

***Abstract*—The performance of optical Phase-Modulated (PM) Radio-over-Fiber (RoF) links assisted with coherent detection and Digital Signal Processing (DSP) (PM-Coh) is analyzed and experimentally demonstrated for next generation wireless over fiber systems. PM-Coh offers high linearity for transparent transport of high frequency microwave signals, and better receiver sensitivity than Intensity Modulated with Direct Detection (IM-DD) systems. By including photonic downconversion in the PM-Coh link, in a form of a pulsed free-running LO, it is possible to receive high RF carrier frequencies, with low bandwidth electronics. Analytical assessment and simulations are used to determine the ultimate performance with respect to laser linewidth, modulation index and receiver sensitivity. Then, two different scenarios are studied and experimentally demonstrated as an application of PM-Coh links: a high capacity multi-antenna RoF system (12 subcarriers of 400 Mbit/s and 6 subcarriers of 800 Mbit/s) and photonic downconversion for the detection of high RF carriers microwave signals (up to 3.2 Gbit/s at 40 GHz).**

***Index Terms*—Distributed antenna systems, coherent detection, next generation wireless systems, radio over fiber.**

I. Introduction

RADIO over fiber (RoF) is a promising technology for next generation wireless networks. It is currently receiving large attention for the transparent optical transport of wireless signal from the Base Station (BS) to the Central Station (CS) as opposed to the current implementation of on-site demodulation and baseband transport [1], [2]. Optical transport presents several advantages over the electrical, among others higher bandwidth, longer reach and lower non-linear effects [3]. Transparent optical transport of the wireless signal allows the signal processing to be moved from the BS to the CS. The centralization of the complex equipment into a single CS and a simple BS increase placement flexibility and decrease overall cost.

The main focus on RoF links has been on IM-DD links, since they rely on already well established technology and can thereby provide low cost implementation [3], [4]. This kind of links has been studied in detail from the microwave design point of view and showed their capacity for the transport of broadband wireless signals, especially for the downlink (from CS to BS to wireless user). The design of a RoF for uplink transmission (wireless to BS to CS), has stringent requirements in dynamic range as the signal comes after wireless transmission. In Fig. 1 (top) is illustrated a basic IM-DD, where the microwave signal modulates the intensity of an optical carrier, and detected after fiber transmission with a single photodectector. Afterwards, electrical downconversion is needed, where an electrical Local Oscillator (LO) at f_{RF} is mixed with the electrical signal at f_s, resulting in a intermediate frequency $f_{IF} = f_{RF} \pm f_s$, which falls within the bandwidth of the Analogue to Digital Convertor (A/D).

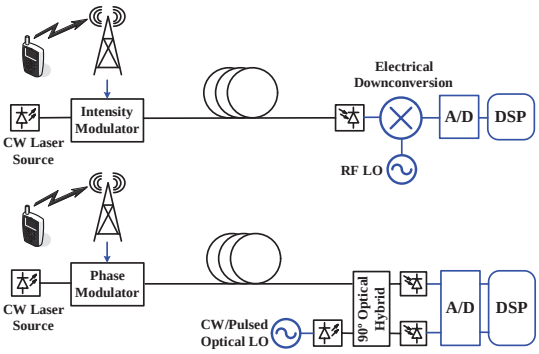

Fig. 1. Schematic description of two different types of RoF link: Intensity-Modulated and Direct Detected (IM-DD) with external optical modulation (top) and Phase-Modulated assisted with digital Coherent detection (PM-Coh) (bottom).

The IM-DD may not be the best solution, as the system needs high received optical power in order to increase the link gain, insufficient dynamic range due to the non-linear intrinsic response of the intensity modulators, and suffers from periodical RF power fading due to chromatic dispersion in the fiber propagation. More sophisticated variations of the IM-DD basic scheme has been proposed [5]–[7] in order to achieve better performance in link gain and link linearity, at the expense of complex schemes on the optical transmitter or receiver.

As an alternative, optical phase modulated RoF links has been proposed and demonstrated to offer low distortion and high linearity for the transport of high speed wireless signals [8]–[13]. The absence of a bias control makes it suitable for simple BS. However, the use of direct detection requires a careful design of the link in terms of dispersion [8] or a phase-tracking receiver [9], [10]. The use of coherent detection

A. Caballero, D. Zibar and I. Tafur Monroy are with DTU Fotonik, Department of Photonics Engineering, Technical University of Denmark, Kgs. Lyngby, Denmark, (email: acaj@fotonik.dtu.dk).

Manuscript received XX XX, 2011; revised XX XX, 2011. This work was supported in part by the Danish Research Council under grant OPSCODER.

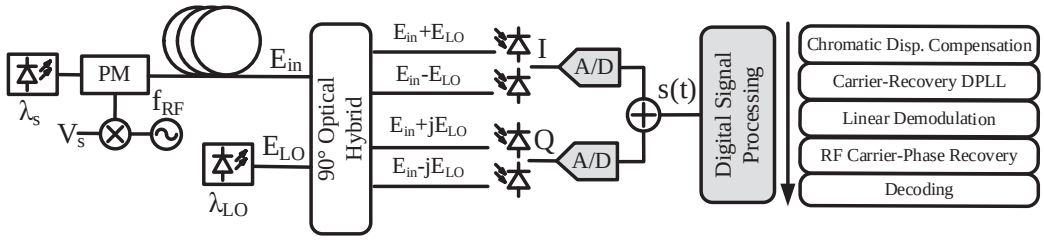

Fig. 2. Detail description of the PM-Coh RoF link, including a block diagram of the algorithms used in the demodulation.

and DSP on a phase modulated RoF signal (PM-Coh) has been demonstrated to offer advantages in dynamic range and digital demodulation by recovering the optical field using a coherent receiver, thus the phase information [11]. By using linear demodulation on the digital domain, it is possible to recover the phase of the optical field. The detection of high RF frequencies, exceeding the bandwidth of the A/D convertor, is possible by performing photonic downconversion. A second phase modulator, modulated with an RF acting as LO, realizes the downconversion to an IF in the optical domain [11]. However, the propose implementation uses homodyne coherent detection, with a single laser source, requiring a second fiber for the transport of the unmodulated optical source and careful matching of the two paths length. This architecture can be suitable for short links requiring high electrical gain and dynamic range, however it is not suitable for access networks, where the BS to CS link is implemented on a single optical fiber with lengths of few kilometers.

Our proposed solution for the integration into next generation hybrid optical-wireless networks is based on intradyne coherent detection. The implementation of the PM-Coh link uses two independent free-running lasers [12], [13]. It avoids the use of the second fiber for the transport of the reference signal, by using a second independent laser at the CS. This architecture presents benefits for the deployment due to the centralization of the more complex LO lasers at the CS and a simple antenna BS. The basic scheme is shown in Fig. 1 (bottom). The microwave signal modulates the phase of the optical carrier, using a phase modulator at BS, and transmitted through the fiber to the CS. In the detection side, an optical coherent receiver is used to recover the optical field. The recovered signal is then process in the digital domain using DSP algorithms, which can compensate transmission impairments such as fiber chromatic dispersion or beating noise from the two laser sources. It also benefits from the integration with Wavelength Division Multiplexing (WDM) Passive Optical Network (PON) networks, by the flexibility in wavelength selection given by coherent detection. Furthermore, Photonic Downconversion (PDC) can be applied in a more flexible way, by creating a pulsed LO optical source, independent from the fiber transmission link and benefiting from the high stability and low jitter of optical pulsed sources.

In this paper we analyze PM-Coh links for the transparent transport of microwave signals, using free-running independent lasers. We evaluate the capacity of the link, in terms of Error Vector Magnitude (EVM), for the transport of broadband microwave signals, for high carrier frequencies with complex modulation formats. In section II we formulate analytically the behavior of the system for continuous wave operation and for PDC. In section III, the performance is evaluated through computer simulations to determine the ultimate requirements on laser linewidths, modulation index and receiver sensitivity. In section IV we present two different scenarios where the PM-Coh link has been experimentally demonstrated.

II. Phase Modulated Radio-over-Fiber Link

A. Transmission Theoretical Model

In this section, we present our theoretical model of the PM-Coh. This analysis derives the equations for the small signal approximation case, extracting the main parameters needed for the design of the link. The scheme of the system is shown in Fig. 2. The description of the continuous wave optical carrier in terms of its optical power, frequency and phase can be written as:

$$E_{in}(t) = \sqrt{P_{in}} e^{j(\omega_0 t + \phi_{in}(t))} \tag{1}$$

Where P_{in} is the input optical power, ω_0 is the wavelength of the optical source, and ϕ_{in} is the signal phase.

The radio-frequency (RF) signal can be written as:

$$V_{RF}(t) = A_s V_s(t) cos(\omega_{RF} t) \tag{2}$$

Where $V_s(t)$ is the baseband normalized signal, A_s is the amplitude and ω_{RF} is the RF frequency. We have not considered a phase term in the RF signal.

The modulation of the optical carrier with an RF signal using a Phase Modulator can, thus be written as:

$$E_{in}(t) = \sqrt{P_{in}} e^{j(\omega_0 t + \phi_{in}(t))} e^{jmV_s(t)\cos(\omega_{RF} t)} \tag{3}$$

Where the Modulation Index (MI) is defined as:

$$m = \frac{\pi \cdot A_s}{V_\pi} \tag{4}$$

being V_π the electro-optical conversion efficiency. We can expand the second term of Eq. (3) by using the Bessel function expansion:

$$e^{jz\cos(\Theta)} = \sum_{n=-\infty}^{\infty} j^n J_n(z) e^{jn\Theta} \tag{5}$$

Applying the variable change $z(t) = mV_s(t)$ and $\Theta = \omega_{RF}t$ we get:

$$E_{in}(t) = \sqrt{P_{in}}e^{j(\omega_0 t+\phi_{in}(t))}.\sum_{n=-\infty}^{\infty} j^n J_n(mV_s(t))e^{jn\omega_{RF}t} \quad (6)$$

In the receiver side we describe the optical field of the LO light source as:

$$E_{LO}(t) = \sqrt{P_{LO}}e^{j(\omega_{LO}t+\phi_{LO}(t))} \quad (7)$$

Where ω_{LO} is the wavelength of the LO and ϕ_{LO} is its phase.

By using a 90° optical hybrid to beat the optical signal and LO, and taking the current outputs of the balanced photodiodes, $i_i(t)$ and $i_q(t)$ (neglecting shot and thermal noise), it is possible to reconstruct the phase field to form the received signal $s(t)$ as:

$$\begin{aligned} s(t) &= i_i(t) + ji_q(t) \\ &= A_r e^{j(\Delta\omega(t)+\Delta\theta(t)+mV_s(t)\cos(\omega_{RF}t))} \quad (8) \\ s(t) &= A_r e^{j(\Delta\omega(t)+\Delta\theta(t))} \\ &\quad \cdot \sum_{n=-\infty}^{\infty} j^n J_n(mV_s(t))e^{jn\omega_{RF}t} \quad (9) \end{aligned}$$

Where $\Delta\omega = \omega_0 - \omega_{LO}$, $\Delta\theta = \theta_0 - \theta_{LO}$ and $A_r = 2R\sqrt{P_{in}}\sqrt{P_{LO}}$.

A Bessel function has a Taylor expansion of the form:

$$J_n(x) = \sum_{n=0}^{\infty} \frac{(-1)^n}{m!\Gamma(m+n+1)}\left(\frac{x}{2}\right)^{2m+n} \quad (10)$$

We can consider that the main contributions of the signal are the zero ($J0$) and first ($J1$) order Bessel function, corresponding to the main and first harmonic component. This is a good approximation while the MI is low, $<< 0.1$, as shown in Fig. 3 (a), while the second order Bessel function (J2) magnitude is still negligible. The overall bandwidth of the receiver gets within ω_{RF}. Whereas for high MI, $>> 0.2$, the component at $2\omega_{RF}$ cannot be neglected and should also be considered, requiring higher signal bandwidth at the receiver side to avoid non-linear distortion [11]. The zero and first order Bessel function, with $x \ll 1$ can be expanded as:

$$J_0(x) \approx 1 - \frac{x^2}{4} \quad (11)$$

$$J_1(x) = -J_{-1}(x) \approx \frac{x}{2} \quad (12)$$

Substituting and neglecting the phase difference of the signal and LO $\Delta\theta(t)$:

$$\begin{aligned} s(t) \approx\ & A_r e^{j\Delta\omega(t)}\Big(J_0(mV_s(t)) \\ & + jJ_1(mV_s(t))e^{j\omega_{RF}t} \\ & - jJ_{-1}(mV_s(t))e^{-j\omega_{RF}t}\Big) \quad (13) \end{aligned}$$

By using the Taylor approximation of the Bessel function, we obtain:

$$\begin{aligned} s(t) \approx\ & A_r e^{j\Delta\omega(t)}\Big(1 - \frac{m^2}{4}V_s^2(t)) \\ & + j\frac{m}{2}V_s(t)e^{j\omega_{RF}t} - j\frac{m}{2}V_s(t)e^{-j\omega_{RF}t}\Big) \quad (14) \end{aligned}$$

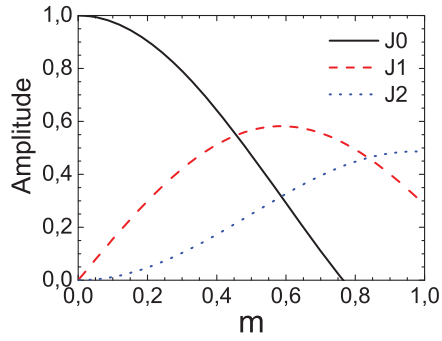

(a)

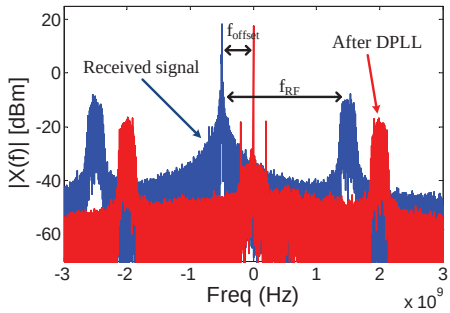

(b)

Fig. 3. (a) Magnitude of the Bessel Functions as a function of modulation index (m). For high modulation index, the carrier component(J0) decrease in power, but the second component (J2) starts being more significant. (b) Spectrum of a received signal after A/D conversion of a PM-Coh link (blue) and after compensating the frequency offset with a DPLL (red). The received signal is a 16QAM at 100 Mbaud, at 2 GHz carrier frequency (f_{RF}). The lasers have 100 kHz of linewidth and an offset between each other (f_{offset}) of 500 MHz.

The Fourier transform of Eq. (14), with $S(\omega) = \mathcal{F}(s(t))$ and $V(\omega) = \mathcal{F}(V_s(t))$ is given by:

$$\begin{aligned} S(\omega) \approx\ & A_r\Big(\delta(\omega-\Delta\omega) - \frac{m^2}{16}(V \times V(\omega-\Delta\omega)\Big) \\ & + j\frac{mA_r}{2}V(\omega-\Delta\omega-\omega_{RF}) \\ & - j\frac{mA_r}{2}V(\omega-\Delta\omega+\omega_{RF}) \quad (15) \end{aligned}$$

where $V \times V(\omega-\Delta\omega)$ is the self-convolution of the signal.

From the analysis of Eq. 15 can be extracted that there are two components in the spectrum of the PM signal. The first one, centered in $\Delta\omega$, contains the optical carrier and the self-convolution of the signal baseband spectrum, attenuated by a factor of m^2. The other terms contain the data signal, centered in $\Delta\omega \pm \omega_{RF}$. The use of high MI decrease the noise influence induced from the lasers and photodetectors, therefore its value is recommended to be maximized. However, the value should be kept within the $(-V_\pi, V_\pi)$ range, to avoid phase uncertainty of 2π multiples. Low V_π voltage modulators are necessary in order to achieve high MI with low driving RF power.

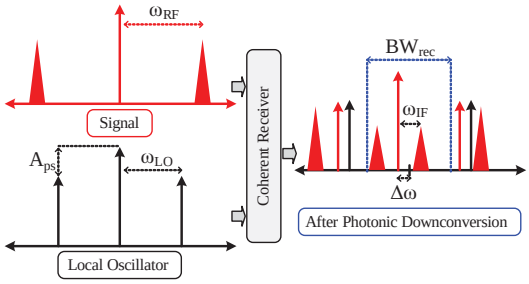

Fig. 4. Scheme for photonic downconversion, where the signal and pulsed LO are mixed in the coherent receiver, resulting in IF components,which can be detected using low-bandwidth components.

B. Digital Coherent Receiver

One of the advantages of coherent detection with digital signal processing is the capability of recovering the phase of the received optical field and compensating various impairments caused by the fiber transmission and optical components, by using DSP algorithms. Fig. 2 shows a detailed description of the PM-Coh link under consideration. After detection, the two photocurrents from the photodiodes, i_i and i_q, are digitized using a high speed D/A convertor and form a complex quantity:

$$K_{rec}(t) = I(t) + jQ(t) \tag{16}$$

The first step is the compensation of chromatic dispersion, which is a linear impairment and can be compensated in the frequency domain as:

$$H(\omega) = \exp\big(-j\frac{\beta_2}{2}L\omega^2\big) \tag{17}$$

being β_2 the second order propagation constant and L the fiber link length. From Eq. (8) it is shown that the desired signal is not at ω_{RF}, but shifted $\Delta\omega$, which should be adjusted before recovering the phase of the optical field. Therefore, the second step is removing the frequency offset between the lasers $\Delta\omega(t)$, by using a carrier-recovery Digital Phase Locked Loop (DPLL) [12], [14]. When the DPLL is locked, the frequency and phase difference between the transmitter and LO laser is removed from the input signal. High laser linewidth can be tolerated by decreasing loop filter bandwidth [12]. The signal after DPLL, $\hat{K}_{rec}$ is therefore a sampled replica of the input optical field E_{in}. The spectrum of the signal before and after DPLL can be shown in Fig. 3 (b) for a simulated PM-Coh link. It can be shown how the DPLL corrects from the frequency offset between the lasers. The RF signal imposed to the phase modulator is later on recovered using linear demodulation, by taking the phase of the recovered optical field [11]:

$$\phi_{rec}(t) = \frac{\pi \cdot V(t)}{V_\pi} = Im[ln(\hat{K}_{rec}(t))] \tag{18}$$

Finally, typical digital RF demodulation is done, consisting on frequency downconversion, carrier-phase recovery, decision and symbol mapping.

C. Photonic Downconversion

One way to extend the frequency range of digital coherent receivers beyond few GHz in PM-Coh systems is using PDC [15]–[17]. This is performed by re-modulating the received phase-modulated signal and benefits from high stability. However, by using an independent pulsed laser source as LO [13], it is possible to achieve high stable optical pulses [18]. As it is shown in Fig. 4, the LO in the receiver is a pulse source with a repetition rate ω_{LO}. After the coherent receiver, the RF signal, with a carrier frequency ω_{RF}, is transferred to an intermediate frequency (IF), $\omega_{IF} = \omega_{RF} \pm \omega_{LO}$. The sum of the maximum estimated frequency deviation of the LO from the signal frequency ω_{offset} and the IF is designed to fall within the operating range of A/D converters: $\omega_{IF} + \omega_{offset} < \omega_{A/D}$.

To a first approximation, we can model the optical sampling system as a center wavelength and two side tones, separated ω_{LO} with a difference of amplitude from the first lobe of A_{ps}. Based on Eq. (7), we can include the sampling term:

$$E_{LOs}(t) = E_{LO}(t)\big(1 + \frac{1}{A_{ps}}(e^{j\omega_{LO}t} + e^{-j\omega_{LO}t})\big) \tag{19}$$

Reformulating eq. (8) using eq.(19) we get:

$$\begin{aligned} s_s(t) &= s(t)\big(1 + \frac{1}{A_{ps}}(e^{j\omega_{LO}t} + e^{-j\omega_{LO}t})\big) \\ &= s(t) + \frac{s(t)}{A_{ps}}e^{(j\omega_{LO}t)} + \frac{s(t)}{A_{ps}}e^{(-j\omega_{LO}t)} \end{aligned} \tag{20}$$

Which has a Fourier transform given by:

$$S_s(w) = S(\omega) + \frac{S(\omega - \omega_{LO})}{A_{ps}} + \frac{S(\omega + \omega_{LO})}{A_{ps}} \tag{21}$$

The RF signal will be placed at an intermediate frequency $\omega_{IF} = \omega_{RF} - \omega_{LO}$. The receiver bandwidth needs to be $BW_{rec} < \omega_{IF} + \Delta\omega$. Neglecting the $V \times V(\omega - \Delta\omega)$ term, for low MI, from eq. (15) we get:

$$\begin{aligned} S_s(w) \approx\ & A_r\delta(\omega - \Delta\omega) + j\frac{mA_r}{2A_{ps}}V(\omega - \omega_{IF} - \Delta\omega) \\ & -j\frac{mA_r}{2A_{ps}}V(\omega - \omega_{IF} + \Delta\omega) \end{aligned} \tag{22}$$

From Eq. (22) it is also possible to extract the limitations in terms of laser linewidth for the election of ω_{RF}. As stated in [11], the IF needs to be placed away from the laser noise sideband, in order to avoid excess noise in the receiver. The gain of the PM-Coh link with PDC, related with the Continuous Wave (CW) case is:

$$G_{PMPDC} = \Big(\frac{mA_r}{2A_{ps}}\Big)^2 = \frac{G_{PMCW}}{A_{ps}^2} \tag{23}$$

The penalty in link gain from the downconversion in terms of received power is cause by the LO peak-to-side-lobe difference, given by A_{ps}. This penalty is directly related to the beating of the signal with the side-lobe peaks, with usually lower optical power than the total LO power.

In the case of photonic downconversion, we need to take into account that the dispersion value is related to ω_{RF} but the signal is centered at ω_{IF} after PDC. Therefore, in order to adequately compensate the chromatic dispersion, a factor

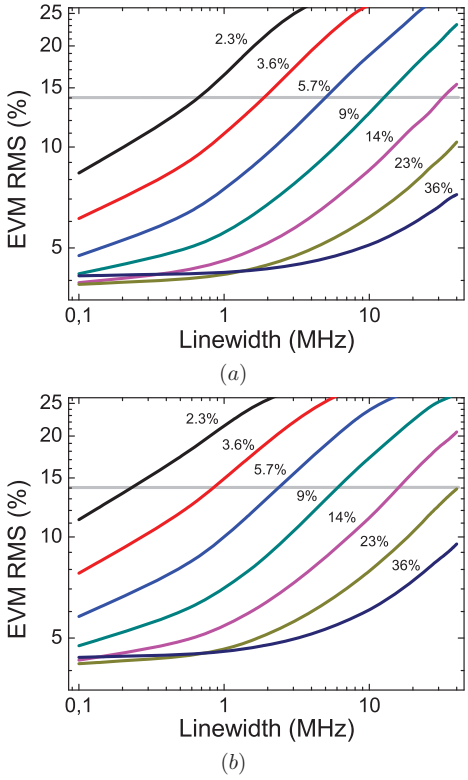

Fig. 5. Linewidth requirements for simulated PM-Coh link at (a) 100 Mbaud (b) 200 Mbaud 16QAM RF signal. $P_{rec} = -15dBm$ and $P_{LO} = -3dBm$.

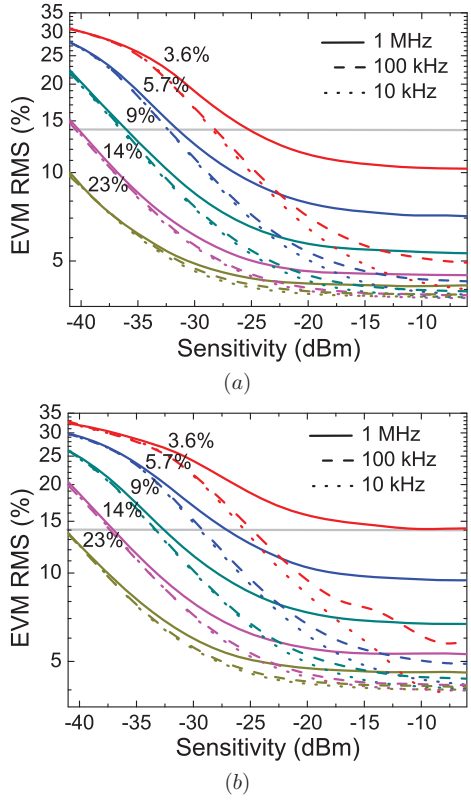

Fig. 6. Receiver sensitivity requirements for a PM-Coh link at diffeent MI and laser linewidths, for (a) 100 Mbaud (b) 200 Mbaud 16QAM RF signal.

D_c should be added to the total dispersion with the following relationship:

$$D_c = \frac{\beta_2 L \omega_{RF}}{\beta_2 L \omega_{IF}} = \frac{\omega_{RF}}{\omega_{IF}} \tag{24}$$

III. Performance Evaluation

In this section, the performance of the PM-Coh link is evaluated by characterizing the distortion on the transport of a high order modulation format (16QAM) RF signal. We have calculated the induced EVM of the demodulated signal. This measure computes the magnitude of the error vector between the ideal constellation point and the received after the transmission link. The purpose of this section is to analyze the parameters involved in the link design for a practical implementation.

The most critical design parameters for this type of systems are:

- MI of the microwave signal on the optical carrier, relating the RF input power and the V_π of the optical phase modulator.
- Laser linewidths of the transmitter and LO lasers.
- Received optical signal power.

For optical fiber access links, where the length of the link is short ($<$ 20 km), the received optical power level is not generally the main limiting factor, especially with the use of optical coherent detection. Eq. (8) formulates the different parameters of the PM-Coh link. The MI and laser linewidth are in the phase term of the optical field: $\Delta\omega(t)+\Delta\theta(t)+mV_s(t)$ where the component $\Delta\theta(t)$ is related to the lasers beating due to phase noise, m is the MI and $\Delta\omega(t)$ the difference in frequency of the transmitter and LO lasers.

The PM-Coh link described in section II has been simulated using Matlab and VPI Transmission Maker Simulation Software, emulating a single carrier RF signal at 2 GHz with a 16QAM modulation format, optically modulated in phase and transmitted over a 20 km optical fiber link. The parameters used in the simulation are gathered in Table I. The Root Mean Squared (RMS) EVM has been calculated, corresponding a BER of 10^{-3} an RMS EVM of 14%. No errors were detected for RMS EVM below 8% over 1 million bits (BER $< 1 \times 10^{-6}$).

Fig. 5 shows the effect of laser linewidth for different MI for (a) 100 Mbaud and (b) 200 Mbaud. To achieve an EVM below 8% with lasers in the range of the MHZ, MI over 9% are needed. This linewidth can easily be achieved with

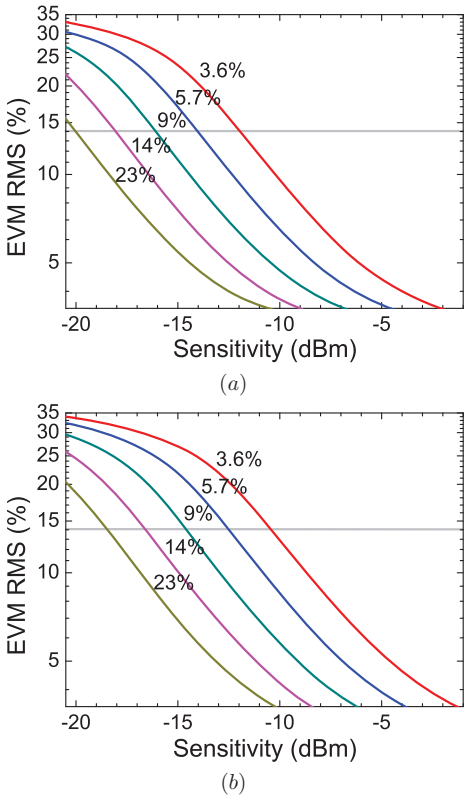

Fig. 7. Receiver sensitivity requirements for an IM-DD link at different MI for (a) 100 Mbaud (b) 200 Mbaud 16QAM RF signal.

TABLE I
SIMULATION VALUES FOR THE PM-COH LINK

Parameter	Value
Modulation type	16QAM
Baudrate	100 and 200 Mbaud
f_{RF}	2 GHz
Photodiode Bandwidth	4 GHz
modulation index	2.3% to 23%
Fiber length	20 km
Received optical power	-15 dBm
Local Oscillator optical power	-3 dBm
RMS EVM for 10^{-3}	14%
Fiber length	20 km

standard DFB lasers. However, for low MI, more stringent requirements are needed on the lasers linewidth, requiring 100 kHz linewdith lasers for MI over 3.6%. In Table II is shown the modulation index achieved with different RF power and V_π values of the modulator. Note that a reduction from 18% in MI to 7.1% in MI means 8 dB lower input RF power.

A performance comparison in terms of overall noise for the PM-Coh link versus the IM-DD can be done by evaluating

TABLE II
VALUES OF MODULATION INDEX (%) RELATED TO RF POWER AND V_π OF THE OPTICAL MODULATOR.

P_{RF} (dBm)	0	4	8	12	16
V_π = 4V	7.9	12.5	20	31.5	44
V_π = 7V	4.5	7.1	11.4	18	25.1
V_π = 11V	2.9	4.5	7.3	11.5	16

their performance with respect to the receiver sensitivity and MI. The results for 100 Mbaud and 200 Mbaud 16QAM RoF are shown in Fig. 6 for PM-Coh and in Fig. 7 for IM-DD using a Mach-Zehnder Modulator (MZM) driven in the linear region. For the case of PM-Coh, different linewidths of the laser were also simulated.

For the case of PM-Coh link at high MI conditions, the influence of the laser linewidth is minimized, being possible to achieve better receiver sensitivity. The system can achieve an EVM $< 8\%$ with received optical power of -20 dBm in a 200 Mbaud 16QAM RF signal, with a MI over 9%. On the contrary, in Fig. 6 (a) is also shown that for low MI, high received power and low linewidth are needed in order to achieve low EVM values. For example, in the case of a 100 Mbaud 16QAM, with a 1 MHz linewidth laser, it is possible to achieve EVM below 8% with a MI over 5.7% and $-20\ dBm$ received optical power. But with a 100 kHz laser, $-27\ dBm$ are needed for the same MI. However, for MI over 14% no penalty is given by the laser linewidth, requiring less than $-30\ dBm$ received optical power.

On the IM-DD link, received power needs to be over $-11\ dBm$, for 5.7% MI, 9 dB more than the PM-Coh link case, yet relaxing the requirements on laser linewidth. Hence, the PM-Coh requires lower receiver optical power than the IM-DD link, thus allowing longer fiber links. The laser linewidth are in the MHz range, which is feasible with standard DFB lasers. It also avoids the periodic power fading of the RF signal due to chromatic dispersion in IM-DD links, allowing higher flexibility in the fiber design. For links with long fiber length and low optical power budget, PM-Coh is a better option than IM-DD.

The evolution of the EVM performance of the PM-Coh link for higher bitrates is shown in Fig. 8. Low linewidth lasers are required in order to get low EVM after the transport of high bitrates signals. For laser linewidths below MHz, the MI has less influence in the system performance, as long as it is maintained over 9% of MI, like in Fig. 5 for $-15\ dBm$ sensitivity. Therefore, for the design of high capacity links in PM-Coh, lasers with $\sim 100\ kHz$ linewidth are required.

We can conclude that for the PM-Coh links, it is possible to achieve low distortion on the microwave signal transport with standard optical components. It performs better than IM-DD in terms of receiver sensitivity and requires not knowledge of the fiber link, especially critical for high RF carrier frequencies. However, it requires low linewidth lasers to achieve high capacity, yet available with current technology.

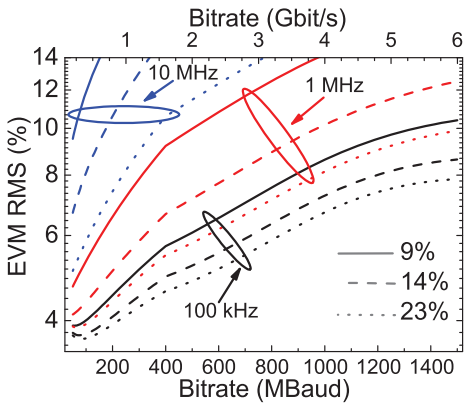

Fig. 8. Evolution of EVM as function of bitrate for different laser linewidth and modulation index in a PM-Coh link.

IV. Experimental validations

In this section, we describe different scenarios were the transparent transport of RF signals can be used and can benefit for the use of a PM-Coh link. Two of these scenarios have been experimentally demonstrated and compared with the simulations.

A. Application scenarios

Next generation wireless systems will be required to support high capacity channels with ubiquitous coverage. The requirement for high capacity implies moving towards high RF frequencies, where more spectrum is available, added to the use of advanced modulation formats in order to increase the spectral efficiency. At high RF frequencies the wireless coverage is limited due to a higher air loss, thus being necessary to increase the density of antennas per area to minimize wireless propagation losses. A solution for improved coverage is simple antenna front ends to increase flexibility in their placement, with transparent transport of the signal to/from the CS. For the uplink transmission, the centralization of the signal processing can benefit from cooperative detection, as the user data can be reconstructed by using the information from the various antenna stations [19]. When multiple RF channels are received from different antennas, they can form an aggregate channel at the BS in order to be optically transported to the CS. The multiplexing for the transparent transport can be done in the RF domain, using different Intermediate Frequency (IF) for every channel, keeping transparency while increasing bandwidth efficiency [20]. The different signals from the BS can be multiplexed in the optical domain by using WDM, where a different wavelength is assigned for each BS. On the receiver side, the optical LO wavelength of the coherent receiver can be tuned to match the assigned wavelength of the BS.

PM-Coh link detection and transparent transport of wireless signals can find application supporting several scenarios, among others:

- Ring cooperative detection
- subcarrier multiplexed PM-Coh link for distributed antenna systems
- Photonic Downconversion of high RF carriers and high speed wireless signals

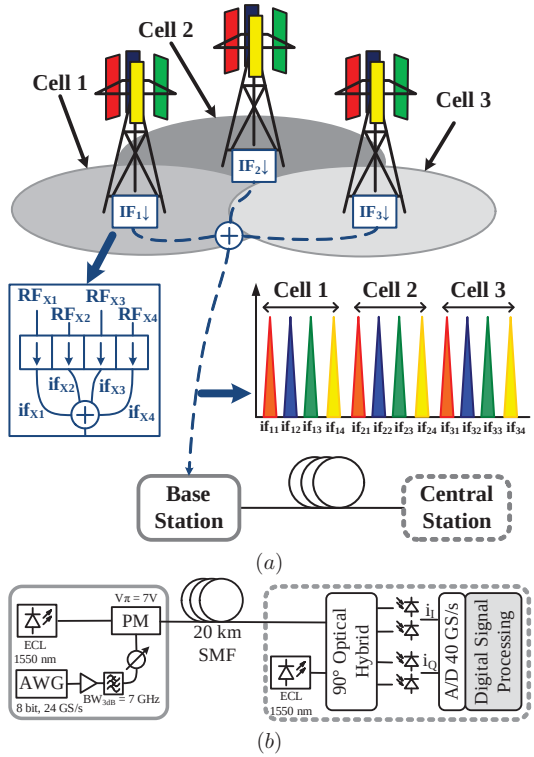

Fig. 9. (a) Scenario for the distributed antenna systems with PM-Coh link. A 3-cell group with 4 antennas/cell, which share the same frequency spectrum. The signals are then multiplexed in the electrical domain at different IF, in the antenna station, to conform a subcarrier multiplexed signal that is transported through the fiber using a PM-Coh link. (b) Experimental setup.

The scenario described in [21] presents an example of an optical fiber ring connecting multiples BS to a CS. Each BS may lie some distance away, e.g. 20 km, from the feeder fibre ring and use a specific assigned wavelength and conventional single mode fibre (SMF) while the feeder ring may use a Non-Zero Dispersion Shift Fibre (NZDSF) that in combination with Raman amplification offers low chromatic dispersion and compensation of fiber transmission loss, with enough power budget for proper detection. At the receiver side, optical coherent detection is used and WDM channel selection is performed by proper wavelength tuning of the local laser oscillator.

B. Multi-Antenna RoF System

1) Scenario: The exponential growth on the demand of high speed wireless data communications has put significant pressure on the cellular operators to improve their cellular access network capacity. Multiple-input and multiple output

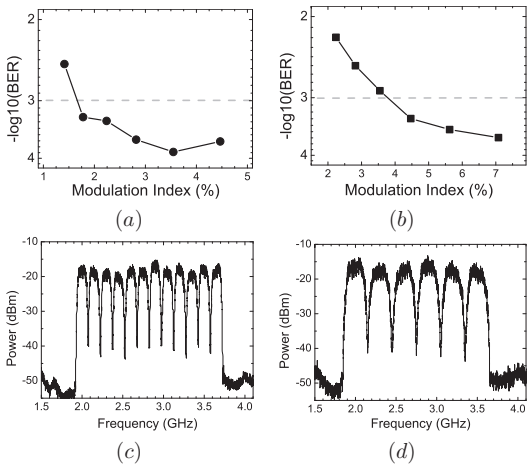

Fig. 10. Experimental averaged BER results for the multicarrier PM-Coh with (a) 12 subcarriers at 100 Mbaud and (b) 6 subcarriers at 200 Mbaud. Electrical spectra of the multicarrier signals driven to the phase modulator for (c) 12 subcarriers at 100 Mbaud and (d) 6 subcarriers at 200 Mbaud.

(MIMO) distributed antenna system (DAS) is a promising technology that can improve system capacity by mitigating inter-cell interferences (ICI) [19]. Conventional cellular base-station encode/decode RF signal independently without coordinating the transmission/reception with its neighboring cells. In MIMO-DAS, RF signals are transported from/to a baseband processing unit to/from multiple cell sites. The BS connects to the CS through a RF transport interface. Standards such as common public radio interface (CPRI) or open base-station initiatives (OBSAI) uses digital formats to represent the demodulated but not-yet decoded RF samples. The digital interface demand large backhaul bandwidth compared to their actual RF bandwidth. A 100 MHz LTE advanced system, for example, would demand an excess of 100 Gbps backhaul bandwidth. This is because digital interface requires large number of bits to describe the RF samples [22]. The use of RoF is an alternative to digitalized radio systems [2]. In order to multiplex the different wireless channels, the use of a multi-carrier IF has been proposed for efficient bandwidth utilization. RoF link with IM-DD of radio signals is a commonly used option for downlink [20].

The application of PM-Coh link for this scenario is realized in the uplink transmission, where the different antenna channels are allocated in a different IF, grouped together and modulated into a single optical carrier. Fig. 9(a) shows a possible scenario for next generation Long Term Evolution (LTE) interface, where 3 cells are connected to a Radio Equipement Controller (REC) using a single fiber link. The data from the 4 antennas at a certain cell, RF_{X1} to RF_{X4} with $X = 1, 2, 3$, is transfer to different intermediate frequencies, if_{X1} to if_{X4}, for every cell. The architecture places the subcarriers in a narrow grid to decrease the total bandwidth of the electro-optical system. The multiplexed antenna channels are then optically modulated using a phase modulator and transported over fiber backhaul. This enables the system to support the proposed point-to-multipoint architecture using also WDM for different sectors allocation. The architecture uses multicarrier IF to multiplex up to 12 high capacity wireless channels (100 Mbaud and 200 Mbaud). The required bandwidth for the multiplexed signals in the proposed architecture is decreased below 4 GHz. We have experimentally demonstrated an emulated multicarrier system, as a proof of concept for this type of architecture. It includes the transport on a single optical carrier of an emulated high capacity cell group and successful demodulation with an overall bit-rate of 4.8 Gbit/s.

2) Experimental Setup: The experimental setup is described in Fig. 9 (b). A multicarrier electrical signal was emulated using an Arbitrary Waveform Generator (AWG) (Tektronix AWG7122B) with 8-bit resolution at 24 GSa/s. This signal was created adding up 6 (3 cells of 2 antennas) or 12 (3 cells of 4 antennas) independent 16QAM modulated signals, emulating the different received information from the group of antennas. Then, this signal was amplified with a maximum RF output power of 10 dBm, driving a PM with a V_π of 7 V. A 100 kHz linewidth laser with +3 dBm output power was used at the transmitter. The optical signal was detected using a 90° optical hybrid with integrated photodiodes (7.5 GHz 3-dB bandwidth) after transmission over 22.8 km of SMF. As a LO, a low linewidth ($\sim$ 200 kHz) external cavity laser was used, with 0 dBm output power. The received optical power was set to -9 dBm in order to avoid saturation of the photodetectors. The two resultant photocurrents (In-phase (I) and Quadrature (Q)) were sampled using a high speed Digital Sampling Oscilloscope (DSO) at 40 GSa/s. Offline processing was used to demodulate the detected signal, consisting on frequency offset compensation between the transmitter laser and LO, and usual digital demodulation of the desired channel. Bit Error Rate (BER) results were obtained by averaging over all the subcarriers, as due to different electrical responses of the amplifier and modulator, each subcarrier had slightly different power.

3) Results: The results in Fig. 10 shows the experimental BER obtained for the two scenarios implemented:

- 12 subcarriers with 100 Mbaud 16QAM with 150 MHz grid spacing
- 6 subcarriers at 200 Mbaud 16QAM with 300 MHz grid spacing

resulting in a total transmitted bitrate of 4.8 Gbit/s. The performance was evaluated for different modulation indexes per subcarrier. BER below 10^{-3}, corresponding to an RMS EVM $< 14\%$, were obtained for both cases being the maximum modulation index plotted the one corresponding to 10 dBm total input power to the PM. In Fig. 11 are shown the same results with the computation of the EVM, with the error plot, in order to show the variation of the EVM between the subcarriers. This variation is due to the non-uniform power distribution of the different subcarriers, which is shown in Fig. 10 The frequency response of the amplification stage was not totally flat at high RF power levels, creating distortion on some subcarriers. A low V_π phase modulator will improve substantially the performance, by decreasing the amplification needed to drive it. In Fig. 11 are also included the simulation

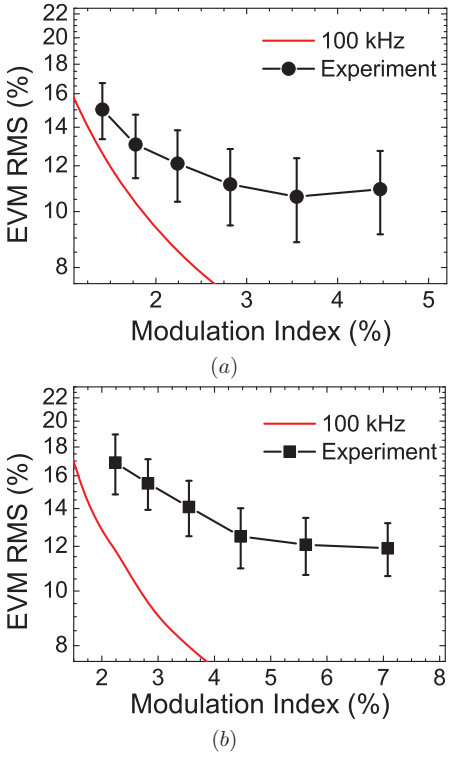

Fig. 11. Experimental EVM simulation results for the multicarrier PM-Coh for (a) 12 subcarriers at 100 Mbaud and (b) 6 subcarriers at 200 Mbaud.

results for different laser linewidths. The results are consistent with the model, however an EVM floor is present when increasing the MI, due to the non-linearities caused by the high electrical power required to drive the phase modulator.

C. Photonic Downconversion for High RF Detection

1) Scenario: The transport of high bitrate signals at mm-wave frequencies posses many technical challenges since it requires very high-speed and linear RF electronics. In this section, we experimentally demonstrate the capabilities of the PM-Coh link for the detection of multi-gigabit mm-wave radio-over-fibre signal. PM-Coh link allows a transparent transport of up to 3.2 Gbit/s 16QAM signal at 40 GHz RF frequency, over 40 km of SMF, with low end-to-end distortion [13]. On the detection side, the use of PDC avoids the need for high frequency electronics in the receiver side, decreasing the bandwdith of the A/D convertor from over 40 GHz to 3 GHz.

2) Experimental setup: The experimental set-up for a PM-Coh link employing PDC is shown in Fig. 12. The transmitter consists of a tuneable external cavity laser at 1550 nm with an average output power of +10 dBm and $< 400\ kHz$ linewidth. A 16QAM signal was generated using a 15-bit AWG at 1.25 GSa/s or a 8-bit AWG at 12 GSa/s, generating I and Q signal components. A Vector Signal Generator (VSG)

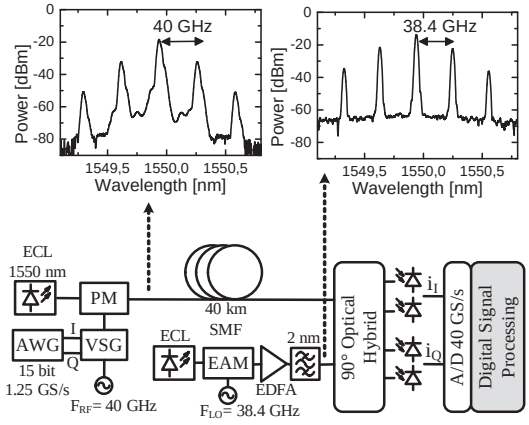

Fig. 12. Setup description for the PM-Coh link with PDC for the transport of 40 GHz RF frequency signals, including optical spectrum of the received signal and LO.

was used to perform up-conversion to 40 GHz RF carrier frequency, with an output power of +14 dBm. The VSG was used to drive an optical phase modulator, with a V_π of 14 V at 40 GHz frequency. resulting on a MI about 14%. The optically phase modulated signal was transmitted through 40 km of standard SMF and detected using a coherent receiver with 7.5 GHz 3-dB bandwidth balanced photodiodes. The pulsed LO was generated by gating light from a continuous wave laser source (linewidth 100 kHz) and by applying a sinusoidal RF signal to an Electro-Absorption Modulator. The frequency of the applied RF signal, F_{LO}, was 38.4 GHz, with 18 dBm RF power and a bias voltage of 2 V in order to obtain the highest extinction ratio of the pulses. The generated pulses had a peak-to-side-lobe difference of 12 dB. The pulses were subsequently amplified by an EDFA and thereafter filtered in order to remove amplified spontaneous emission which lies outside the signal bandwidth. The average output power of the optical pulse train was set to 0 dBm, in order to operate within the linear regime of the photodiodes of the coherent receiver. Due to the mixing process in the coherent receiver, the original data signal at 40 GHz RF carrier frequency was downconverted to an IF frequency: $\mathrm{F_{IF} = F_{RF} - F_{LO} = 1.6GHz}$ The output signals of the balanced photodiodes were then digitized using an 8 bit real time sampling-scope with 3 GHz analog bandwidth. The frequency difference between the transmitter and LO laser, measured to be up to 1 GHz, could be successfully removed by the carrier-recovery DPLL.

3) Results: The optical spectra of the data signal and pulsed LO are also included in Fig. 12. The peaks of the spectra were separated at 40 GHz for the optical data signal, and 38.4 GHz for the LO, so the resulting downconverted frequency component was at approximately 1.6 GHz. Fig. 13 (a) shows the results for the EVM as a function of the increasing bitrate. The theoretical results are also plotted for the single carrier at 2 GHz, showing the best performance possible for a MI of 14%.

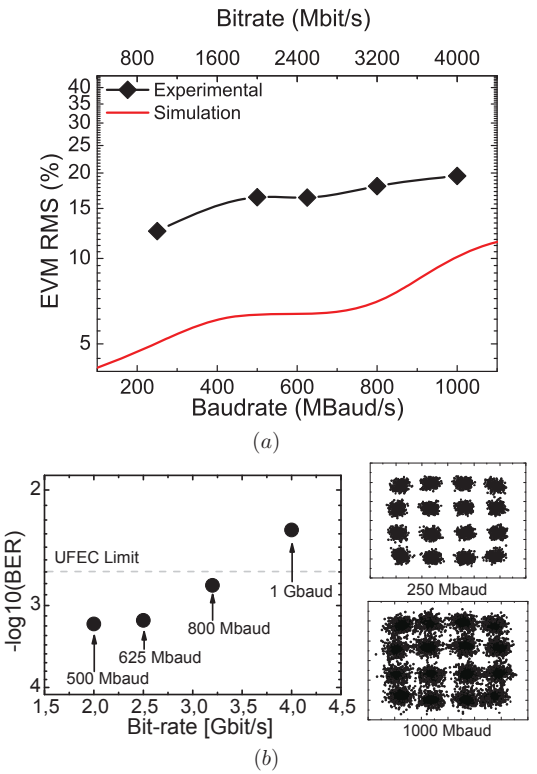

Fig. 13. Experimental results for the 40 GHz PM-Coh link using PDC to 1.6 GHz IF: (a)EVM performance, including simulation results for a 2 GHz RF system, without photonic downconversion, 200 kHz linewidth lasers and 14% MI. (b) BER results for higher bitrates, including the constellations obtained for 250 Mbaud and 1000 Mbaud.

There is a penalty from the simulations to the experimental results. The main cause is the distortion of the constellation, due to the high electrical power (14 dBm) needed to modulate the phase modulator, which has a high V_π at such a high frequency. The second is the PDC penalty in receiver sensitivity and noise. The signal components are mixed with the side-lobs of the LO that are 12 dB lower in power than the principal, creating mixing products with lower power than the pure LO. For the bitrates of up to 3.2 Gbit/s, Fig. 13 (b), we were able to demodulate the signals with error rate below the threshold for forward error correcting coding (FEC). For the bitrates above 3.2 Gb/s, we were still able to perform signal demodulation, however, the BER is above the FEC limit.

V. Conclusion

We have propose and analyzed the performance of PM-Coh links assisted with DSP, with independent free-running lasers, for the detection of high speed wireless signals. We evaluate its performance with respect to EVM induced by the optical transport of a microwave signal. PM-Coh links offer high linearity and better receiver sensitivity than IM-DD. The experimental results show the capacity of the system for transparent transport of multicarriers complex signals and high RF carriers (up to 40 GHz) broadband signals (up to 4 Gbit/s). Despite requiring a complex receiver, we have shown that high capacity links can be achieved with low linewidth lasers, in the sub-MHz range, together with low V_π modulators and low RF imput power.

Acknowledgment

The authors would like to thank Yenista optics, Tektronix and Mr. Thomas Jul of Nortelco Electronics Denmark for allowing us to use their equipment.

References

[1] J. Capmany and D. Novak, "Microwave photonics combines two worlds," *Nature Photon.*, vol. 1, pp. 319–332, 2007.
[2] D. Wake, A. Nkansah, and N. J. Gomes, "Radio over fiber link design for next generation wireless systems," *J. Lightw. Technol.*, vol. 28, no. 16, pp. 2456–2464, Aug. 2010.
[3] A. Seeds, "Microwave photonics," *IEEE Trans. Microw. Theory Tech.*, vol. 50, no. 3, pp. 877–887, Mar 2002.
[4] I. Cox, C.H., E. Ackerman, G. Betts, and J. Prince, "Limits on the performance of rf-over-fiber links and their impact on device design," *IEEE Trans. Microw. Theory Tech.*, vol. 54, no. 2, pp. 906–920, Feb. 2006.
[5] T. Kurniawan, A. Nirmalathas, C. Lim, D. Novak, and R. Waterhouse, "Performance analysis of optimized millimeter-wave fiber radio links," *IEEE Trans. Microw. Theory Tech.*, vol. 54, no. 2, pp. 921–928, 2006.
[6] J. Yao, "Microwave photonics," *J. Lightw. Technol.*, vol. 27, no. 3, pp. 314–335, Feb.1, 2009.
[7] C. Lim, A. Nirmalathas, M. Bakaul, P. Gamage, K.-L. Lee, Y. Yang, D. Novak, and R. Waterhouse, "Fiber-wireless networks and subsystem technologies," *J. Lightw. Technol.*, vol. 28, no. 4, pp. 390–405, 2010.
[8] H. Chi, X. Zou, and J. Yao, "Analytical models for phase-modulation-based microwave photonic systems with phase modulation to intensity modulation conversion using a dispersive device," *J. Lightw. Technol.*, vol. 27, no. 5, pp. 511 –521, 2009.
[9] R. Kalman, J. Fan, and L. Kazovsky, "Dynamic range of coherent analog fiber-optic links," *J. Lightw. Technol.*, vol. 12, no. 7, pp. 1263–1277, Jul 1994.
[10] Y. Li and P. Herczfeld, "Coherent pm optical link employing acp-ppll," *J. Lightw. Technol.*, vol. 27, no. 9, pp. 1086–1094, May1, 2009.
[11] T. Clark, S. O'Connor, and M. Dennis, "A phase-modulation i/q-demodulation microwave-to-digital photonic link," *IEEE Trans. Microw. Theory Tech.*, vol. 58, no. 11, pp. 3039–3058, 2010.
[12] D. Zibar, X. Yu, C. Peucheret, P. Jeppesen, and I. Monroy, "Digital coherent receiver for phase-modulated radio-over-fiber optical links," *IEEE Photon. Technol. Lett.*, vol. 21, no. 3, pp. 155–157, Feb.1, 2009.
[13] A. Caballero Jambrina, D. Zibar, and I. Tafur Monroy, "Digital coherent detection of multi-gigabit 40 ghz carrier frequency radio-over-fibre signals using photonic downconversion," *Electron. Lett.*, vol. 46, no. 1, pp. 58–58, 2010.
[14] D. Zibar, L. Johansson, H.-F. Chou, A. Ramaaswamy, M. Rodwell, and J. Bowers, "Phase-locked coherent demodulator with feedback and sampling for optically phase-modulated microwave links," *J. Lightw. Technol.*, vol. 26, no. 15, pp. 2460–2475, Aug.1, 2008.
[15] I. Kim, C. Kim, and G. Li, "Requirements for the sampling source in coherent linear sampling," *Opt. Express*, vol. 12, no. 12, pp. 2723–2730, 2004.
[16] M. Bystrom, Y. Li, N. Vacirca, P. Herczfeld, and W. Jemison, "A coherent fiber-optic link with optical-domain down-conversion and digital demodulation," *Proceedings of the 2007 International Topical Meeting on Microwave Photonics* Oct. 2007, pp. 164–167.
[17] V. R. Pagan, B. M. Haas, and T. E. Murphy, "Linearized electrooptic microwave downconversion using phase modulation and optical filtering," *Opt. Express*, vol. 19, no. 2, pp. 883–895, Jan 2011.
[18] K. Sato, A. Hirano, N. Shimizu, and I. Kotaka, "High-frequency and low-jitter optical pulse generation using semiconductor mode-locked lasers," *IEEE Trans. Microw. Theory Tech.*, vol. 47, no. 7, pp. 1251 –1256, Jul. 1999.
[19] M. Karakayali, G. Foschini, and R. Valenzuela, "Network coordination for spectrally efficient communications in cellular systems," *IEEE Wireless Commun. Mag.*, vol. 13, no. 4, pp. 56 –61, 2006.

[20] D. Wake, A. Nkansah, N. J. Gomes, G. de Valicourt, R. Brenot, M. Violas, Z. Liu, F. Ferreira, and S. Pato, "A comparison of radio over fiber link types for the support of wideband radio channels," *J. Lightw. Technol.*, vol. 28, no. 16, pp. 2416–2422, Aug. 2010.
[21] A. Caballero Jambrina, N. Guerrero Gonzalez, A. Fernandez, F. Orlando, D. Zibar, and I. Tafur Monroy, "Long reach and enhanced power budget dwdm radio-over-fibre link supported by raman amplification and coherent detection," in *Proc. ECOC'09* , 2009, Paper P6.09.
[22] C. Hoymann, L. Falconetti, and R. Gupta, "Distributed uplink signal processing of cooperating base stations based on iq sample exchange," in *Proc. ICC '09.*, 2009, pp. 1 –5.

PLACE PHOTO HERE

Antonio Caballero was born in 1985 in Zaragoza, Spain. He received the B.Sc. and M.Sc. degree in Telecommunications Engineering from Centro Politcnico Superior, Zaragoza, Spain, in 2008. He is currently pursuing a Ph.D. in optical communications engineering at DTU Fotonik, Technical University of Denmark. He was a Visiting Researcher at The Photonics and Networking Research Laboratory (PNRL) at Stanford University from February to June 2010, under supervision of Prof. Leonid G. Kazovsky. His research interests are in the area of coherent optical communications as well as high capacity radio-over-fiber links.

PLACE PHOTO HERE

Darko Zibar was born on December 9th, 1978, in Belgrade former Yugoslavia. He received the M.Sc. degree in Telecommunication in 2004 from the Technical University of Denmark and the Ph.D. degree in 2007 from the Department of Communications, Optics and Materials, COM•DTU within the field of optical communications. He was a Visiting Researcher with Optoelectronic Research Group led by Prof. John E. Bowers, at the University of California, Santa Barbara (UCSB) from January 2006 to August 2006, and January 2008 working on coherent receivers for phase-modulated analog optical links. From February 2009 until July 2009, he was Visiting Researcher with Nokia-Siemens Networks working on digital clock recovery for 112 Gb/s polarization multiplexed systems. Currently, he is employed at DTU Fotonik, Technical University of Denmark as the Assistant Professor. His research interests are in the area of coherent optical communication, with the emphasis on digital demodulation and compensation techniques.

PLACE PHOTO HERE

Idelfonso Tafur Monroy received the M.Sc. degree in multichannel telecommunications from the Bonch-Bruevitch Institute of Communications, St. Petersburg, Russia, in 1992, the Technology Licenciate degree in telecommunications theory from the Royal Institute of Technology, Stockholm, Sweden, and the Ph.D. degree from the Electrical Engineering Department, Eindhoven University of Technology, The Netherlands, in 1999. He is currently Head of the metro-access and short range communications group of the Department of Photonics Engineering, Technical University of Denmark. He was an Assistant Professor until 2006 at the Eindhoven University of Technology. Currently, he is an Associate Professor at the Technical University of Denmark. He has participated in several European research projects, including the ACTS, FP6, and FP7 frameworks (APEX, STOLAS, LSAGNE, MUFINS). At the moment, he is in involved the ICT European projects Gi-GaWaM, ALPHA, BONE, and EURO-FOS. His research interests are in hybrid optical-wireless communication systems, coherent detection technologies and digital signal processing receivers for baseband and radio-over-fiber links, optical switching, nanophotonic technologies, and systems for integrated metro and access networks, short range optical links, and communication theory.

Paper 5: Long reach and enhanced power budget DWDM radio-over-fibre link supported by Raman amplification and coherent detection

A. Caballero, N. Guerrero Gonzalez, F. Amaya, D. Zibar, and I. Tafur Monroy, "Long reach and enhanced power budget DWDM radio-over-fibre link supported by Raman amplification and coherent detection," in *Proc. 35th European Conference on Optical Communication, ECOC'09*, Vienna, Austria, 2009, paper P6.09.

Long Reach and Enhanced Power Budget DWDM Radio-over-Fibre Link Supported by Raman Amplification and Coherent Detection

A. Caballero(1), N. Guerrero (1), F. Amaya(1,2), D. Zibar(1), I. Tafur Monroy(1)

(1) Department of Photonics Engineering, Technical University of Denmark, Lyngby, Denmark,acaj@fotonik.dtu.dk
(2) GIDATI, Universidad Pontificia Bolivariana, Medellin, Colombia, foamaya@javerianacali.edu.co

Abstract We report on a scalable and enhanced power budget radio-over-fibre system for hybrid-wireless access networks operating at *12.5 GHz DWDM spacing for 5 GHz RF carriers over a* 60 km fibre link with Raman amplification**.**

Introduction

Radio-over-Fibre (RoF) transmission systems are currently finding an application in Hybrid Wireless-Optical Broadband-Access Network (WOBAN)[1].The WOBAN network provides the advantages in terms of high capacity and transparency of a Passive Optical Network (PON) with the flexibility and cost-savings of a wireless network[1,2]. However, superimposing a conventional optical intensity modulated wireless signals over a PON architecture demands careful design to accommodate required optical power budgets, optical bandwidth efficiency and overall system linearity[2]. The use of optical phase modulation for RoF systems offers several advantageous features in WOBAN, such as enhanced linearity[3,4] and absence of required driving bias in the optical Phase Modulator (ΦM). This allows for passive antenna base stations with potentially lower power consumption compared to traditional approaches. In this paper, we propose and experimentally demonstrate a RoF system addressing the challenges of power budget, spectral efficiency and linearity based on optical phase modulation and digital coherent detection. We also propose to use fibre distributed Raman amplification and its advantageous features (high OSNR, possible centralize pump location, wide spectral gain range) to extend reach and scalability of the fibre access link and benefit from the enhanced receiver sensitivity. We report on the experimental demonstration of a combined wireless and fiber link of 5 RF channels at 5 GHz carrier frequency, 250 Mbps BPSK modulated, over a 12.5 GHz spaced DWDM link.

WOBAN Scenario

Figure 1 shows the description of the considered

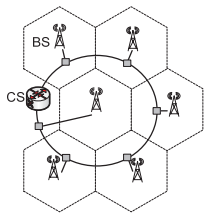

Fig. 1: Proposed WOBAN scenario

WOBAN scenario. An optical fiber ring connects multiples Base Stations (BS) to a Central Station (CS) where signal detection and demodulation take place. Each BS may lie some distance away, e.g. 20 km, from the feeder fibre ring and may use a specific assigned wavelength and conventional single mode fibre (SMF) while the feeder ring may use a Non-Zero Dispersion Shift Fibre (NZDSF) that in combination with Raman amplification offers low chromatic dispersion and compensation of transmission loss, with enough power budget for proper detection. At the receiver side, optical coherent detection is used and channel selection is performed by proper wavelength tuning of the local laser oscillator. A DSP receiver is envisaged to perform linear phase demodulation.

Setup Description

The experimental setup is shown in Fig. 2. The transmitter consists on 5 tuneable Distributed Feedback Laser (DFB) with an average output power before ΦM of +1 dBm and ~3 MHz linewidth. The wavelengths are from 1552.22 nm to 1552.62 nm, following the 12.5 GHz ITU grid spacing. A 250 Mbps BPSK is generated using an Arbitrary Waveform Generator (AWG) at 1.25 GSa/s that drives a Vector Signal Generator (VSG), which performs up conversion to the 5 GHz carrier Radio-Frequency

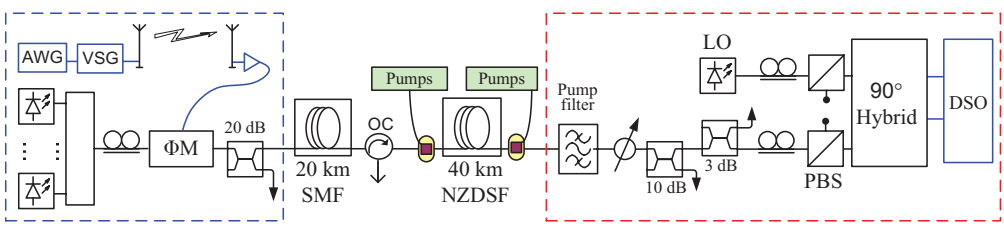

Fig. 2: Experimental setup description

978-3-8007-3173-2

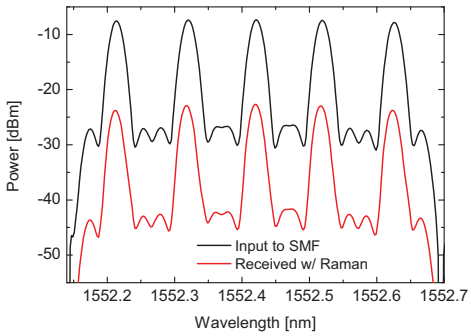

Fig. 3: Spectrum of WDM channels

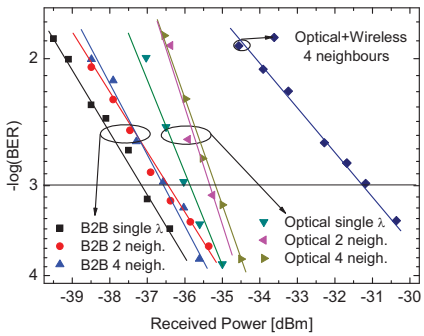

Fig. 4: BER curves for B2B, fiber transmission, fiber transmission with wireless link

(RF). The output power of the VSG is 8 dBm and it is used to drive an omnidireccional antenna with 12 dBi gain. Due to the in-door laboratory space limitations, 2 m away, another similar antenna detects the signal and, after a 37 dB gain RF amplifier, drives the ΦM with 6 dBm RF power. The optically phase modulated signal is transmitted through 20 km of SMF before entering the 40 km NZDSF feeder ring span. To compensate for the ring fiber losses, a bidirectional distributed fiber Raman amplification was employed with co pumping wavelengths at 1455 nm and 1427 nm, and counter pumping at 1463 nm. The pump powers were 200 mW, 100 mW and 240 mW respectively, with an average on-off Raman gain of 12 dB. A circulator and a wideband filter are used to reject the pumps wavelength into the transmitter and receiver, respectively. As a Local Oscillator (LO), a tunable external cavity laser is used, with ~100 kHz linewidth and 0 dBm input power to the 90° optical hybrid. Both signals are passed through Polarization Beam Splitters (PBS) so the beating of both lasers is maximized. In practice, a polarization diversity scheme or polarization tracking can also be implemented. The resultant in-phase and quadrature signals are detected with two pairs of balance photodiodes, with 7.5 GHz bandwidth. The detected photocurrents are digitalized using a sampling oscilloscope at 40 Gs/s (Agilent Infinium DSO91304A) for offline signal processing. The demodulation algorithms[4] consists on a carrier recovery digital PLL, linear demodulation for phase extraction, carrier recovery and symbol decision.

Experimental Results

The measured optical spectrum is shown in Fig. 3. For comparison purposes we relate the performance relative to the central wavelength channel (1552.42 nm) and its neighbour channels. Further, we assessed the penalty in Bit Error Rate (BER) for detecting the central wavelength alone, and for the case of simultaneous transmission of two and four neighbouring channels spaced 12.5 GHz. The BER comparison level is set to 10^{-3}, corresponding to the lower bound for Forward Error Correction (FEC) algorithms.

Fig. 4 shows the measured results for Back-to-Back (B2B), after the fiber link, with direct modulation of the ΦM from the VSG (no air link) and after 2 m wireless transmission. A penalty of 0.5 dB is incurred from single wavelength to two 12.5 GHz spaced neighbours, whereas almost no additional penalty is measured for four 12.5 GHz spaced neighbours. A penalty of only 1.5 dB is shown from B2B to 60 km fiber transmission link. We can also observe that in our experiment the main source of penalty is due to the two closest channels and not by the number of channels, indicating low or no cross phase modulation (XPM) during fibre transmission. The wireless link introduced a measured 5.5 dB penalty, however signal detection was still possible. Our DSP receiver did not include any compensation schemes to deal with signals distortions due to the wireless link nor for fibre chromatic dispersion, and therefore performance improvement is still possible.

Conclusions

We have experimentally demonstrated the first wireless and fiber link using optical phase modulation supported by coherent detection and a DSP receiver. 5 DWDM channels spaced 12.5 GHz where transmitted through the fiber, with receiver sensitivity above -30 dBm for 60 km fibre transmission, including 2 m wireless link. To compensate the attenuation of the 40 km NZDSF feeder ring distributed Raman amplification was used. This result indicates the prospects of using coherent detection and DSP for RoF links in WOBAN due to its enhanced received sensitivity, linearity and spectral efficiency.

References

1 S. Sarkar et al., J. Lightwave Technol. **25**, 3329-3332 (2007)
2 Z. Jia et al., J. Lightwave Technol. **25**, 3452-3471 (2007)
3 T. R. Clark et al., PTL **19**, 1206-1208 (2007)
4 D. Zibar et al., PTL **21**, 155-157 (2009)

Paper 6: Distributed MIMO antenna architecture for wireless-over-fiber backhaul with multicarrier optical phase modulation

A. Caballero, S. Wong, D. Zibar, L. Kazovsky and I. Tafur Monroy, "Distributed MIMO antenna architecture for wireless-over-fiber backhaul with multicarrier optical phase modulation," in *Proc. Optical Fiber Communication Conference and Exposition, OFC/NFOEC*, Los Angeles, CA, 2011, paper OWT8.

Distributed MIMO Antenna Architecture for Wireless-over-Fiber Backhaul with Multicarrier Optical Phase Modulation

Antonio Caballero[1], Shing-Wa Wong[2], Darko Zibar[1], Leonid G. Kazovsky[2], Idelfonso Tafur Monroy[1]
1. DTU Fotonik, Department of Photonics Engineering, Technical University of Denmark, Ørsteds Plads, B. 343, DK 2800 Kgs. Lyngby
email:acaj@fotonik.dtu.dk
2. Department of Electrical Engineering, Stanford University, Stanford, CA 94305, USA

Abstract: A novel optical phase-modulated wireless-over-fiber backhaul architecture for next generation cellular network is presented and experimentally demonstrated for high capacity wireless multicarrier uplink transmission on a single wavelength.
OCIS codes: (060.1660) Coherent communications; (120.5060) Phase modulation; (060.5625) Radio frequency photonics

1. Introduction

The exponential growth on the demand of high speed wireless data communications has put significant pressure on the cellular operators to improve their cellular access network capacity. Multiple-input and multiple output (MIMO) distributed antenna system (DAS) is a promising technology that can improve system capacity by mitigating inter-cell interferences [1]. In a MIMO-DAS, as shown in figure 1, RF signals are transported to a baseband processing unit (radio equipment controller, REC) from multiple cell sites (radio equipment, RE), through a RF transport interface, thus allowing communication between neighboring cells. Standards such as common public radio interface (CPRI) or open base-station initiatives (OBSAI) uses digital formats to represent the demodulated but not-yet decoded RF samples. However, they demand large backhaul bandwidth compared to their actual RF bandwidth, due to the high resolution bits needed for the digitalization process of the RF samples [2].

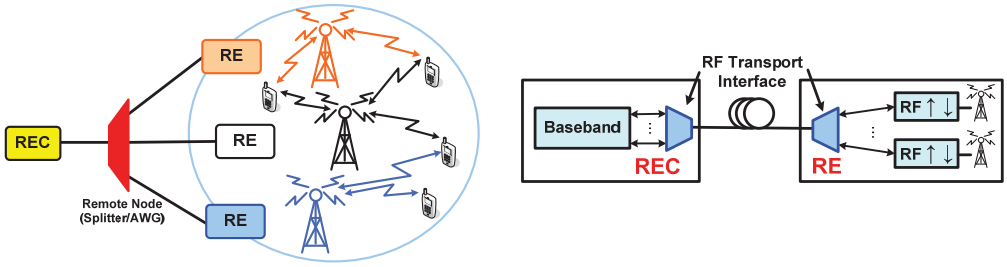

Figure 1(a): Point-to-multi-point backhaul architecture for multi-cell sites MIMO-DAS. Figure 1(b): MIMO-DAS system separates baseband unit from RF units. They are connected by RF transport interface to exchange RF IQ samples

The use of radio-over-fiber (RoF), where the analog signals are transported transparently through the optical fiber link, is an alternative to digitalized radio systems. In order to multiplex the different wireless channels, the use of a multicarrier intermediate frequency (IF) has been proposed for efficient bandwidth utilization [3]. RoF link with optical intensity modulation and direct detection (IM-DD) of radio signals is a commonly used option for downlink. However, for uplink transmission (antenna to REC), where the requirements on linearity are more stringent, the performance of IM-DD is suboptimal due to the high optical power required and limited linearity, especially for high capacity wireless links. Recently, optical phase-modulated RoF (PM-RoF) links has been proposed and demonstrated to offer both high linearity and high sensitivity for high speed wireless signals [4,5]. By using linear demodulation on the digital domain, it is possible to recover the phase of the optical field and compensate for link impairments. However, they require a second laser source as a local oscillator (LO) and a 90° optical hybrid receiver. The centralization of both components in the REC in the proposed point-to-multipoint architecture allows the system to become cost-effective for high capacity cellular backhaul.

This paper investigates the use of PM-RoF for the MIMO-DAS uplink. The architecture uses multicarrier IF to multiplex up to 12 high capacity wireless channels (100 Mbaud and 200 Mbaud). We have analyzed the requirements of the PM-RoF link in terms of laser linewidth and optical phase modulation index. Experimental demonstration of an emulated multicarrier system is reported as a proof of concept, including the transport on a single optical carrier of an emulated high capacity cell group and successful demodulation with an overall bit-rate of 4.8 Gbit/s.

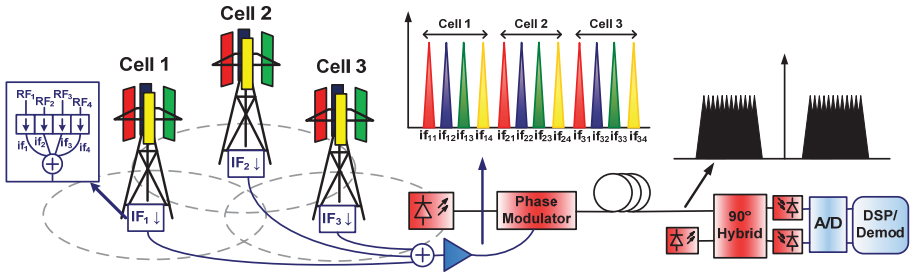

Figure 2: Proposed scenario where 3 cells of 4 antennas each are connected to a central station using an IF-ROF link. The 12 channels are electrically multiplexed in frequency in the electrical domain and transparently transported through the fiber.

2. Proposed architecture

As in MIMO-DAS uplink, received signals for all the cellular antennas occupy the same frequency range; the data from the different antennas are subcarrier multiplexed in a narrow grid, thus decreasing the total bandwidth of the electro-optical system. Figure 2 shows the proposed architecture, where the multiplexed antenna channels are then optically modulated using a phase modulator and transported over fiber backhaul to the REC. The phase of the optical carrier is recovered there using coherent detection. Transmission impairments from electrical and optical components can be compensated by digital signal processing. The required receiver sensitivity is significantly improved, making the use of optical amplification or high power laser sources unnecessary. The architecture can be easily scaled to a wavelength division multiplexed (WDM) system, using different wavelength for different groups of cells. Figure 2 also shows a possible scenario for next generation long-term evolution (LTE) interface, where 3 cells are connected to a REC using a single fiber link. Each RE has four antennas, giving a total of 12 independent channels of about 200 MHz each. The required bandwidth for the multiplexed signals in the proposed architecture is decreased below 4 GHz.

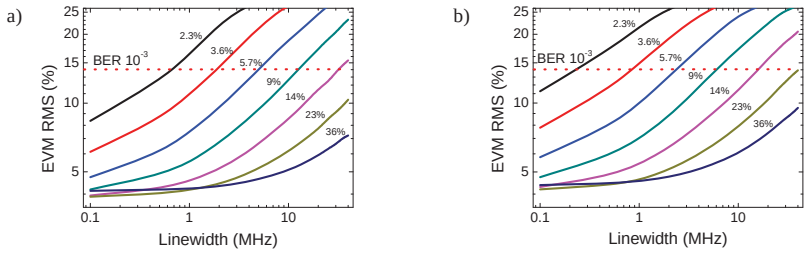

Figure 3: Error vector magnitude (EVM) at different modulation index as a function of lasers linewidth (transmitter and local oscillator equal linewidth). Transmitted single carrier 100 Mbaud (left) and 200 Mbaud (right) 16QAM RF signal over the phase-modulated optical link with 20 km SMF and coherent detection.

3. System performance requirements

The main limitations for a PM-RoF systems are the modulation index of the electrical signal and the induced phase noise due to the linewidth of the transmitter and local oscillator lasers. The received power is not the main limiting factor due to the short length of the link and the use of optical coherent detection. The use of high modulation index decrease the noise influence induced from the lasers and photodetectors, therefore its value is recommended to be as high as possible, within the ($-V_\pi$, V_π) range, to avoid phase uncertainty.

The proposed architecture has been simulated using Matlab and VPI Transmission Maker software, emulating a single carrier at 2 GHz with 100 or 200 Mbaud 16QAM over a 20 km optical phase modulated fiber link, with coherent detection. The root-mean-square error vector magnitude (RMS EVM) has been calculated, to show the induced distortion of the link for a high order modulation format. In the system, a BER of 10^{-3} is obtained with EVM of 14%. A laser linewidth value of less than 2 MHz is requested to assure low signal distortion in the link, which can be easily achievable with a standard DFB laser; as well as a modulation index over 10% per subcarrier. Therefore, low V_π voltage modulators are necessary in order to achieve high modulation index with low driving RF power.

4. Experimental results

The experimental setup is also described in figure 2. A multicarrier electrical signal was emulated using an arbitrary waveform generator (Tektronix AWG7122B) at 24GSa/s. This signal was created adding up 6 (3 cells of 2 antennas) or 12 (3 cells of 4 antennas) independent 16QAM modulated signals, emulating the different antennas. Then, this signal was amplified with a maximum RF output power of 10 dBm, driving a PM with a V_π of 7 V. A 1 MHz linewidth laser with +3 dBm output power was used at the transmitter. The optical signal was detected using a 90^o optical hybrid with integrated photodiodes (7.5 GHz bandwidth) after transmission over 22.8 km of SMF. As a LO, a low linewidth (~200 kHz) external cavity laser was used, with 0 dBm output power. The received optical power was set to -9 dBm in order to avoid saturation of the photodetectors. The two resultant photocurrents (I&Q) were sampled using a high speed digital sampling scope (DSO) at 40 GSa/s. Offline processing was used to demodulate the detected signal, consisting on frequency offset compensation between the transmitter laser and LO, and common digital demodulation of the desired channel [5]. BER results were obtained by averaging over all the subcarriers, as due to different electrical responses of the amplifier and modulator, each subcarrier had slightly different power.

Figure 4 shows the results for two considered cases: 12 subcarriers with 100 Mbaud 16QAM in 150 MHz grid spacing and 6 subcarriers at 200 Mbaud 16QAM, 300 MHz grid spacing (4.8 Gbit/s total bit-rate transmitted). The performance was evaluated for different modulation indexes per subcarrier. BER below 10^{-3}, corresponding to an RMS EVM <14%, were obtained for both cases being the maximum modulation index plotted the one corresponding to 10 dBm total input power to the PM. The frequency response of the amplification stage was not totally flat at high RF power levels, creating distortion on some subcarriers. A low V_π PM will improve substantially the performance, by decreasing the amplification needed to drive the PM.

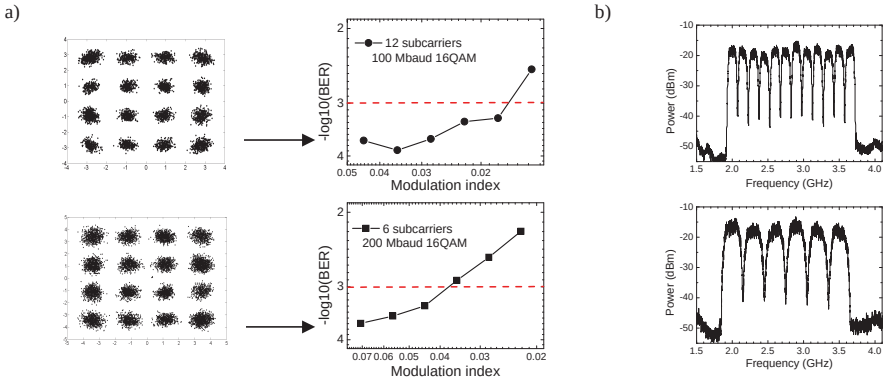

Figure 4: a) BER results as a function of the individual modulation index for 12 x 100 Mbaud 16QAM (top) and 6 x 200 Mbaud 16QAM (bottom) including constellation of the received symbols. b) Electrical spectrum of the transmitted subcarrier systems.

5. Conclusion

We have proposed and experimentally demonstrated a novel architecture for transparent transport of multiple wireless channels over a single laser source for MIMO-DAS. This architecture is highly linear and capable to support multiple users with high individual bandwidth requirements. We have reported experimental demonstration of a cellular coverage of 12x400 Mbit/s (3 cells x 4 antennas, 100 Mbaud 16QAM) and 6x800 Mbit/s (3 cells x 2 antennas, 200 Mbaud 16QAM) on a single optical carrier, showing the potential integration of the proposed architecture into the next generation cellular networks.

References

[1] M. K. Karakayali, G. J. Foschini, and R. A. Valenzuela, “Network coordination for spectraly efficient communications in cellular systems,” IEEE Wireless Communications, vol. 13, pp. 56-61, August 2006.

[2] C. Hoymann, L. Falconetti, and R. Gupta, “Distributed Uplink Signal Processing of Cooperating Base Stations based on IQ Sample Exchange,” in Proc. ICC, pp. 5, June 2009.

[3] D. Wake, A. Nkansah, and N. J. Gomes, “A Comparison of Radio Over Fiber Link Types for the Support of Wideband Radio Channels,” J. Lightwave Technol., vol 28, n. 16, August 2010

[4] T. R. Clark and M. L. Dennis, “Coherent Optical Phase-Modultion Link,” Photon. Techhnol. Lett., vol. 19, no. 6, August 2007.

[5] A. Caballero, D. Zibar and I. Tafur Monroy, “Digital coherent detection of multi-gigabit 40 GHz carrier frequency radio-over-fibre signals using photonic downconversion,” El. Letters, vol. 46, issue 1, pp. 58-59, 2010.

Paper 7: Reconfigurable digital coherent receiver for metro-access networks supporting mixed modulation formats and bit-rates

N. Guerrero Gonzalez, A. Caballero, R. Borkowski, V. Arlunno, T. T. Pham, R. Rodes, X. Zhang, M. B. Othman, K. Prince, X. Yu, J. B. Jensen, D. Zibar, and I. Tafur Monroy, "Reconfigurable digital coherent receiver for metro-access networks supporting mixed modulation formats and bit-rates," in *Proc. Optical Fiber Communication Conference and Exposition, OFC/NFOEC*, Los Angeles, CA, 2011, paper OMW7.

Reconfigurable Digital Coherent Receiver for Metro-Access Networks Supporting Mixed Modulation Formats and Bit-rates

Neil Guerrero Gonzalez, Antonio Caballero Jambrina, Robert Borkowski, Valeria Arlunno, Tien Thang Pham, Roberto Rodes, Xu Zhang, Maisara Binti Othman, Kamau Prince, Xianbin Yu, Jesper Bevensee Jensen, Darko Zibar, and Idelfonso Tafur Monroy

DTU Fotonik, Department of Photonics Engineering, Technical University of Denmark, DK-2800 Kgs. Lyngby, Denmark.
nggo@fotonik.dtu.dk.

Abstract: Single reconfigurable DSP coherent receiver is experimentally demonstrated for mixed-format and bit-rates including QPSK, OFDM, IR-UWB for wireline and wireless signal types. Successful transmission over a deployed fiber link is achieved.
OCIS codes: (060.1660) Coherent communications, (120.5060) Phase modulation

1. Introduction:

Next generation metro-access networks will need to support diverse broadband services including converged wireless and wireline optical access over a unified fiber platform, satisfying bandwidth requirements [1] as well as fulfilling stringent power budget and chromatic dispersion constrains [2]. Another important attribute of future metro-access networks is agile re-configurability to seamlessly accommodate for emerging new services and increased bandwidth requirements [1]. Furthermore, the introduction of mixed modulation formats, bit-mixed rates, support for burst mode transmission into the metro-access networking scenario is creating a highly heterogeneous environment that represents a new challenge to tackle in the near future. Approaches looking for solutions to one or more of the above issues are radio-over-fiber systems for integrating baseband and wireless service delivery over optical fiber access networks [3]. Another approach is developing multi-rate receivers for optical network units (ONUs) from 2.5 Gbit/s-40 Gbit/s to accommodate for mixed bit-rate or service bit-rate on demand [4]. Another promising approach proposed recently is coherent detection based passive optical networks to support closely spaced channels with increased receiver sensitivity to cope with the required large number of users and to extend the reach of metro-access networks [5]. Although experimental demonstrations of converged service delivery have been reported in the literature [2, 3] they use a dedicated receiver for each modulation or bit-rate. In this paper we present and experimentally demonstrate a single, reconfigurable, digital receiver supporting mixed modulation formats, baseband and wireless-over-fiber, with reconfiguration in the digital signal processing domain. We successfully demonstrate its operation for 20 Gbps non-return-to-zero quadrature phase-shift keying (NRZ-QPSK), optically phase-modulated 5 GHz OFDM radio-over-fiber and 2 Gbps impulse radio ultrawideband (IR-UWB), and 5 Gbps directly modulated vertical cavity surface emitting laser (VCSEL) after 78 km of deployed fiber link.

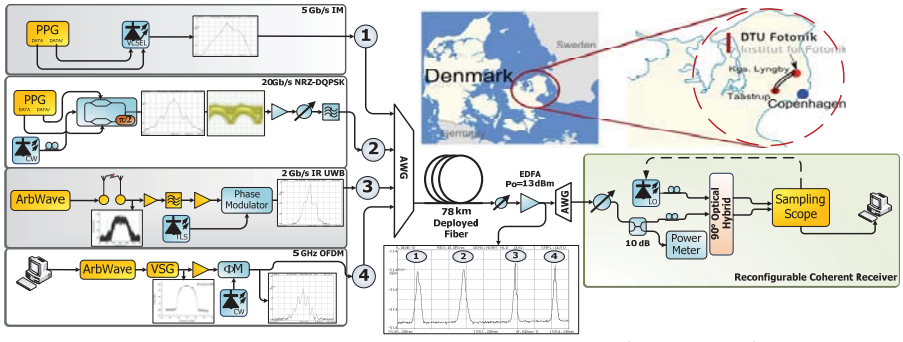

Fig.1 Experiment layout, showing optical and electrical RF spectra at key points; route of installed optical fiber are also shown. Reconfigurable receiver construction allows local oscillator (LO) tuning for channel selection. PPG: pulse pattern generator; ArbWave: arbitrary waveform; VSG: vector signal generator.

2. System description

Fig. 1 shows a block diagram of the heterogeneous optical network and setup used in the experiment. The field-deployed fiber connects the Kgs. Lyngby campus of the Technical University of Denmark (DTU) and the Taastrup suburb of Copenhagen. The fiber is a G.652 standard single-mode fiber (SMF) type (16.5 ps/nm km chromatic dispersion, 0.20 dB/km attenuation). The total link loss was 27 dB. ITU standard operating wavelengths were used for all channels at 200 GHz separation due to equipment availability. Total launch power into the deployed fiber was kept to +4 dBm. At the receiver side, emulating the central office, an erbium doped fiber amplifier (EDFA) was used as preamplifier followed by an optical bandpass filter to reduced ASE noise. The optical power level to the receiver was set to -11 dBm. A tunable external cavity laser was used as local oscillator (LO) for all the received signal types; with a linewidth of 100 kHz. The in-phase and quadrature signals after the 90° optical hybrid were detected with two pairs of balanced photodiodes, having full width at half maximum bandwidth of 7.5 GHz. The detected photocurrents were digitized using a sampling oscilloscope at 40 GSa/s for offline processing. The employed single digital receiver used a digital dispersion compensation module followed by an optical carrier-recovery digital phase-locked loop (PLL) and linear signal demodulation [6] for phase-modulated OFDM and IR-UWB RoF subsystems. Instead of a DPLL, a frequency offset compensation module was used for the NRZ-QPSK optical signal. Reconfiguration for each modulation format was performed by digitally switching between the signal demodulation DSP blocks. Below we present the set-up for each of the signal formats considered.

Gbps Intensity-modulated VCSEL: a pulse pattern generator (PPG) at 5 Gbps directly modulated a 1550 nm VCSEL. Single drive configuration was used for the VCSEL with a driving peak-peak voltage of 1 V. A pseudo random binary sequence (PRBS) with a length of 2^{15}-1 was used for this experiment. The bias current of the VCSEL was used to tune the wavelength to the assigned AWG channel. Bias current was set to 14 mA. The output power of the VCSEL launched into the fiber was measured to be 0.5 dBm.

20 Gbps QPSK baseband: the transmitter of the baseband QPSK subsystem included a PPG to providing a PRBS (215-1) and a MZ modulator to generate a QPSK signal at the wavelength of 1550.5 nm. The value of the signal laser linewidth was 2 MHz.

2 Gbps phase-modulated IR-UWB: an Arbitrary Waveform Generator (AWG) with 24 GSa/s sampling rate was utilized to program a 5th order derivative Gaussian pulse for good compliance with FCC mask [7]. A PRBS with a word length of 2^{11}-1 with bipolar modulation at a bit rate of 2 Gbps was used. The UWB signal was transmitted using a Skycross omni-directional antenna (SMT-3TO10M-A, 0dBi gain) and received after 1 m wireless transmission by a Geozondas directive antenna (AU-3.1G10.6G-1, from +4.65 dBi to +12.4 dBi gain within the UWB frequency range). The received signal was amplified by a low noise amplifier, filtered by a high-pass filter and then amplified again to drive the optical phase modulator. The wavelength of this channel was set at 1552.54 nm. The DSP algorithm in the receiver side included matched filtering and a decision block.

5 GHz OFDM RoF: the OFDM baseband signal was generated in software using a 2^{15}-1 PRBS as input data stream. 256 4-QAM subcarriers were used with 26 samples (10%) cyclic prefix per OFDM symbol. The OFDM frame is composed of two Schmidl training symbols [8] followed by eight data symbols. The signal was fed to an AWG with a 1.25 GSa/s rate which results in a bit rate of 500 Mbps. The signal is then upconverted to a frequency of 5 GHz using a free-running Vector Signal Generator (VSG) whose output is amplified to drive an optical phase modulator supplied with a continuous wave (CW) light at 1553.78 nm. At the receiver, the DSP algorithm implemented a digital PLL, timing offset estimation using a smoothed Schmidl timing metric followed by a carrier frequency offset estimation [8]. The training sequence enabled equalization of each OFDM sub-channel.

3. Results

To demonstrate the performance of our reconfigurable digital coherent receiver, we show in Fig. 2 the measured bit error rate (BER) curves for back-to-back (B2B) and after 78 km of deployed fiber transmission (considering both single and all simultaneous channel performance) as a function of the received optical power. For all four subsystems, a BER value below 10^{-3} (FEC threshold) is achieved for all considered scenarios. **5 Gbps coherently detected, intensity-modulated VCSEL:** as we can see in Fig. 2(a), the VCSEL coherently detected subsystem achieves a sensitivity of -24 dBm for both B2B and 78 km deployed fiber. Chromatic dispersion was completely compensated by DSP, and no penalty was appreciated compared with the B2B case. **20 Gbps QPSK baseband:** Fig. 2(b) shows that fiber transmission incurred 1 dB power penalty (at 10^{-3} BER) difference. Moreover in the simultaneous presence of the other three channels, there was an observable 0.5 dB penalty both for back to back and after transmission; however the reconfigurable receiver showed successful operation.

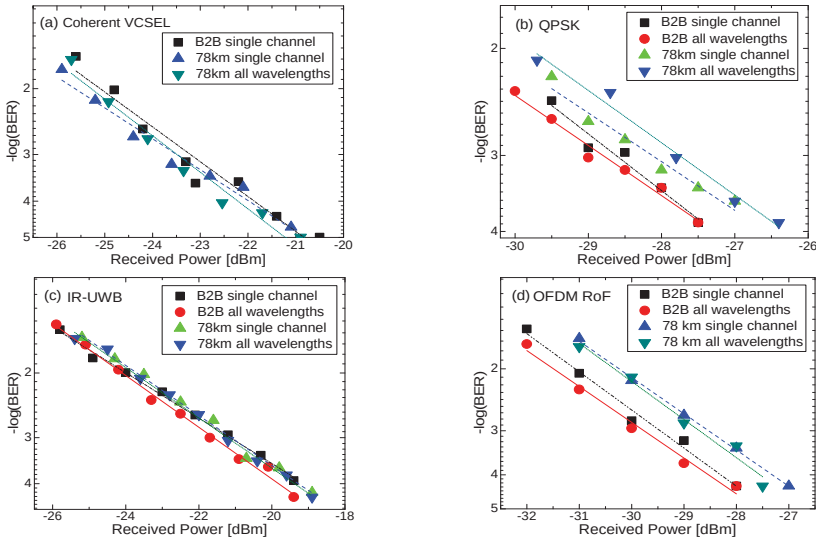

Fig.2 Measured BER performances for (a) 5 Gbps intensity-modulated VCSEL, (b) 20 Gbps QPSK baseband, (c) 2 Gbps phase-modulated IR-UWB, and (d) 5 GHz OFDM RoF.

2 Gbps phase-modulated IR-UWB: as shown in Fig. 2(c) the measured BER performances of the UWB subsystem were consistent for all cases. Errors occurred when the received optical power was less than -21.5 dBm. The BER performance is below the FEC limit when the received power was higher than -23 dBm. **5 GHz OFDM RoF:** Fig. 2(d) shows that for the case of four simultaneously integrated channels, OFDM suffered nearly 0.5 dB of power penalty, for both B2B and 78 km fiber transmission compared to single OFDM channel transmission yielding a receiver sensitivity at a BER of 10^{-4} of 28 dBm for the B2B system, and -27.5 dBm for the 78 km optical transmission link, respectively. The reconfigurable receiver showed stable operation for the 4-QAM OFDM RoF subsystem.

4. Conclusions

A single reconfigurable DSP enabled coherent receiver is experimentally demonstrated for mixed modulation formats and bit rates. In our reported experiment, four different types of wireline and wireless services including 20 Gbps QPSK baseband, 5Gbps OOK, 5 GHz OFDM RoF and 2 Gbps IR-UWB are successfully demodulated after transmission over 78 km deployed fiber link. The receiver used the same optical front-end, is able to switch among baseband and wireless types of signals by DSP reconfiguring to baseband only. This demonstrated digital reconfigurable coherent receiver has potential to enable unified support for signal detection on highly heterogeneous next generation metro- access networks.

5. References

[1]. K, Sato and H. Hasegawa, “Optical Networking Technologies That Will Create Future Bandwidth Abundant Networks”, JOCN **1**, 81-83 (2009).

[2]. K. Prince, J. B. Jensen, A. Caballero, X. Yu, T. B. Gibbon, D. Zibar, N. Guerrero, A. V. Osadchiy, and I. Tafur Monroy, “Converged Wireline and Wireless Access Over a 78-km Deployed Fiber Long-Reach WDM PON”, PTL **21**, 1274-1276, (2009).

[3]. M. Popov, “The Convergence of Wired and Wireless Services Delivery in Access and Home Networks”, in Proc. OFC (San Diego, CA 2010), paper OWQ6.

[4]. H. Kimura, Y. Sakai, N. IIyama and K. Kumozaki, “Service Rate Matching Optical Receiver Module with Bit Rates Over 40Gb/s for PS-based WDM PON Systems”, in Proc. LEOS (Newport Beach, CA 2008), pp. 669-70.

[5]. H. Rohde, S. Smolorz, E. Gottwald and K. Kloppe, “Next Generation Optical Access: 1 Gbit/s for Everyone”, in Proc. ECOC (Vienna, Austria 2009), paper 10.5.5

[6]. D. Zibar, X. Yu, C. Peucheret, P. Jeppesen and I. Tafur Monroy, “Digital Coherent Receiver for Phase-Modulated Radio-Over-Fiber Optical Links”, PTL **21**, 155-157 (2009).

[7]. X. Yu, T. B. Gibbon, M. Pawlik, S. Blaaberg, and I. Tafur Monroy, “A Photonic Ultra-Wideband Pulse Generator Based on Relaxation Oscillations of a Semiconductor Laser”, Optics Express **17**, 9680-9687 (2009).

[8]. T. Schmidt and D. Cox, “Robust Frequency and Timing Synchronization for OFDM”, IEEE Trans Commun **45**, 1613-1621. (1997).

Paper 8: Radio-frequency transparent demodulation for broadband hybrid wireless-optical links

D. Zibar, R. Sambaraju, R. Alemany, A. Caballero, J. Herrera, and I. Tafur Monroy, "Radio-frequency transparent demodulation for broadband hybrid wireless-optical links," *IEEE Photon. Technol. Lett.*, vol. 22, no. 11, pp. 784–786, 2010.

Radio-Frequency Transparent Demodulation for Broadband Hybrid Wireless-Optical Links

Darko Zibar, Rakesh Sambaraju, Ruben Alemany, Antonio Caballero, Javier Herrera, and Idelfonso T. Monroy

***Abstract*—A novel demodulation technique which is transparent to radio-frequency (RF) carrier frequency is presented and experimentally demonstrated for multigigabit wireless signals. The presented demodulation technique employs optical single-sideband filtering, coherent detection, and baseband digital signal processing. Multigigabit wireless signal demodulation of 1.25-Gbaud quadrature phase-shift-keying modulated data at 40- and 35-GHz RF carrier frequency is experimentally demonstrated using the proposed demodulation scheme.**

***Index Terms*—Coherent communication, digital receivers, digital signal processing, microwave photonics, modulation.**

I. Introduction

THE increase in the data capacity demand is pushing the development of multigigabit wireless systems. Currently, there is much research effort underway in order to develop multigigabit wireless systems addressing applications like local area network (LAN) bridging, interbuilding communications, mobile backhaul, etc. [1]–[3]. Several frequency bands in the millimeter-wave frequency regime (60, 70/80, $>$100 GHz, etc.) have a few gigahertz of available bandwidth, which could potentially enable gigabit wireless transmissions. However, in order to achieve multigigabit capacity in the limited available millimeter-wave bandwidth, spectrally efficient modulation formats like quadrature phase-shift-keying (QPSK) and M-quadrature amplitude modulation (QAM) are required. Radio-frequency (RF)-over-fiber technologies [3] provide a good solution for generation and transport of wireless signals. Wireless signal generation with the bit rate up to 10 Gb/s, has been generated using on–off keying and spectral efficient QAM modulation [2], [5]. However, the detection of these vector modulated multigigabit signals using conventional electrical methods becomes complicated when the bit rate increases and RF carrier frequency approaches millimeter-wave frequencies. Recently, several photonic techniques for demodulation of M-QAM signals have been proposed ([4], [5] and references therein), but they still require relatively complex high-bandwidth analog phase-locked-loop and RF components. Additionally, digital coherent receiver structures have also been proposed for RF-over-fiber links [6], [7]. Although, the demonstrated digital coherent techniques do not require electronic or optical phase-locked loops, they still require electronics such as analog-to-digital (A/D) converters or signal sources at high RF carrier frequencies [8]. In this letter, we consider the optical link between the remote antenna unit and the central station for the delivery of high RF carrier frequency broadband wireless signals. We present a novel technique for demodulation of high-frequency multigigabit RF signals using coherent detection and baseband digital signal processing. The advantage of the proposed technique is that it is transparent to RF carrier frequency and only requires A/D converters at the baseband/data rate frequency. In order to demonstrate the RF frequency transparency, demodulation of 2.5-Gb/s QPSK modulated data signal, at 40- and 35-GHz RF carrier frequency, is experimentally demonstrated. To the best of our knowledge, this is the first experimental demonstration where a combination of optical single-sideband filtering, coherent detection, and baseband digital signal processing is employed for fiber transport and subsequent demodulation of high RF carrier frequency, phase-shift-keyed modulated wireless signals. It is this unique combination that makes our proposed technique transparent to the RF carrier frequency as well as broadband.

Manuscript received January 06, 2010; revised February 16, 2010; accepted March 07, 2010. Date of publication March 18, 2010; date of current version May 07, 2010. This work has been supported by the European Commission FP7 under Network of Excellence project EUROFOS (22402).

D. Zibar, A. Caballero, and I. T. Monroy are with DTU Fotonik, Department of Photonics Engineering, Technical University of Denmark, Kgs. Lyngby, DK-2800, Denmark (e-mail: dazi@fotonik.dtu.dk; dz@com.dtu.dk; acaj@fotonik.dtu.dk; idtm@fotonik.dtu.dk).

R. Sambaraju, R. Alemany, and J. Herrera are with Valencia Nanophotonics Technology Center, Universidad Politécnica de Valencia, 46022 Valencia, Spain (e-mail: rsambaraju@ntc.upv.es; ralemany@ntc.upv.es; jherrera@ntc.upv.es).

Color versions of one or more of the figures in this letter are available online at http://ieeexplore.ieee.org.

Digital Object Identifier 10.1109/LPT.2010.2045752

II. Experimental setup and Digital Coherent Demodulation

The schematic of the experimental setup is shown in Fig. 1. The system incorporates fiber to attain a simplified remote antenna base station and thereby locate all the signal processing parts at the central station. The idea is to keep the remote antenna station as simple as possible [3]. In order to emulate the received RF signal at the remote antenna station, a pattern generator is used to generate in-phase and quadrature components of the 1.25-Gbaud QPSK data signal which are then up-converted to an RF carrier frequency of $f_{\mathrm{RF}} = 40$ GHz by a vector signal generator. The electrical power of the QPSK modulated RF signal was set to $+2$ dBm. An optical carrier at the wavelength of $\lambda_1 = 1554.68$ nm generated from an external cavity tunable laser (TLS) was amplitude modulated with the 1.25-Gbaud QPSK modulated data signal at the 40-GHz RF carrier frequency using a Mach–Zehnder modulator (MZM) biased at the quadrature point. The output of the MZM consists of the optical carrier at $\lambda_1 = 1554.68$ nm, and two sidebands, at $\lambda_1 - \lambda_{\mathrm{RF}} = 1554.36$ nm and $\lambda_1 + \lambda_{\mathrm{RF}} = 1555.0$ nm, each modulated with 1.25-Gbaud QPSK data and separated by

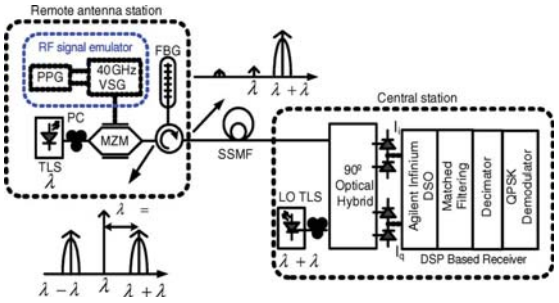

Fig. 1. General outline for the experimental setup for demonstration of RF transparent demodulation of multigigabit RF-over-fiber link. PPG: pulse pattern generator; VSG: vector signal generator; FBG: fiber Bragg grating; MZM: Mach–Zehnder modulator; PC: polarization controller; TLS: tunable laser source; LO: local oscillator; λ_1: wavelength of the TLS; $\lambda_1 + \lambda_{\rm RF}$: wavelength of the LO TLS; $f_{\rm RF}$: RF carrier frequency of the signal from VSG.

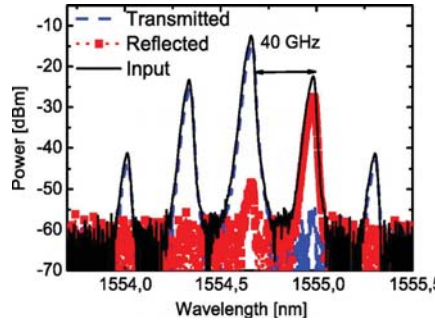

Fig. 2. Optical spectrum of the input signal to the FBG, and reflected and transmitted optical signal through the FBG.

40 GHz/0.32 nm from λ_1 (see Fig. 1). The main idea behind our approach is now to filter out one of the sidebands of the modulated optical carrier ($\lambda_1 + \lambda_{\rm RF}$ or $\lambda_1 - \lambda_{\rm RF}$), and in this way only transmit baseband data making this scheme RF carrier frequency independent, and also dispersion tolerant since only the baseband data is transmitted. This is illustrated in Fig. 1. To filter out the sideband at $\lambda_1 + \lambda_{\rm RF} = 1555.0$ nm, a fiber Bragg grating (FBG) centered at $\lambda_1 + \lambda_{\rm RF} = 1555.0$ nm with an optical bandwidth of 25 GHz is used in combination with an optical circulator. The reflected signal from the FBG at the wavelength $\lambda_1 + \lambda_{\rm RF} = 1555.0$ nm which is then sent to the receiver contains purely 2.5-Gb/s QPSK data modulation. The optical data signal at $\lambda_1 + \lambda_{\rm RF} = 1555.0$ nm, carrying 2.5 Gb/s of QPSK data, is then transmitted over a 26-km standard single-mode fiber (SMF) prior to coherent detection, which only requires baseband signal processing at twice the data rate. At the receiver, an optical local oscillator (LO) signal, generated from another tunable external cavity laser (~100-kHz linewidth), and with the wavelength approximately set to $\lambda_1 + \lambda_{\rm RF} = 1550.0$ nm is mixed with the filtered sideband carrying 2.5-Gb/s QPSK data in the 90° optical hybrid. We have a polarization controller after the LO laser output so that the polarization of the LO optical signal is manually aligned to maximize the power input to the optical hybrid. In practice, a polarization diversity scheme or polarization tracking could be employed. The in-phase I_i and quadrature I_q optical components are detected using two pairs of balanced photodiodes (BW 7.5 GHz), which were inbuilt in the optical 90° optical hybrid. The photodetected signals were then digitized using a high bandwidth real-time oscilloscope. The digitized signals $I_i[k]$ and $I_q[k]$, where k is an integer, are later used for offline digital signal processing consisting of matched filtering, decimation, and a QPSK demodulation module. The matched filter is a finite impulse response (FIR) raised cosine filter and is used to maximize the signal-to-noise ratio of the detected signal. The decimator down-samples the digitized signals $I_i[k]$ and $I_q[k]$ to one sample per bit prior to QPSK demodulation block. The QPSK demodulation block is a decision directed feedback structure which removes phase and frequency offset between the transmitter and LO laser and, thereby, performs QPSK data signal demodulation [9]. The frequency offset between the transmitter laser and the LO may approach up to 500 MHz, making its removal quite challenging by using conventional digital estimation methods like Viterbi & Viterbi, for which frequency offset values up to approximately 10% of the baud rate can be tolerated [9]. Therefore, we use a feedback structure employing a digital phasor-locked loop such that frequency offset values up to 500 MHz can be removed by optimizing the loop bandwidth and still keeping the loop stable. Since the power of the received RF signal may in some cases be very low, it would result in very low sideband powers as well. If no optical single sideband filtering is used, then the gain of the optical amplifiers would be distributed over the entire optical signal, including the carrier and the other sideband which is not desired. The optical single-sideband filtering can be placed either at the antenna or central office all depending on the transmissions scenario.

III. Experimental Results

In Fig. 2, optical spectra of the input signal at the FBG, as well as the optical spectra of the transmitted and the reflected signal from the FBG, are shown. It is the reflected signal at $\lambda_1 + \lambda_{\rm RF} = 1550.0$ nm containing only baseband 2.5-Gb/s QPSK data modulation that is sent to the transmission span of 26 km and subsequent signal demodulation as mentioned earlier. It is observed from Fig. 2 that the FBG suppresses the optical carrier at λ_1 and the lower sideband at $\lambda_1 - \lambda_{\rm RF}$ by more than 30 dB, allowing for pure baseband transmission.

In Fig. 3(a), the frequency spectrum of the sampled photocurrent $I_i[k]$ is shown. It is observed that the signal is in baseband and is symmetric around zero since the frequency offset between the transmitter and LO laser has been removed by the DSP. The frequency spectra has nulls at 1.25 GHz as expected. In Fig. 3(b), the constellation diagram of the demodulated 2.5-Gb/s QPSK signal is shown for the RF power of 2 dBm. The constellation points look clear and well separated indicating that the digital signal-processing-based receiver can be successfully used for QPSK signal demodulation. Next, in order to test the demodulation scheme, we investigate the system performance as a function of optical signal-to-noise ratio (OSNR). Fig. 4(a) shows the bit-error-ratio (BER) curves plotted as a function of the OSNR measured in 0.1-nm resolution bandwidth. To begin with, we focus on the data signal at

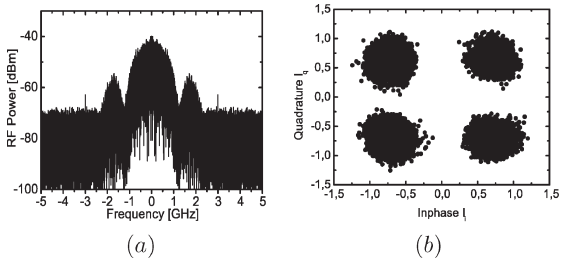

Fig. 3. (a) Frequency spectra of the sampled photocurrent, $I_i[k]$ at the output from one of the arms of the 90° optical hybrid. (b) Constellation diagram of the demodulated 2.5-Gb/s QPSK data signal.

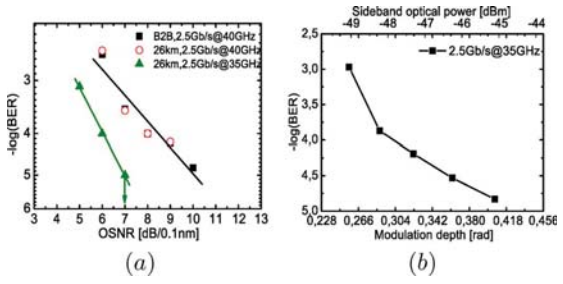

Fig. 4. (a) BER plotted as a function of OSNR. The RF power is maintained constant at 2 dBm, which converts to a modulation depth of 0.51 rad. V_π of the modulator is 4.9 V. (b) BER plotted as a function of the modulation depth.

40-GHz RF carrier frequency. First, the BER was measured in a back-to-back scenario, and then a 26-km fiber transmission was performed. Fig. 4(a) shows that for the back-to-back scenario, successful signal demodulation is achieved with the receiver sensitivity of 8 dB in order to obtain the BER of 10^{-4}. Additionally, it can be observed from Fig. 4(a), that the 26-km fiber transmission did not induce any penalty for the demodulation of a 2.5-Gb/s QPSK signal at 40-GHz RF carrier, proving the dispersion tolerance of the proposed scheme. In order to demonstrate the RF transparency of the demodulation scheme, the RF carrier frequency was changed to 35 GHz while still keeping the 1.25-Gbaud QPSK data signal modulation. Changing the RF carrier frequency from 40 to 35 GHz has moved the sideband center wavelength, so in order to be able to filter the sideband properly, the transmitter laser was detuned to maximize the filtered optical power. In Fig. 4(a), the BER as a function of OSNR is plotted when the RF carrier frequency is 35 GHz. The error-free (zero errors counted) signal demodulation is achieved when the OSNR is 7 dB, which is indicated by an arrow in Fig. 4(a). We define an error-free operation when we observe no errors for the considered 100.000 bits. An improvement in the BER is observed compared to the case when the RF carrier frequency was 40 GHz, which is due to the increased frequency response of the MZM at 35 GHz compared to 40 GHz. From the specifications of the used MZM provided by the manufacturer, a difference of 2 dB in S_{21} is noted and this difference is reflected in the measured OSNR penalty (for BER of 10^{-4}) when moving from 35 to 40 GHz.

In order to analyze the effect of the RF power on the performance of the demodulation scheme, the BER was measured as a function of the modulation depth without any additional optical noise and plotted in Fig. 4(b). The modulation depth was varied from 0.25 to 0.40 rad, and the corresponding optical sideband power was also measured and is shown as well in Fig. 4(b). Fig. 4(b) shows that the BER well below 10^{-4} is obtainable. Also, for relatively low sideband optical power of -48 dBm, a BER of approximately 10^{-4} is achievable. This proves the high sensitivity of the proposed demodulation scheme. In general, decreasing the modulation depth results in decreasing the signal-to-noise-ratio of the received signal and this translates into increased BER, as shown in Fig. 4(b).

IV. Conclusion

We demonstrate by a proof-of-principle a solution/system for transport of wireless signals from the antenna base station to the central office which is transparent to the RF carrier frequency and only needs electronics at twofold of the wireless signal data rate. The proposed technique is based on optical single-sideband filtering, coherent detection, and baseband digital signal processing. A successful experimental demodulation of 2.5-Gb/s QPSK data signal at 40- and 35-GHz RF carrier frequency is successfully demonstrated using the same receiver structure thereby demonstrating the RF transparency of the scheme.

References

[1] V. Dyadyuk, J. D. Bunton, J. Pathikulangara, R. Kendall, O. Sevimli, L. Stokes, and D. A. Abbott, "A Multigigabit millimeter-wave communication cystem with improved spectral efficiency," *IEEE Microw. Theory Tech.*, vol. 55, no. 12, pp. 2813–2820, Dec. 2007.

[2] A. Hirata, M. Harada, and T. Nagatsuma, "120-GHz wireless link using photonic techniques for generation, modulation, and emission of millimeter-wave signals," *J. Lightw. Technol.*, vol. 21, no. 10, pp. 2145–2153, Oct. 2003.

[3] J. Capmany and D. Novak, *Nature Photon.*, vol. 1, pp. 319–330, 2007.

[4] G. K. Gopalakrishnan, R. P. Moeller, M. M. Howerton, W. K. Burns, K. J. Williams, and R. D. Esman, "A low-loss downconverting analog fiber-optic link," *IEEE Microw. Theory Tech.*, vol. 43, no. 9, pp. 2318–2323, Sep. 1995.

[5] R. Sambaraju, J. Palaci, R. Alemany, V. Polo, and J. L. Corral, "Photonic vector demodulation of 2.5 Gbit/s QAM modulated wireless signals," in *Proc. Int. Topical Meeting Microwave Photonics 2008*, 2008, pp. 117–120.

[6] T. R. Clark and M. L. Dennis, "Coherent optical phase modulation link," *IEEE Photon. Technol. Lett.*, vol. 19, no. 16, pp. 1206–1208, Aug. 15, 2007.

[7] D. Zibar, X. Yu, C. Peucheret, P. Jeppesen, and I. T. Monroy, "Digital coherent receiver for phase modulated radio-over-fibre optical links," *IEEE Photon. Technol. Lett.*, vol. 21, no. 3, pp. 155–157, Feb. 1, 2009.

[8] A. Caballero, D. Zibar, and I. T. Monroy, "Digital coherent detection of multi-gigabit 16-QAM signals at 40 GHz carrier frequency using photonic downconversion," in *Proc. Eur. Conf. Optical Communications*, 2009, pp. 58–59, Paper PD3.3.

[9] H. Meyr, M. Moeneclaey, and S. A. Fechtel, *Digital Communication Receivers*. Hoboken, NJ: Wiley, 1998.

Paper 9: 100-GHz wireless-over-fibre links with up to 16 Gb/s QPSK modulation using optical heterodyne generation and digital coherent detection

R. Sambaraju, D. Zibar, A. Caballero, I. Tafur Monroy, R. Alemany, and J. Herrera, "100-GHz wireless-over-fibre links with up to 16 Gb/s QPSK modulation using optical heterodyne generation and digital coherent detection," *IEEE Photon. Technol. Lett.*, vol. 22, no. 22, pp. 1650–1652, 2010.

100-GHz Wireless-Over-Fiber Links With Up to 16-Gb/s QPSK Modulation Using Optical Heterodyne Generation and Digital Coherent Detection

Rakesh Sambaraju, Darko Zibar, Antonio Caballero, Idelfonso T. Monroy, Ruben Alemany, and Javier Herrera

***Abstract*—In this letter, a novel technique for direct conversion of an optical baseband quadrature phase-shift keying (QPSK) signal to a millimeter-wave wireless signal and subsequent signal demodulation is reported. Optical heterodyne mixing of the optical baseband QPSK signal with a free-running unmodulated laser for the wireless signal generation is employed. To correct for the phase and frequency offset originating from the heterodyne mixing of the two free-running lasers, wireless signal demodulation based on optical coherent detection in combination with baseband digital signal processing is implemented. As a proof of concept, 5-Gb/s amplitude-shift keying and up to a 16-Gb/s QPSK wireless signal in the band of 75–110 GHz was generated and successfully demodulated. All-photonic millimeter-wave wireless signal generation and digital coherent detection at baud-rate are employed without complex optical phase-locked loop.**

***Index Terms*—Coherent detection, digital signal processing, microwave photonics, wireless communication.**

I. Introduction

OPTICAL communication systems are going through a radical change with the return of coherent detection in combination with digital signal processing. This allows for spectrally efficient modulation formats, such as quadrature phase-shift keying (QPSK) or quadrature amplitude modulation (M-QAM), to be used to generate high-speed data signals with the bit rates of up to 112 Gb/s while keeping the baud rates at either 10 or 28 Gbaud [1]. The digital signal processing assisted optical coherent detection is maturing very fast [2], and is expected to enter the commercial applications within a few years. On the other hand, wireless technology is also advancing at a rapid pace, especially in the millimeter-wave frequency bands like 60, 70/80, and $>$100 GHz, where several gigahertz of bandwidth are available [3]. Wireless links with capacities of 10 Gb/s, and even up to 28 Gb/s have been demonstrated, using microwave photonic techniques [4]. However, the current technologies for generation of high-capacity wireless signals either employ spectrally inefficient on–off-keying modulation which are limited to 10 Gb/s [5], or use complex electronic arbitrary waveform generators [4].

In this letter, we report for the first time, a novel technique for generation and demodulation of spectrally efficient QPSK wireless signals in the 75- to 110-GHz band. The wireless QPSK signal generation is obtained by directly converting an optical baseband signal into an millimeter-wave wireless signal as explained next. The proposed wireless signal generation is based on heterodyne mixing of a high-speed optical (baseband) QPSK signal with a free-running continuous-wave (CW) laser in a photodiode. The subsequent wireless signal demodulation is based on optical single sideband filtering, coherent detection and baseband digital signal processing, i.e., radio-frequency (RF) transparent signal demodulation [6]. We experimentally demonstrate a successful generation and demodulation of 5-Gb/s amplitude shift keying (ASK) and up to 16-Gb/s QPSK wireless signals in the 75- to 110-GHz frequency band. The proposed technique does not incorporate any millimeter-wave components for the wireless signal generation or detection, and digital coherent detection with electronic components only at twice the data signal baud rate are used. The proposed technique is also highly scalable and does not require any kind of optical phase-locking techniques for the wireless signal generation [7], and detection. The phase and frequency drift originating from wireless signal generation and coherent detection, both employing free-running lasers, are fully compensated using digital signal processing based detection. This concept significantly simplifies the system complexity and achieves the breakthrough demanded from simple and seamless integration between high-capacity optical fiber links and wireless connections.

II. Experimental Setup

Fig. 1 shows the schematic of the experimental setup for the generation and detection of QPSK wireless signals. In order to generate an optical data signal, a CW external cavity laser (ECL) at wavelength λ_1 (1555 nm) is used. The output of the ECL is then phase-modulated by two data streams I_k and Q_k using a nested dual-parallel Mach–Zehnder modulator (MZM) structure (in-phase/quadrature (I/Q) modulator) to generate an optical baseband QPSK signal. The optical I/Q modulator is driven with up to 8-Gb/s electrical data signals from a bit pattern generator with a PRBS (pseudorandom bit sequence) pattern of length $2^{15}-1$ to generate 16-Gb/s optical baseband QPSK signals. The optical baseband signal is then amplified, and filtered using a 1-nm bandwidth optical bandpass filter (OBPF) to remove the out-of-band amplified spontaneous emission (ASE)

Manuscript received June 08, 2010; revised July 23, 2010; accepted September 03, 2010. Date of publication September 16, 2010; date of current version October 22, 2010. This work has been supported by the European Commission FP7 under Network of Excellence project EUROFOS (22402) www.eurofos.eu.

R. Sambaraju, R. Alemany, and J. Herrera are with the Universidad Politécnica de Valencia, 46022 Valencia, Spain (e-mail: r.sambaraju@ieee.org; rualser@hotmail.com; jaherllo@ntc.upv.es).

D. Zibar, A. Caballero, and I. T. Monroy are with the DTU Fotonik, Tecnical University of Denmark, 2800 Kgs-Lyngby, Denmark (e-mail: dazi@fotonik.dtu.dk; acaj@fotonik.dtu.dk; idtm@fotonik.dtu.dk).

Color versions of one or more of the figures in this letter are available online at http://ieeexplore.ieee.org.

Digital Object Identifier 10.1109/LPT.2010.2076801

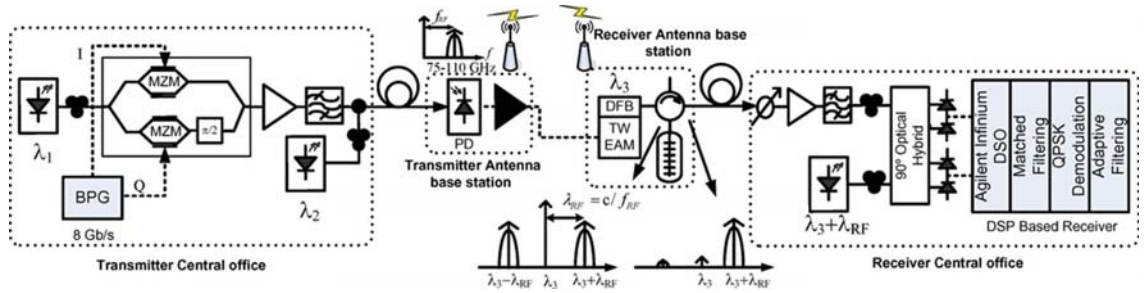

Fig. 1. Experimental setup of a QPSK wireless-over-fiber link. (Antenna at the transmitter and receiver are just for illustration purposes; no wireless transmission is performed).

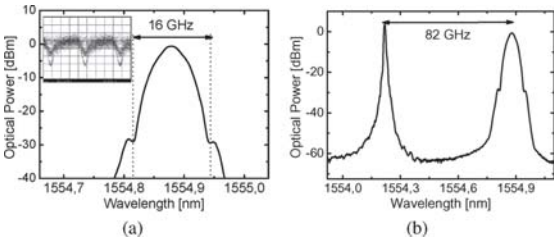

Fig. 2. (a) Optical spectrum of a 16-Gb/s baseband QPSK signal with the direct detected eye diagram (inset). (b) Optical spectrum of the combined optical baseband 16 QPSK signal and an unmodulated optical carrier with a frequency separation of $\Delta f = f_{\mathrm{RF}} = 82$ GHz.

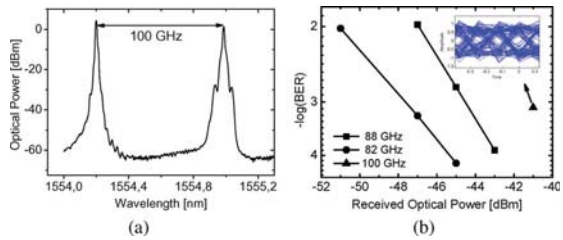

Fig. 3. (a) Optical spectrum showing the 5-Gb/s ASK optical data signal and an unmodulated optical carrier prior to the RF up-conversion. (b) BER plots versus the received optical power of the wireless 5-Gb/s ASK signals at RF frequencies of 82, 88, and 100 GHz.

noise. The optical spectrum of the 16-Gb/s optical QPSK signal is plotted in Fig. 2(a) together with the directly detected eye diagram of the optical QPSK signal [inset Fig. 2(a)]. The eye diagram shows the characteristic intensity dips of a QPSK signal when generated using a nested I/Q MZM. Prior to the up-conversion to the RF carrier frequency, the baseband optical QPSK signal is combined in an optical coupler with another CW optical signal at wavelength λ_2 (1554.32 nm) emitted from an ECL (see Fig. 1). The frequency difference between the two optical sources, $\Delta f = f_{\mathrm{RF}}$, is chosen to the desired RF carrier frequency. The optical spectrum of the combined optical signals is plotted in Fig. 2(b). The combined optical signals are then transmitted, using 50-m-long single-mode fiber (SMF), to a remote transmitter antenna site (see Fig. 1). At the remote transmitter antenna site, the two optical carriers are heterodyne mixed in a 100-GHz bandwidth photodiode, generating a 16-Gb/s QPSK modulated radio signal at an RF carrier frequency of $f_{\mathrm{RF}} = 82$ GHz. The wireless signal at 82 GHz with 16-Gb/s QPSK data modulation is then amplified using a W-band amplifier (from Radiometer Physics GmbH). At the reception point (receiver antenna base station, see Fig. 1), the wireless QPSK signal modulates an optical carrier at wavelength λ_3 (1549.34 nm) emitted from a distributed-feedback laser integrated with a 100-GHz travelling wave electroabsorption modulator (DFB TW-EAM), developed in the European Project ICT-HECTO. The optical output of the TW-EAM contains a central carrier at λ_3 and the two sidebands at wavelengths $\lambda_3 \pm \lambda_{\mathrm{RF}}$ (see Fig. 1), where $\lambda_{\mathrm{RF}} = c/f_{\mathrm{RF}}$ and c is the velocity of light. The sidebands $\lambda_3 \pm \lambda_{\mathrm{RF}}$ are separated by $f_{\mathrm{RF}} = 82$ GHz from the optical carrier at λ_3, and contain the QPSK data modulation. Using a fiber Bragg grating (FBG) with >25 dB of rejection and centered at 1550 nm, one of the sidebands is filtered out such that only pure baseband QPSK signal at $\lambda_3 + \lambda_{\mathrm{RF}}$ (1550 nm) is sent to the coherent receiver at the receiver central station, after 50 m of transmission. Prior to demodulation, the baseband QPSK signal is amplified using an optical preamplified receiver, and intradyne mixed in a optical 90° hybrid with an optical local oscillator emitting from an ECL with a linewidth of 100 kHz, and tuned to $\lambda_3 \pm \lambda_{\mathrm{RF}}$. The photodetected I and Q signals are then sampled at a rate of 20 GS/s using a real-time digital sampling scope, and subsequently off-line processed using a digital signal processing-based receiver [6].

III. Results

The system performance is tested by first setting the system baud rate to 5 Gbaud and applying an ASK modulation format for the following RF carrier frequencies: 82, 88, and 100 GHz. Fig. 3(a) shows the optical spectrum at the input of the photodiode, of the optical baseband 5-Gb/s ASK signal together with an unmodulated CW optical carrier 100 GHz away in frequency, prior to wireless signal generation. At the receiver (receiver central office), the ASK wireless signals were successfully demodulated using the DSP-based receiver and the bit-error ratio (BER) is plotted versus the received optical power, as shown in Fig. 3(b). The received optical power to the preamplified receiver is varied using the variable optical attenuator (VOA) present in the receiver central office (see Fig. 1). Power penalty is observed as the RF carrier frequency increases, which is due to the bandwidth limitation of the RF components. Later the modulation format was changed to QPSK, resulting in a 10-Gb/s QPSK wireless signal at a carrier frequency of 82 GHz. At the receiver, the 10-Gb/s QPSK wireless signal is successfully demodulated with BER values below 10^{-3}, as shown in Fig. 4. Using digital signal processing, demodulation of the 10-Gb/s

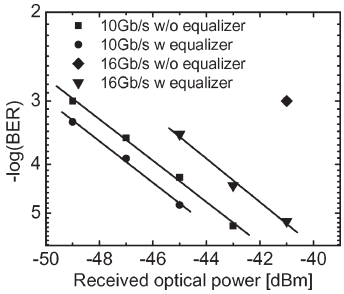

Fig. 4. BER as a function of the received optical power of a 10- and 16-Gb/s wireless QPSK signal at the RF carrier frequency of 82 GHz, with and without adaptive equalization.

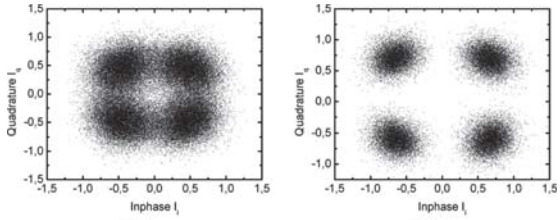

Fig. 5. Constellation diagrams of a 16-Gb/s 82-GHz wireless signal. (a) Without and (b) with baud rate adaptive equalizer.

QPSK signals is performed with and without adaptive equalizer at baud rate, and relatively small improvement of around 1 dB is observed in the performance indicating that no severe inter symbol interference (ISI) due the bandwidth limitations of the RF components is experienced. Then, the baud rate is changed to 8 Gbaud resulting in a 16-Gb/s QPSK wireless signal, and the BER of the 16-Gb/s signals is also plotted versus the received optical power in Fig. 4. It is observed that for 8-Gbaud case, the adaptive equalizer pushes down the BER from 10^{-3} to 10^{-5} for a received optical power of -41 dBm indicating strong ISI arising from the bandwidth limitations of the RF components. It can also be noted that when changing the bit rate from 10 to 16 Gb/s and by using adaptive equalization, a penalty of around 3 dB is induced, which is mainly attributed to the frequency response of the RF components. For instance, the photodiode has a 3-dB cut-off at 90 GHz, and the W-band amplifier has a 2-dB lower gain at 90 GHz. In order to demonstrate the effect of adaptive digital equalization, the constellation diagrams of the demodulated QPSK signal with and without digital equalization for $P_{\mathrm{rec}} = -43$ dBm are plotted in Fig. 5(a) and (b), respectively. It is observed from Fig. 5(a), where digital equalization is not applied, that it is very difficult to distinguish data points and no successful demodulation can be performed. After applying the equalization [see Fig. 5(b)], the constellation points look clear and well separated with successful signal demodulation at a BER below 10^{-4}. The applied equalizer has only seven taps and can be thereby easily implemented in hardware. Apart from the bandwidth limitations of the RF components, the critical parameter for the system performance is the amount of the total frequency offset which can be tracked by the digital carrier-recovery scheme. For the wireless signal generation and subsequent detection, four different lasers are used in total, therefore, the frequency offset may be large. In general, the ratio between the total frequency offset and the baud rate should not exceed 10%, otherwise, advanced frequency tracking algorithms must be employed. Another issue is that the total amount of phase noise, which may set the limitations for the choice of the employed modulation format.

IV. Conclusion

Using digital coherent detection for wireless signal demodulation, all-optical generation of multigigabit-per-second spectrally efficient wireless signals can be obtained by simple heterodyne mixing of an optical baseband signal with another free-running laser in a photodiode. Successful wireless signal generation and demodulation of a 5-Gb/s ASK and 16-Gb/s QPSK wireless signal in the 75- to 110-GHz band is performed demonstrating the modulation format transparency. The proposed system does not involve any millimeter-wave components (only electronics at twice the baud rate are employed) or any high-frequency analogue phase-locking mechanism, resulting in the reduced overall system complexity.

Acknowledgment

The authors acknowledge U. Westergren of the project ICT-HECTO (www.hecto.eu) for providing the 100-Gb/s DFB-TWEAM; A. Walber from Radiometer Physics GmbH for providing the 100-GHz amplifier; D. Gonzalo from Agilent Spain, Vedran Furtula DTU • Electro and S. Bojanic from Anritsu Denmark.

References

[1] P. Winzer, A. Gnauck, C. Doerr, M. Magarini, and L. Buhl, "Spectrally efficient long-haul optical networking using 112-Gb/s polarization-multiplexed 16-QAM," *J. Lightw. Technol.*, vol. 28, no. 4, pp. 547–556, Feb. 1, 2010.

[2] C. R. Doerr, L. Zhang, and P. J. Winzer, "Monolithic InP multi-wavelength coherent receiver," in *Proc. Optical Fiber Communication Conf. (OFC'10)*, San Diego, CA, 2010, Paper PDPB1.

[3] J. A. Wells, "Faster than fiber: The future of multi-G/s wireless," *IEEE Microw. Mag.*, vol. 10, no. 3, pp. 104–112, May 2009.

[4] C.-T. Lin, E.-Z. Wong, W.-J. Jiang, P.-T. Shin, J. Chen, and S. Chi, "28-Gb/s 16-QAM OFDM radio-over-fiber system within 7-GHz license-free band at 60 GHz employing all-optical up-conversion," in *Proc. Conf. Lasers and Electro-Optics/Quantum Electronics and Laser Science (CLEO/QELS 2009)*, 2009, Paper CPDA8.

[5] R. W. Ridgway and D. W. Nippa, "Generation and modulation of a 94-GHz signal using electrooptic modulators," *IEEE Photon. Technol. Lett.*, vol. 20, no. 8, pp. 653–655, Apr. 15, 2008.

[6] R. Sambaraju, D. Zibar, R. Alemany, A. Caballero, and J. Herrera, "Radio frequency transparent demodulation for broadband wireless links," in *Proc. Optical Fiber Communication Conf. (OFC'10)*, San Diego, CA, 2010, Paper OML1.

[7] L. A. Johansson and A. J. Seeds, "36-GHz 140-Mb/s radio-over-fiber transmission using an optical injection phase-lock loop source," *IEEE Photon. Technol. Lett.*, vol. 13, no. 8, pp. 893–895, Aug. 2001.

Paper 10: High-capacity wireless signal generation and demodulation in 75- to 110-GHz band employing all-optical OFDM

D. Zibar, R. Sambaraju, A. Caballero, J. Herrera, U. Westergren, A. Walber, J. B. Jensen, J. Marti, and I. Tafur Monroy, "High-capacity wireless signal generation and demodulation in 75- to 110-GHz band employing all-optical OFDM," *IEEE Photon. Technol. Lett.*, vol. 23, no. 12, pp. 810 –812, 2011.

High-Capacity Wireless Signal Generation and Demodulation in 75- to 110-GHz Band Employing All-Optical OFDM

Darko Zibar, Rakesh Sambaraju, Antonio Caballero, Javier Herrera, Urban Westergren, Achim Walber, Jesper Beevense Jensen, Javier Marti, and Idelfonso Tafur Monroy

***Abstract*—We present a radio-frequency (RF) and bit-rate scalable technique for multigigabit wireless signal generation based on all-optical orthogonal frequency-division multiplexing (OFDM) and photonic up-conversion. Coherent detection supported by digital signal processing is used for signal demodulation and data recovery. In order to demonstrate the RF frequency scalability and bit-rate transparency, the system is tested at 60 GHz and in the 75- to 110-GHz band at the baud rates of 5 and 10 Gbaud. In terms of the bit rate, the proposed system is experimentally tested up to 40 Gb/s for wireless signal generation and demodulation. The wireless transmission is not considered in this letter. Additionally, a novel digital carrier phase/frequency recovery structure is employed to enable robust phase and frequency tracking between the beating lasers.**

***Index Terms*—Coherent communication, digital receivers, digital signal processing, microwave photonics, modulation.**

I. Introduction

WIRELESS links that can provide the same capacity as baseband optical communication systems will provide a cost-effective solution for future's wireless/wireline seamless network integration and future data interconnects [1]. Additionally, future high capacity wireless links will probably require optical fiber backbone to feed gigabit-per-second capacities into the core network. Therefore, future hybrid optical fiber-wireless links should be highly transparent with optical links and be able to provide capacities in proximity of 100 Gb/s. To realize high capacity wireless links approaching 40 Gb/s and beyond, we must move to millimeter (mm)-wave frequency range, where we have a few gigahertz of available bandwidth, and employ spectrally efficient modulation formats. Current approaches for achieving record wireless capacities in 60 GHz band is obtained by using electrical OFDM and optical modulators for up-conversion to the desired RF carrier frequency [2], [3] and references therein. The techniques presented in [2], [3] have some severe limitations: they require high-bandwidth complex arbitrary waveform generators and high-frequency RF components for signal generation and demodulation. Scaling those approaches to 40 Gb/s, and beyond, at mm-wave frequencies, is very challenging. What is most important is that in a converged wireless/wireline network scenario, seamless integration between the optical and wireless signal formats with RF/bit-rate transparency and scalability is crucial. What we mean with transparency and scalability is that one can take an optical baseband signal, either single carrier amplitude/binary phase/quaternary phase shift keying or multicarrier OFDM, and convert it directly to the wireless signal by heterodyne beating. This is currently not achievable using conventional approaches such as those presented in [2], [3]. As we move to 75–110 GHz band, we have recently experimentally demonstrated as a proof of concept, a technique for direct conversion of single-carrier optical baseband Quadrature Phase Shift Keying (QPSK) signal to a mm-wave wireless signal based on free-running heterodyne mixing and digital coherent detection [4]. In this letter, we present a novel concept for high-capacity wireless links, based on all-optical OFDM [5] and RF transparent signal demodulation. The proposed technique relies on seamlessly converting a high-capacity all-optical OFDM baseband signal to a desired RF carrier frequency, without changing its modulation format, see Fig. 1. To demonstrate the scalability of the proposed, system, mm-wave wireless signals at different baud-rates and with various numbers of OFDM subcarriers were generated at both the 60 GHz and 75–110 GHz band. The maximum achievable bit rate for the experiment for which Forward Error Correction (FEC) codes can correct is 24 Gb/s. For the 40 Gb/s wireless signal generation, the signal can be demodulated and we show the demodulated constellation diagrams. However, the average error rate is above the FEC limit due to the severe bandwidth limitations of the components.

Manuscript received December 02, 2010; revised January 31, 2011; accepted March 26, 2011. Date of publication April 15, 2011; date of current version May 25, 2011. This work was supported by the Danish Research Council project OPSCODER and by the European Commission FP7 under Network of Excellence project EUROFOS (22402).

D. Zibar, A. Caballero, J. B. Jensen, and I. T. Monroy are with DTU Fotonik, Department of Photonics Engineering, Technical University of Denmark, Kgs. Lyngby, DK-2800, Denmark (e-mail: dazi@fotonik.dtu.dk; acaj@fotonik.dtu.dk; jebe@fotonik.dtu.dk; idtm@fotonik.dtu.dk).

R. Sambaraju, J. Herrera, and J. Marti are with Valencia Nanophotonics Technology Center, Universidad Politécnica de Valencia, 46022 Valencia, Spain (e-mail: rsambaraju@ntc.upv.es; jherllo@upvnet.upv.es; j.marti@upvnet.es).

U. Westergren is with the Royal Institute of Technology, Photonics and Microwave Engineering, SE-164 40 Kista, Sweden (e-mail: urban@kth.se).

A. Walber is with Radiometer Physics GmbH, 53340 Meekenheim, Germany (e-mail: walber@radiometer-physics.de).

Color versions of one or more of the figures in this letter are available online at http://ieeexplore.ieee.org.

Digital Object Identifier 10.1109/LPT.2011.2139201

II. Experimental Setup and Demodulation

The experimental setup for the generation and digital coherent detection of high-capacity wireless OFDM signals is shown in Fig. 1. First, a high-capacity all-optical OFDM signal is generated. In the experiment, we generate up to three subcarriers all-optical OFDM signal where each subcarrier is QPSK modulated. For the generation of two subcarriers all-optical OFDM signal, an optical carrier emitted from an external cavity laser (ECL, $\lambda_1 = 1549.8$ nm) is modulated by a sinusoidal

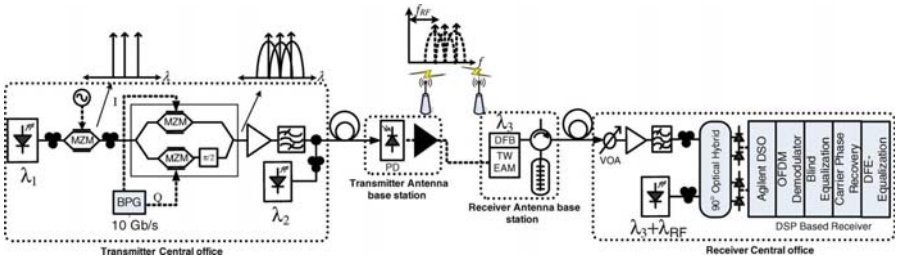

Fig. 1. Experimental setup for the generation and demodulation of wireless signals based on all-optical OFDM and digital coherent detection. BPG: bit pattern generator. VOA: variable optical attenuator. (Antenna at the transmitter and receiver are for illustration purposes.)

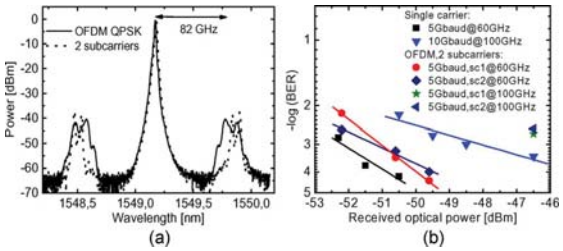

Fig. 2. (a) Optical spectrum at the output of the TW-EAM of the wireless signal with and without the OFDM QPSK data modulation. (b) BER plotted as a function of received optical power for single and multicarrier OFDM signal in 60-GHz and 75- to 110-GHz band.

electrical clock signal (running at frequency which is half of the baud rate), in a Mach–Zehnder Modulator (MZM) biased at its minimum transmission point. The minimum transmission point generates an Optical Carrier Suppression (OCS) modulation where the two OFDM subcarriers separated by the baud rate are generated. Similarly, for generating three subcarriers all-optical OFDM signal, the electrical clock signal frequency is changed to the baud rate and the MZM bias is chosen by optimizing the power of the three subcarriers (the optical carrier, and the sidebands). The optical subcarriers are then fed into an optical I/Q modulator, where two independent data streams (pseudo random bit sequence of length $2^{15}-1$) at baud rate modulate the phase of the subcarriers resulting in QPSK modulation on the subcarriers. The output of the optical I/Q modulator is an all-optical OFDM-QPSK modulated signal. The all-optical OFDM-QPSK modulated signal is then amplified and combined with another unmodulated CW optical carrier (λ_2). The combined all-optical OFDM-QPSK signals and the unmodulated CW carrier are then transmitted to the remote antenna site (see Fig. 1) where they are heterodyne mixed in a ($\sim$75 GHz bandwidth) Photo-Diode (PD). The output power after the photodiode is approximately -3 dBm. In reality, one would need to code independent data bit streams for each subcarrier. One way of doing this would be to use different lasers sources separated by the baud rate and modulate the output of each laser in the I/Q modulator by the QPSK data signal. The modulated laser sources would then be optically combined in a coupler to generate an all-optical OFDM signal as shown in [5]. The output of the photo-diode is a high-capacity OFDM-QPSK electrical signal at the desired RF carrier frequency. The desired RF carrier frequency is simply chosen by varying the wavelength of the unmodulated CW optical source. The electrical mm-wave OFDM-QPSK modulated signal is received at the receiver antenna site (Fig. 1) and transmitted through a few meter of fiber ($\sim$20 m) prior to signal demodulation using the RF transparent demodulation technique [6]. Prior to demodulation, the mm-wave signal is electrically amplified and modulated on an optical carrier at λ_3 (1549.2 nm), emitted from a Distributed Feed-Back laser integrated with a 100 GHz Travelling Wave Electroabsorption Modulator (DFB-TW-EAM), developed in the European Project ICT-HECTO. Fig. 2(a) shows the output of the TW-EAM when modulated using a 10 Gbaud two subcarrier OFDM-QPSK wireless signal in the 75–110 GHz band (the set RF carrier frequency is: $f_{RF} = 82$ GHz). From Fig. 2(a), it can be seen that the sidebands are 82 GHz apart from the optical carrier (λ_3) containing the two subcarrier OFDM-QPSK signal. To perform the demodulation, only one of the sidebands is required, which is filtered out using a fiber Bragg's grating (FBG extinction ratio $>$25 dB). The filtered sideband is fed into an optical preamplified receiver prior to detection. The preamplified optical signals are intradyne mixed with an optical local oscillator (LO) in an optical 90° hybrid. The photo-detected in-phase and quadrature outputs of the optical hybrid are sampled using a 20 GSa/s real-time oscilloscope and demodulated offline. The demodulation process consists of OFDM demodulation block, blind equalization based on Constant Modulus Algorithm (CMA), carrier phase and frequency estimation and Decision Feedback Equalizer (DFE) for nonlinear equalization. A novel digital carrier phase and frequency recovery structure which is a hybrid between Viterbi & Viterbi (V&V) algorithm and digital phase-locked loop for signal demodulation is employed, see Fig. 3. The novelty behind the proposed carrier phase and frequency recovery structure is that the (V&V) algorithm is embedded inside a digital phase-locked loop to produce an error signal for the feedback loop. The $W(z)$ is the corresponding low-pass loop filter. The advantages of the proposed structure is that it uses blind (robust) phase estimation by employing V&V and feedback loop to track the fast phase and frequency fluctuations. The DFE nonlinear equalizer consists of Feedforward Equalizer (FFE) and Feedback Equalizer (FBE) each updated with Least Mean Squares (LMS) algorithm.

III. Experimental Results

In order to test the scalability to the RF carrier frequency and bit rate, the system is tested in 60 GHz and 75–110 GHz band.

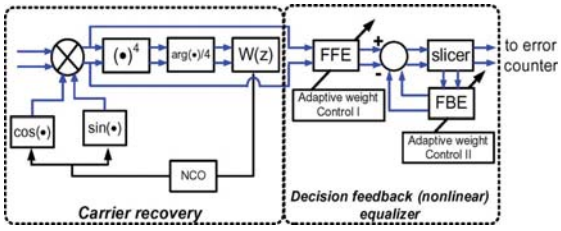

Fig. 3. Digital carrier phase and frequency recovery structure and nonlinear decision feedback equalizer. NCO: Number controlled oscillator.

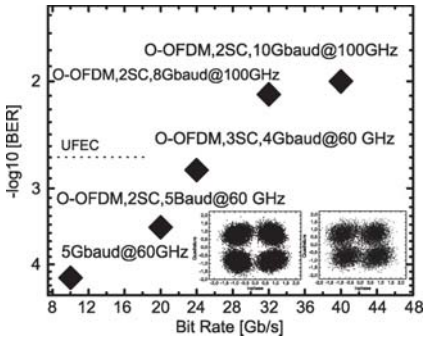

Fig. 4. BER as a function of generated bit rate for all-optical OFDM-QPSK wireless signal generation in 60-GHz and 75- to 110-GHz band. Inset: Constellation diagrams of the demodulated 40-Gb/s two subcarrier OFDM-QPSK wireless signals.

First, the baud rate is set to 5 Gbaud, and the RF carrier frequency is chosen to 60 GHz. In, Fig. 2(b), the BER, versus the received optical power, of the single carrier QPSK and two subcarriers OFDM-QPSK wireless signal are plotted. It is observed that for the single carrier and multicarrier OFDM modulation format, the BER below 10^{-3}, is achieved indicating successful signal demodulation. The given BER is obtained by counting the number of errors after the signal has been demodulated offline. For the error counting we consider 100000 bits. Additionally, the results indicate that it is possible to use all-optical OFDM for high-capacity wireless signal generation. By moving from 60 GHz to 75–110 GHz band, we have more available bandwidth and the baud rate is therefore increased from 5 Gbaud to 10 Gbaud, resulting in the total bit rate of 20 Gb/s, and the BER curve is shown in Fig. 2(b) We also tested the wireless signal generation and demodulation using two subcarriers all-optical OFDM at 5 Gbaud in 75–110 GHz band. The BER for the received power of -46.5 dBm, is shown in Fig. 2(b), and a relatively large penalty is observed compared to the single carrier 10 Gbaud case. The two subcarriers OFDM-QPSK signal at 5 Gbaud occupy less bandwidth compared to the single carrier at 10 Gbaud, so the bandwidth limitation is not causing the penalty. In stead, we believe that it is the nonlinearity of the RF components that is resulting in the penalty and that is the main reason why the BER for the two subcarrier OFDM in the 75 GHz–110 GHz band is above the FEC limit. The nonlinearity will destroy the orthogonality among the OFDM signal subcarriers and introduce ISI which is difficult to get rid of. In Fig. 4, we have summarized the highest achieved bit-rates when all-optical OFDM is used for wireless signal generation in 60 GHz and 75–110 GHz band. At 60 GHz, we push the system performance by employing three subcarriers all-optical OFDM-QPSK for wireless signal generation. Taking into consideration the bandwidth limitations of components, the baud rate is set to 4 GBaud, resulting in a total bit rate of 24 Gb/s. It is observed in Fig. 4, that the average BER of the three subcarriers is below the UFEC limit. In the 75–110 GHz band, the baud rate is first increased to 8 GBaud and two subcarriers all-optical OFDM is used for wireless signal generation resulting in the total bit rate of 32 Gb/s. Next, the baud rate is increased to 10 GBaud, resulting in the total bit rate of 40 Gb/s by applying two subcarriers OFDM-QPSK, see Fig. 4. The constellation diagrams of demodulated 10 Gbaud subcarriers of a two subcarrier OFDM-QPSK signal in the 75–110 GHz band are plotted as an inset in Fig. 4. It is observed that in spite of the sever bandwidth limitations, constellation diagrams can be recovered. The BER of the subcarrier 1 and subcarrier 2 is -2.7 (below UFEC) and -1.8, respectively.

IV. Conclusion

We have presented a novel scalable high-capacity wireless signal generation technique based on a conversion of an all-optical OFDM baseband signal, to the wireless signal, by simple heterodyning and coherent detection at the receiver. Wireless signal capacities of up to 24 Gb/s have been demonstrated in 75–110 GHz band using three subcarrier all-optical OFDM. One issue which remains to be investigated is wireless transmission and the optimum number of subcarriers. However, in order to make the proposed system transparent with QPSK baseband optical links, the system should operate at 10 Gbaud. It will therefore be the bandwidth of RF components that will set an upper limit for the number of subcarriers. Taking into consideration that horn antennas with 24 dBi gain as well as RF amplifiers with up to 20 dB of gain are commercially available today, we believe that wireless transmission for the proposed system is feasible.

References

[1] J. Wells, "Faster than fiber: The future of multi-Gb/s wireless," *IEEE Microw. Mag.*, vol. 10, no. 3, pp. 104–112, May 2009.

[2] C.-T. Lin, E.-Z. Wong, W.-J. Jiang, P.-T. Shin, J. Chen, and S. Chi, "28-Gb/s 16-QAM OFDM radio-over-fibre system within 7 GHz licence free band at 60 GHz employing all-optical upconversion," presented at the Proc. Conf. Lasers and Electro-Optics 2009 (CLEO), Baltimore, MD, 2009, Paper CPDA 8.

[3] M. Weiss, A. Stohr, F. Lecoche, and B. Carbonnier, "27 Gb/s photonic wireless 60 GHz transmission system using 16 QAM OFDM," presented at the Proc. Int. Topical Meeting on Microwave Photonics (MWP 2009), Valencia, Spain, Postdeadline Paper.

[4] R. Sambaraju, D. Zibar, A. Caballero Jambrina, I. Tafur Monroy, R. Alemany, and J. Herrera, "100-GHz wireless-over-fibre links with up to 16 gb/s qpsk modulation using optical heterodyne generation and digital coherent detection," *IEEE Photon. Technol. Lett.*, vol. 22, no. 22, pp. 1650–1652, Nov. 15, 2010.

[5] S. Chandrasekhar and X. Liu, "Experiemntal investigation on the performance of closely spaced multi-carrier PDM-QPSK with digital coherent detection," *Opt. Express*, vol. 17, pp. 21350–21361, 2009.

[6] D. Zibar, R. Sambaraju, R. Alemany, A. Caballero, J. Herrera, and I. Tafur Monroy, "Radio-frequency transparent demodulation for broadband hybrid wireless-optical links," *IEEE Photon. Technol. Lett.*, vol. 22, no. 11, pp. 784–786, Jun. 1, 2010.

Paper 11: High-capacity 60 GHz and 75-110 GHz band links employing all-optical OFDM generation and digital coherent detection

A. Caballero, D. Zibar, R. Sambaraju, J. Marti and I. Tafur Monroy, "High-capacity 60 GHz and 75-110 GHz band links employing all-optical OFDM generation and digital coherent detection," *IEEE/OSA J. Lightw. Technol.*, accepted for publication, 2011.

High-Capacity 60 GHz and 75-110 GHz Band Links Employing all-Optical OFDM Generation and Digital Coherent Detection

Antonio Caballero, Darko Zibar, Rakesh Sambaraju, Javier Herrera, Javier Martí and Idelfonso Tafur Monroy

***Abstract*—The performance of wireless signal generation and detection at mm-wave frequencies using baseband optical means is analyzed and experimentally demonstrated. Multi-gigabit wireless signal generation is achieved based on all-optical Orthogonal Frequency-Division Multiplexing (OFDM) and photonic upconversion. The received wireless signal is optically modulated and detected using digital coherent detection. We present a theoretical model, ultimate performance limitations based on simulations as well as experimental validation of the proposed architecture. In order to demonstrate the RF frequency scalability and bit-rate transparency of our proposed approach, we experimentally demonstrated generation and detection in the 60 GHz and 75-110 GHz band of an all-optical OFDM QPSK, with 2 and 3 subcarriers, for a total bitrate over 20 Gbps.**

***Index Terms*—High-speed wireless, optical heterodyning, coherent detection, optical OFDM, radio over fiber.**

I. Introduction

HIGH bitrate wireless signals can be generated and detected using photonic methods due to the high capacity that optics can provide [1]. The use of high carrier frequencies, such as in the 60 GHz or 75-110 GHz bands and beyond [2], are necessary to provide very high capacity wireless links, as they offer several GHz of available bandwidth [3]. The application of this high-capacity wireless links are numerous. The flexibility given by wireless links allows a faster deployment than fiber. For instance, they could be used as an alternative for fiber backbone in temporal installations or with difficult access. So far, high-speed arbitrary waveform generators has been used to drive optical modulators for the generation of high bitrates in wireless for frequencies up to 60 GHz achieving bitrates over 30 Gbps within the 7 GHz of bandwidth available based on OFDM [4], [5]. For the 75-110 GHz band, On-Off Keying wireless systems has been demonstrated employing optical generation and electrical envelope detection at 10 Gbps [6] and 20 Gbps [7] 1.25 Gbps link was achieved at 105 GHz RF frequency using IF optical upconversion [9] The use of all-optical transmitter was reported in [10] using a DQPSK optical modulator, with up to 4.6 Gbps at 92 GHz RF frequency. For gigabit generation beyond 100 GHz, 8 Gbps was achieved at 250 GHz by optical heterodyning [11].

A different approach for the photonic generation and detection of high speed microwave signals in frequencies over 60 GHz is the combination of high spectral-efficient modulation formats achievable by optical modulators using baseband electronics and digital coherent detection [12], [13]. For example in [13], it has been demonstrated over 20 Gbps links in the 60 GHz and 75-110 GHz bands. At the transmitter side, the use of photonic generation of advance modulation formats (QPSK, m-QAM) can provide high capacity and spectral efficient baseband optical signals. The use of Optical OFDM (O-OFDM) [14], [15] has been demonstrated to enable highly spectral-efficient optical channels, while decreasing the requirements of the baseband electronics. In the reception, the microwave signal is re-modulated in the optical domain using a high speed electro-optical modulator, such as an Electro-Aborption Modulator (EAM). By filtering the optical sideband generated, the signal is converted back to baseband, where digital coherent detection is applied for demodulation [16]. Based on the robustness of the receiver, it is possible to compensate for link impairments, such as laser beating from the optical heterodyning RF generation and coherent detection or non-ideal response of the opto-electrical components [17]–[19].

In this paper we derive an analytical model for a link comprising photonic generation and detection of high speed wireless signals using baseband components at the transmitter and receiver. We also describe the Digital Signal Processing (DSP) algorithms needed to demodulate the signals and analyze their behaviour under different impairments. The link and algorithms performance was evaluated under the presence of various optical and electrical impairments, such as linewidth of the lasers, Optical Signal-to-Noise Ratio (OSNR), response of the Photodiode (PD) as well as electrical amplifier nonlinear distortion. We also provide the designing engineering rules for this type of links.

The text of this paper is organized as follows: In section II we formulate analytically the behaviour of the system and describe the digital coherent receiver structure, including the algorithms used for signal demodulation. In section III, the performance is evaluated in terms of Bit Error Rate (BER) through computer simulations, to determine the ultimate requirements of the link for generation and detection of 10 Gbaud wireless links at 100 GHz. In section IV we present

A. Caballero, D. Zibar and I. Tafur Monroy are with DTU Fotonik, Department of Photonics Engineering, Technical University of Denmark, Kgs. Lyngby, Denmark, (email: acaj@fotonik.dtu.dk)

R. Sambaraju and J. Marti are with Valencia Nanophotonics Technol. Center, Universidad Politcnica de Valencia, Camino de Vera s/n, Ed.8F, 46022 Valencia, Spain

Manuscript received XX XX, 2011; revised XX XX, 2011. This work was supported in part by the European Comission FP7 under Network of Excellence project EUROFOS (22402) and the Danish Research Council under grant OPSCODER.

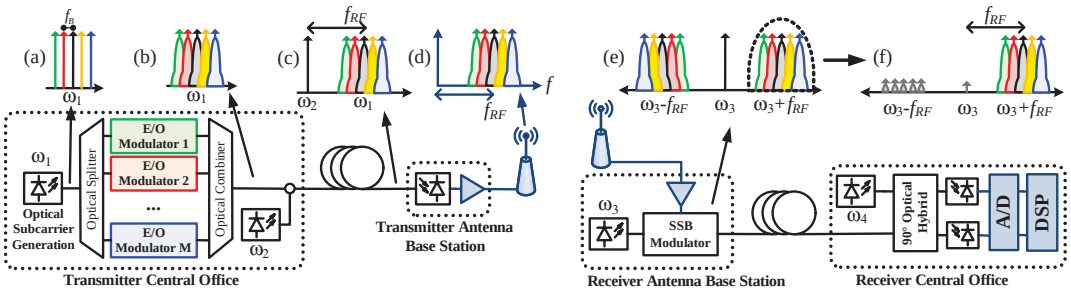

Fig. 1. Block diagram for the generation and detection of mm-wave carrier frequency signals using Optical-OFDM (O-OFDM) baseband generation and optical reception using SSB modulation combined with digital coherent detection. (a) Multicarrier generation, (b) O-OFDM baseband signal, (c) Optical signals for RF optical heterodyning, (d) mm-wave RF signal generated, (e) Optical modulated received RF signal, (f) SSB baseband signal containing the transmitted O-OFDM signal.

experimental results of over 20 Gbps generation and detection in the 60 GHz and 75-110 GHz band using 10 Gbps baseband electronics. In section V we provide a summary conclusion and a future work overview.

II. Principle of High-Capacity Photonic Generation and Detection of MM-Wave Signals

In this section the principle of high-capacity photonic generation and detection of wireless signals is described mathematically, in order to identify the characteristics of the link, such as RF power generation, influence of laser beating in the generation and detection and receiver sensitivity. Based on this analysis, we propose and describe the algorithms needed for the demodulation of the recovered signal.

The block diagram of this architecture is shown in Fig. 1. For the generation of the high-speed wireless signal, at the Central Office (CO) are placed a multicarrier optical generator, O-OFDM modulator consisting on independent I/Q optical modulators and the beating laser source. The optical signal is transported to the transmitter antenna base station, consisting on a high-speed PD and the transmitter antenna. For the detection of the wireless signal, at the receiver antenna base station is placed a Single Side-Band (SSB) optical modulator, which impose the received wireless signal into an optical carrier and transported to the CO. At the CO, there is an optical digital coherent receiver that performs optical signal detection and demodulation.

A. Theoretical description

The generation of an O-OFDM signal requires a multiple subcarrier laser source, with a carrier separation equal to the baud rate of the signal. Each laser output is then optically demultiplexed and each subcarrier is individually modulated using I/Q modulators. Complex modulation formats, such as Quadrature Phase Shift Keying (QPSK) or M-Quadrature Amplitude Modulation (QAM) can be generated generating multiple QPSK data signal. The modulated laser sources are then be optically combined, to generate an all-optical OFDM signal [14]. In our architecture, the O-OFDM transmitter will be placed at the Transmitter Central Office, as shown in Fig. 1.

The output signal of a multicarrier laser source, represented in Fig. 1 (a), consisting on M carriers separated by ω_s, can be mathematically represented as:

$$E_{mc}(t) = \sqrt{P_i} e^{j(\omega_1 t + \phi_1(t))} \sum_{m}^{M} e^{j\omega_s n t} \tag{1}$$

Where P_i is the individual optical power per carrier, ω_1 is the central wavelength of the optical source and ϕ_1 is the signal phase. An array of I/Q modulators individually modulates each optical subcarrier, with $A_n(t)e^{j\theta_n(t)}$ being the imposed modulation at ω_s baudrate. Afterwards, all subcarriers are optically combined again, to comform an O-OFDM modulated signal, as:

$$\begin{aligned} E_{mod}(t) &= \sqrt{P_i} e^{j(\omega_1 t + \phi_i(t))} \sum_{m}^{M} A_n(t) e^{j\omega_s n t + j\theta_n(t)} \\ &= \sqrt{P_i} e^{j(\omega_1 t + \phi_i(t))} S_o(t) \end{aligned} \tag{2}$$

The resulting signal can be represented as an optical carrier centered at ω_1 with an optical OFDM signal, $S_o(t)$, as shown in Fig. 1 (b). The generation of a mm-wave signals is performed by the beating of the signal $E_{mod}(t)$ and a second Continious Wave (CW) laser source in the photodiode. A CW laser source, centered at ω_2 can be written as:

$$E_b(t) = \sqrt{P_b} e^{j(\omega_2 t + \phi_2(t))} \tag{3}$$

The combination of $E_{mod}(t)$ and $E_b(t)$ in a 3 dB coupler, Fig. 1 (c), is transported to the Antenna Base Station (BS) and detected using a high speed PD. The output signal of the PD is an RF electrical signal at the frequency defined by the difference of the two wavelengths of the lasers:

$$\omega_{RF} = |\omega_1 - \omega_2| \tag{4}$$

The generated RF signal, shown in Fig. 1 (d), can be written as:

$$s_{tx}(t) = A_{tx} S_o \cos(\omega_{RF} t + \Delta\phi_{RF}(t)) + DC \tag{5}$$

With $\Delta\phi_{RF}(t) = |\phi_1(t) - \phi_2(t)|$. The generated RF power, related to a baseband normalized power, is:

$$P_{out} = |A_{tx}|^2 = R_L P_b P_i \left(R\right)^2 / 2 \tag{6}$$

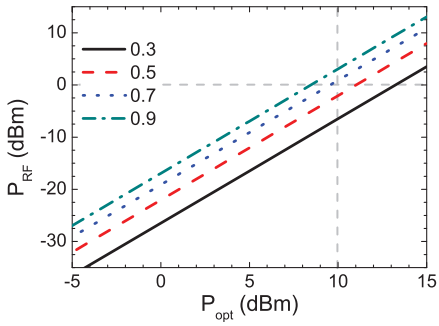

Fig. 2. Generated RF power at the output of the PD as a function of optical input power of signal and beating tone, for different photodiode responsivities ($R = [0.3, 0.5, 0.7, 0.9]$).

With R the PD responsivity and RL the resistance load. Fig. 2 shows the RF power generated with optical heterodyning, as a function of incoming optical power (P_i and P_b) for different PD responsivities, assuming a linear response of the PD. It is possible to achieve high RF power with this configuration, due to the high input optical power than the PD can support before saturation [20], Therefore, it is possible to avoid the RF power amplifier at the transmitted antenna for short wireless links. . For instance, with 10 dBm optical power, it is possible to achieve over 0 dBm RF power for R over 0.7. The transmitted RF signal has a component of uncertainty in the phase and frequency of the generated signal, $\Delta\phi_{RF}(t)$, caused by the heterodyne mixing of the lasers.

The received RF signal is modulated into the optical domain using a high-speed amplitude modulator. A SSB is generated by filtering out one of the side lobes of the optical signal, containing just baseband information. After, a coherent receiver is used to recover the signal. High-speed electro-optical modulation, capable to achieve bandwidths over 90 GHz, are nowadays only achievable by EAM [21]. An EAM can be modeled, in a small signal approximation, as [22]:

$$p_m(t) = A_m(1 - r_m s_{rx}(t)) \tag{7}$$

with r_m the slope of the EAM modulated at the linear bias point and A_m the insertion losses caused by the modulator absorption at the bias point. From a third laser source at ω_3, the optically modulated RF signal, shown in Fig. 1 (e), is:

$$\begin{aligned} E_{rx}(t) &= \sqrt{P_{rx}} e^{j(\omega_3 t + \phi_3(t))} A_m \\ &\quad (1 - r_m A_{rx} S_o \cos(\omega_{RF} t + \Delta\phi_{RF}(t))) \end{aligned} \tag{8}$$

with A_{rx} the received amplitude of the wireless signal, after receiver antenna and low-noise amplifier.

The modulated optical signal consists on an optical carrier and two side-bands $\pm\omega_{RF}$ away, containing the signal information. In order to detect the signal using a baseband receiver, the upper side-band is filtered out from the modulated optical field, generating a SSB modulation, as shown in Fig. 1 (f). The resulting SSB optical signal is:

$$E_{SSB}(t) = \sqrt{P_{rx}} \frac{A_m r_m A_{rx}}{2} S_o e^{j((\omega_3 + \omega_{RF})t + \phi_3(t) + \Delta\phi_{RF}(t))} \tag{9}$$

The attenuation caused by the SSB modulation, reflected in results in low values of optical power of the received signal. In practical scenarios, this can be in the order of -40 dBm [12], [13]. This is caused by the high insertion losses of the EAM, $A_m r_m A_{rx}$, and the high losses of the optical filter to perform a narrow SSB filtering. Therefore, high optical amplification is needed before detection, for example using a high-gain Erbium Doped Fiber Amplifier (EDFA), resulting in a low OSNR signal. At the receiver, for intradyne coherent detection, the wavelength of the LO laser needs to be placed closed to the incoming SSB signal:

$$\omega_4 = \omega_3 + \omega_{RF} + \Delta\omega \tag{10}$$

with $\Delta\omega$ the wavelength offset from the receiver signal and the LO. We describe the optical field of the Local Oscillator (LO) light source as:

$$E_{lo}(t) = \sqrt{P_o} e^{j(\omega_4 t + \phi_4(t))} \tag{11}$$

with ϕ_4 its optical phase variation. The beating of the optical signal and LO at the 90° optical hybrid, results in two photocurrents outputs from the balanced PD, $i_i(t)$ and $i_q(t)$, used to reconstruct the optical field to form the received signal $s(t)$, as:

$$\begin{aligned} s(t) &= i_i(t) + j i_q(t) \\ s(t) &= 2R\sqrt{P_{rx} P_o} A_m r_m S_o e^{j(\Delta\omega + \Delta\phi_{RF}(t) + \Delta\phi_2(t))} \end{aligned} \tag{12}$$

Where $\Delta\phi_2 = \phi_3 - \phi_4$. As a result, the detected signal has the influence of three beating components. First, a component from the free-running beating of the two lasers at the transmission, $\Delta\phi_{RF}(t)$. Second one from the beatings of the SSB signal and LO at the coherent receiver, $\Delta\phi_2$. The third one is the beating caused by the combination of both incoherent beating of the lasers at transmitter and receiver.

The performance of the system in the generation and especially in the detection is degraded due to impairments in the optical and electrical domain. From the optical domain, the beating of the four lasers in the system results in stringent requirements on the linewidth magnitude of the lasers, increasing also the complexity of the DSP algorithms for carrier-phase recovery. Secondly, the design of the PD placed at the transmitter antenna should be adequate for wireless generation. In order to achieve maximum efficiency, the PD should be able to provide high output photocurrent, high quantum efficiency and high-power handling capabilities at mm-wave frequencies, so transmitter RF amplifier can be removed. Thirdly, SSB modulation of the optical signal at high carrier frequency results in low electro-optical efficiency, requiring high optical amplification and as a result low OSNR. The modulator design should be optimized to improve modulation index and have also a flat response in the microwave band.

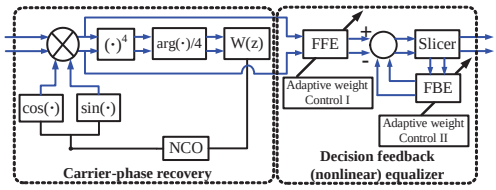

Fig. 3. carrier-phase recovery and non-linear equalizer structure.

B. Digital Receiver Structure

The algorithms for the demodulation are similar to the one used in baseband digital coherent receivers, as the detected signal after SSB generation, eq. (9), is a baseband optical signal. However, the signal is degraded due to the various impairment mentioned in section II. Consequently, exhaustive DSP is needed to compensate for the distortion induced by the link. The algorithms need to be able to track the frequency and phase changes caused by the three beating components. Also, they need to compensate for the non-linear response of the optical and electrical components, such as transmitter PD, electrical amplifier, antennas, wireless media and SSB modulator. The algorithms are based on standard digital coherent receivers, still designed to operate with severe distorted signals. The algorithms consists on OFDM demodulation block, blind equalization based on Constant Modulus Algorithm (CMA), carrier phase and frequency estimation and Decission Feedback Equalizer (DFE) for nonlinear equalization.

In order to track the phase changes of the signal, it is necessary to implement a robust carrier phase and frequency recovery scheme. Afterwards, a post-equalization algorithm should be place, to compensate for residual distortion. In Fig. 3, the proposed digital carrier phase and frequency recovery structure is shown together with a nonlinear decision feedback equalizer. The novelty behind the proposed carrier phase and frequency recovery structure is that the Viterbi&Viterbi (V&V) algorithm is embedded inside a digital phase-locked loop [18], [23] to produce an error signal for the feedback loop. The $W(z)$ is the corresponding low-pass loop filter. The advantages of the proposed structure is the robustness of blind phase estimation by employing V&V and feedback loop to track the fast phase and frequency fluctuations.

The operation of the digital carrier phase and frequency recovery structure is as follows. The Numerical Controlled Oscillator (NCO) generates a complex locally generated signal from the sine and cosine phase samples. The phase rotator performs a complex multiplication between the incoming signal and the locally generated signal to produce complex frequency difference signal. A phase detector algorithm consists on a V&V algorithm, including a digital filter $W(z)$ and produces an error signal. The error signal is then applied to the NCO. When the structure reaches stable steady state operation, the frequency and phase difference between the transmitter and LO laser is removed from the incoming signal. The output of the carrier-phase recovery feeds a nonlinear decision feedback equalizer, consisting of a Feedforward Equalizer (FFE) and Feedback Equalizer (FBE). The taps of the FFE and FBE equalizers are adjusted by Least Mean Squares (LMS) algorithm.

TABLE I
SIMULATION VALUES FOR RF TRANSPARENT GENERATION AND DETECTION LINK

Parameter	Value
Modulation type	QPSK
Baudrate	10 Gbaud
f_{RF}	100 GHz
PD Bandwidth	90 GHz
Receiver PD Bandwidth	7.5 GHz
Optical filter Bandwidth	0.3 nm
Laser linewidth	100 kHz to 2 MHz

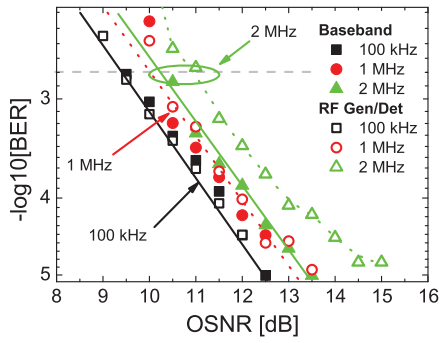

Fig. 4. Simulated BER performance as a function of OSNR for QPSK for baseband and wireless generation and detection, for three different linewidth values for the lasers (100 kHz, 1 MHz and 2 MHz).

III. THEORETICAL PERFORMANCE EVALUATION

In this section we analyze the receiver performance for the generation and detection of high speed wireless signals using the proposed architecture. The system described in section II has been simulated using Matlab and VPI transmission maker. A single carrier QPSK has been simulated at 10 Gbaud for 100 GHz RF frequency generation and detection. The parameters used in the simulations are shown in Table I.

Fig. 4 shows the BER results as a function of OSNR. The proposed architecture has been compared with an standard baseband system at the same baudrate, consisting on an I/Q modulator and digital coherent detection. Different values of lasers linewidth were simulated, from 100 kHz to 2 MHz. An OSNR of 9.5 dB is required to achieve BER below 2×10^{-3}, limit of Ultra Forward Error Correction (UFEC), for 100 kHz linewidth lasers, with no penalty from Back-to-Back (B2B) baseband detection to RF generation and detection. Less than 1 dB penalty was observed from 100 kHz to 1 MHz linewidth lasers. However, for laser linewidth values of 2 MHz, the influence of the beating of the 4 lasers in the RF generation-detection schemes becomes more prominent, leading a penalty of 1 dB from baseband to RF generation.

Next, we have evaluated the performance of the receiver algorithms for a fixed OSNR of 10 dB and 100 kHz linewidth

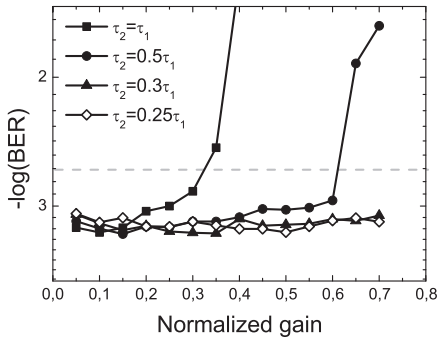

Fig. 5. BER as a function of the normalized gain of the DPLL for a frequency offset of 200 MHz, (10 Gbaud QPSK, 100 kHz linewidth lasers, 10 dB OSNR).

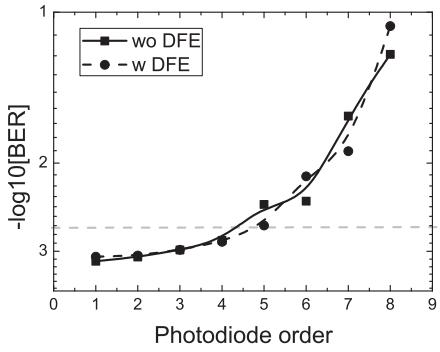

Fig. 6. BER penalty for different photodiode filter order response at the transmitter, (10 Gbaud QPSK, 100 kHz linewidth lasers, 10 dB OSNR).

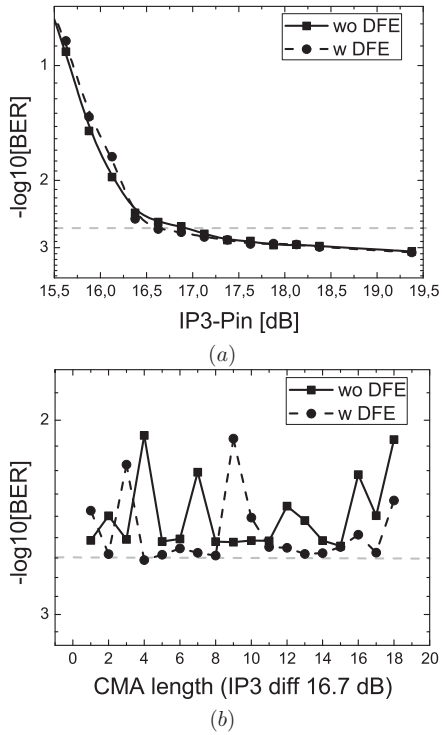

Fig. 7. (a) Influence in BER of the 3^{rd} order interception point of the RF amplifier at the receiver versus the received electrical power. (b) CMA length with and without DFE at 4.6 dB difference in IP3 vs input RF power, (10 Gbaud QPSK, 100 kHz linewidth lasers, 10 dB OSNR).

lasers. First, we evaluate the performance of the DPLL for frequency tracking of a 200 MHz offset received signal. The result is shown in Fig. 5, showing that a proper design of the τ_2/τ_1 filter taps is needed in order to achieve good performance for a wide range of DPLL gain values.

To study the influence of the PD at the transmitter antenna station, we have evaluated the penalty in BER for different filtering responses of the PD. In Fig. 6 it is shown the influence of the PD filtering based on different orders of Butterworth filter. The influence of high order filtering degrades the signal generation, when equivalent filtering order is over 4 (24 dB per octave). Thus, design of the PD for millimeter wave frequencies is required for the generation of high capacity wireless signals.

To test the performance in terms of linearity of the RF amplifier at the receiver, prior the optical modulation, a 3^{rd} order non-linear distortion amplifier model, quantified in terms of Interception Point of 3^{rd} order (IP3) has been simulated. The penalty of the amplifier as a function of the ratio between RF signal power and amplifier IP3 is shown in Fig. 7 (a). For a difference over 17 dB the distortion of the amplifier causes a non-linear distortion starts overpassing the influence of the OSNR. In Fig. 7 (b) is plotted the performance of the CMA length for a difference of 16.7 dB. There is an optimum CMA filter length, that combined with the DFE equalizer results in compensation of the non-linearities induced by the components, such as, in this case, the RF amplifier.

IV. Experimental validations

In this section we report the experimental validation of the proposed architecture for the generation of mm-wave signal in the 60 GHz and 75-110 GHz bands, using standard baseband optics transmitters and receivers.

A. Experimental Setup

The experimental set-up for the generation and digital coherent detection of high-capacity wireless OFDM signals is shown in Fig. 8. In the transmitter side, an External Cavity Laser (ECL) at λ_1= 1549.8 nm and 100 kHz linewidth, was used as laser source and modulated to generate up to three subcarriers using a MZM. For the generation of 2 subcarriers, the MZM was biased at minimum point to generate an optical carrier-suppressed signal and driven with an RF electrical signal at half of the baudrate. The 3 subcarriers were generated driving the MZM with an RF electrical signal at the baudrate

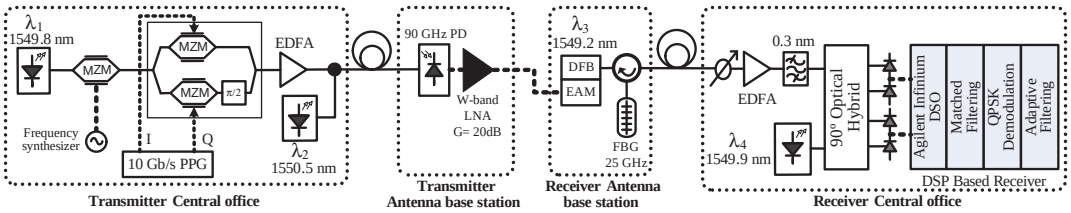

Fig. 8. Detail description of the experimental setup used for the generation and detection of high-speeed wireless signals. PPG: Pulse Pattern Generator.

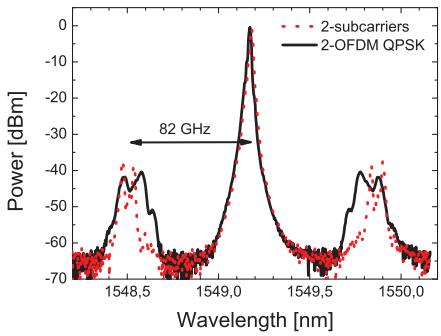

Fig. 9. Optical spectrum at the output of the optical modulator in the receiver, with and without O-ODFM QPSK modulation.

of the baseband signal and biased in a way that the three subcarriers had the same amplitude. The optical subcarriers were then fed into an optical I/Q modulator, driven with two independent data streams (pseudo random bit sequence of length 2^{15}-1) to generate a QPSK modulation on each subcarrier at a baudrate up to 10 Gbaud. The output of the optical I/Q modulator was an all-optical OFDM-QPSK modulated signal. The optical signal was then amplified using an EDFA and combined with another un-modulated CW optical carrier (λ_2), from a second ECL laser source. The combined all-optical OFDM-QPSK signals and the un-modulated CW carrier were then transmitted to the remote antenna site, where they were heterodyne mixed in a $\sim$ 90 GHz bandwidth PD. The electrical output resulted high-capacity OFDM-QPSK electrical signal with a power after the PD of approximately -4 dBm. To modulate the received mm-wave signal we used two different configurations for 60 GHz and 75-110 GHz bands. For the case of 60 GHz, the generated mm-wave signal was electrically amplified using a 55-65 GHz amplifier with 19 dB gain. A 60 GHz reflective EAM (EAM-R-60-C-V-FCA) was used to modulate a third ECL source. For 75-110 GHz, a W-band amplifier with 20 dB gain was used to drive a Distributed Feed-Back laser integrated with a 100 GHz Traveling Wave Electro-Absorption Modulator (DFB-TW-EAM), developed in the European Project ICT-HECTO. The optical carrier was λ_3 (1549.2 nm). The spectrum of the emitted optical signal from the DFB-TW-EAM is shown in Fig. 9, for a two subcarrier 10 Gbaud OFDM-QPSK wireless signal at f_{RF} = 82 GHz, with and without modulation. In Fig. 9, it can be seen that the sidebands are 82 GHz apart from the optical carrier (λ_3) containing the two subcarrier OFDM-QPSK signal.

The SSB signal was generated by filtering out the upper side-lobe of the optically modulated mm-wave signal, using a fibre Bragg's grating with 25 GHz (0.2 nm) bandwidth and an extinction ratio over 25 dB. The filtered sideband was fed into an optical pre-amplified receiver prior to detection. The maximum received power was -46.5 dBm. After EDFA amplifier, a 0.3 m filter was used to remove excess noise from ASE. The pre-amplified optical signals were intradyne mixed with an optical LO at λ_4 centered at $\sim$1550 nm, in an 90° hybrid with integrated PDs (7.5 GHz 3-dB bandwidth). The LO consisted on an ECL with 100 kHz linewidth. The photo-detected In-phase (I) and Quadrature (Q) outputs of the optical hybrid were sampled using a 40 GSa/s real-time oscilloscope and demodulated offline. The demodulation process consisted of OFDM demodulation block [16], CMA blind equalization, carrier phase and frequency estimation and DFE nonlinear equalizer, described in section II.

B. Experimental Results

We evaluate the performance of the system in both 60 GHz and 75-110 GHz bands by performing BER measurements over 100,000 bits. First, the RF carrier frequency was chosen to 60 GHz. The baud rate was set to 5 Gbaud, as 10 GHz bandwidth was available from the RF amplifiers. In Fig. 10 (a) the BER versus the received optical power, of the single carrier QPSK and two subcarriers OFDM-QPSK wireless signal are plotted. It is observed that for both single carrier and multi-carrier O-OFDM modulation format, BER below 2×10^{-3} was achieved indicating successful signal demodulation.

In the 75-110 GHz band the baud rate was increased from 5 Gbaud to 10 Gbaud, resulting in the total bit rate of 20 Gb/s. The BER curve is shown in Fig. 10 (b). We also tested the system with two subcarriers all-optical OFDM at 5 Gbaud in 75-110 GHz band. The BER for the received power of -46.5 dBm is shown in Fig. 10. There is a large penalty compared to the single carrier 10 Gbaud case. The two subcarriers OFDM-QPSK signal at 5 Gbaud occupy less bandwidth compared to the single carrier at 10 Gbaud, so bandwidths limitation were not causing the penalty. We believe that the penalty was due to the nonlinearity of the RF components, destroying the orthogonality among the OFDM signal subcarriers and introduce inter-symbol interference.

In Fig. 11, we have summarized the highest achieved bit-rates when all-optical OFDM is used for wireless signal

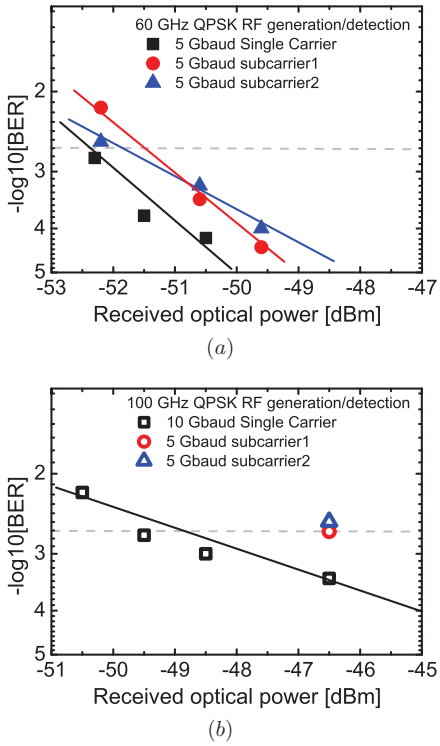

Fig. 10. Experimental BER as a function of the received optical power at the receiver, for all-optical OFDM-QPSK mm-wave signal generation and detection in (a) 60 GHz and (b) 75-110 GHz bands for single-carrier and 2 subcarriers OOFDM.

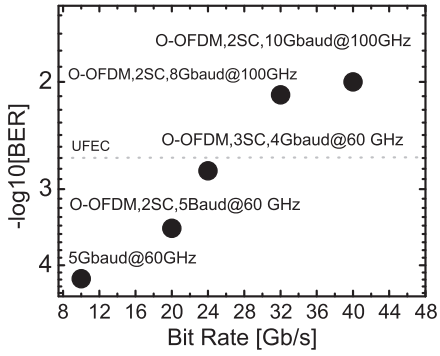

Fig. 11. The BER as a function of generated bit-rate for all-optical OFDM-QPSK mm-wave signal generation and detection in the 60 GHz and 75-110 GHz band.

generation in 60 GHz and 75-110 GHz band. At 60 GHz, we employed three subcarriers O-OFDM-QPSK for RF signal generation. Taking into consideration the bandwidth limitations of components, the baud rate was set to 4 GBaud, resulting in a total bit rate of 24 Gb/s. It is observed in Fig. 11, that the average BER of the three subcarriers is

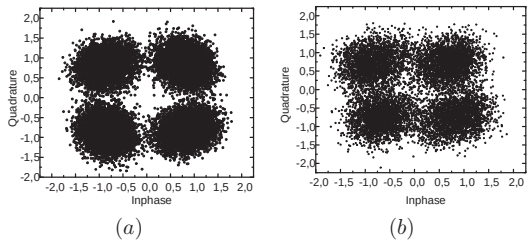

Fig. 12. Constellation of the demodulated 40 Gbit/s OOFDM signal at 82 GHz for (a) first subcarrier (BER $2 \cdot 10^{-3}$) and (b) second subcarrier (BER $1.6 \cdot 10^{-2}$).

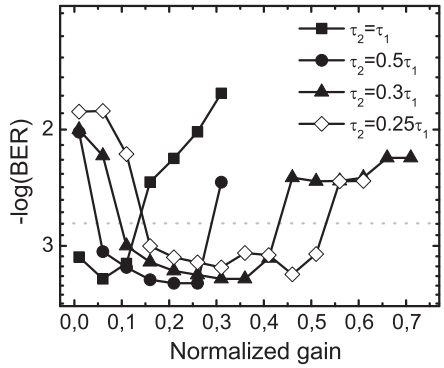

Fig. 13. Experimental BER as a function of the normalized loop gain for 20 Gb/s single-carrier received signal at 82 GHz carrier frequency, for various values of digital filter.

below the UFEC limit. In the 75-110 GHz band, the baud rate was first increased to 8 GBaud and two subcarriers O-OFDM was used for wireless signal generation resulting in the total bit rate of 32 Gb/s. Next, the baud rate is increased to 10 GBaud, resulting in the total bit rate of 40 Gb/s by applying two subcarriers OFDM-QPSK, see Fig. 11. The constellation diagrams of demodulated 10 Gbaud subcarriers of the two subcarrier OFDM-QPSK signal in the 75-110 GHz band are plotted in Fig. 12. It is observed that in spite of the sever bandwidth limitations, constellation diagrams could be recovered. The BER of the subcarrier 1 and subcarrier 2 were 2×10^{-3} (below UFEC) and 1.6×10^{-2}, respectively.

C. Performance of the Carrier-phase recovery DPLL with non-linear equalizer

We tested the carrier phase and frequency recovery structure shown in Fig. 3, for a single carrier 20 Gb/s QPSK at 82 GHz RF carrier frequency. The receiver is tested for relatively low received optical power of -47 dBm. The BER is plotted a function of a normalized loop gain for various values of digital filter W(z) coefficients τ_1/τ_2, see Fig. 13. In general, it can be observed that by varying the normalized loop gain the BER below FEC threshold can be obtained. Additionally, Fig. 13 shows that there exists an optimum value for the normalized loop gain, which results in the minimized BER as it is expected

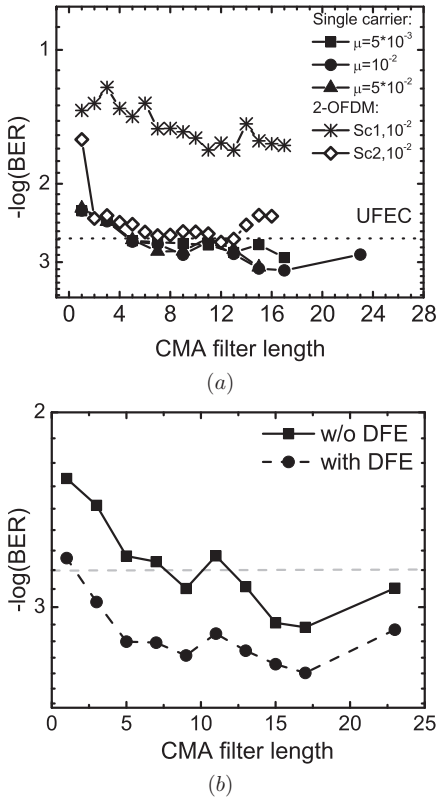

Fig. 14. (a) Experimental BER as a function of FIR CMA for 10 Gbaud QPSK single carrier and 2-O-OFDM at 82 GHz. (b) Experimental BER as a function of FIR CMA length with and without DFE equalizer, for single carrier 20 Gb/s QPSK.

from the theory and simulations performed in section III. By decreasing the ratio between the digital filter coefficients τ_1/τ_2, the BER becomes more invariant to the normalized loop gain.

Next, we investigate the impact of CMA on the system performance using the results showed in Fig. 13, for an optimized carrier phase and frequency recovery structure. In Fig. 14 (a), the BER is plotted as a function of the length of the CMA filter for the single carrier 20 QPSK at 82 GHz and 2 subcarriers O-OFDM signal at abaudrate of 10 Gbaud. In general, the BER performance improves as the CMA length is increased. However, for very long filter length the CMA cannot converge, due to noise amplification. For single carrier 20 Gb/s QPSK system, we also varied the step size parameter μ and as observed that within the varied range the system is not sensitive. For the 2 subcarrier O-OFDM system with the total capacity of 40 Gb/s, only one subcarrier can be obtained below UFEC threshold due to sever components limitations. However, the required CMA filter length is relatively small, indicating the feasibility for real-time implementation. In Fig. 14 (b), the BER is plotted as function of CMA filter length with and without decision feedback equalizer, consisting of 1 tap for FFE and 6 taps for FBE. It can be observed from Fig. 14 (b), that the DFE was able to decrease the BER and improve the overall system performance. Also, it should be noticed that the length of FBE is 6 taps, compared to 1 tap for FFE, indicating that the signal is impaired by nonlinearities.

V. Conclusion

We have described and analyzed the generation and detection of high-capacity wireless signals at mm-wave frequencies using baseband photonic technologies. The generation is based on optical heterodyning of a high-speed I/Q modulated baseband optical signal, and detection is performed using a digital coherent receiver. We have identified the requirements for the design of this link and showed that, by using lasers with linewidth values in the 100 kHz range together with broadband opto-electrical components, it is possible to generate high speed mm-wave signals in the 60 GHz and 75-110 GHz bands. We have also experimentally demonstrated the generation and detection of up to 24 Gbps O-OFDM QPSK signals in the 60 GHz and 75-110 GHz band.

We believe this architecture is feasible to provide high speed wireless transmission, due to the high RF power that can be generated, the high sensitivity of the electro-optical receiver and robustness and flexibility of the DSP algorithms. Future work and efforts should focus on pass-band match design of the electro-optical components to obtain higher efficiency and lower distortion as well as the implementation of the wireless transmission link. The presented results shows the potential and good prospects of this architecture for the generation and detection of high capacity wireless links over 100 Gbps, comparable in capacity with the current baseband optical links.

Acknowledgment

The authors would like to thank Urban Westergren from Royal Institute of Technology and Achim Walber from Radiometer Physics GmbH.

References

[1] A. Stöhr, "10 Gbit/s wireless transmission using millimeter-wave over optical fiber systems," in *Optical Fiber Communication Conference*, Optical Society of America, 2011, p. OTuO3.

[2] J. Federici and L. Moeller, "Review of terahertz and subterahertz wireless communications," *J. Appl. Phys.*, vol. 107, no. 11, pp. –, 2010.

[3] J. Wells, "Faster than fiber: The future of multi-G/s wireless," *IEEE Microw. Mag.*, vol. 10, no. 3, pp. 104 –112, may 2009.

[4] W.-J. Jiang, C.-T. Lin, L.-Y. W. He, C.-C. Wei, C.-H. Ho, Y.-M. Yang, P.-T. Shih, J. Chen, and S. Chi, "32.65-gbps ofdm rof signal generation at 60ghz employing an adaptive i/q imbalance correction," in *36th European Conference and Exhibition on Optical Communication (ECOC), 2010*, p. Th.9.B

[5] C.-T. Lin, A. Ng'oma, L.-Y. W. He, W.-J. Jiang, F. Annunziata, J. J. Chen, P.-T. Shih, and S. Chi, "31 Gbps rof system employing adaptive bit-loading OFDM modulation at 60 Ghz," in *Optical Fiber Communication Conference*. Optical Society of America, 2011, p. OWT7.

[6] A. Hirata, H. Takahashi, R. Yamaguchi, T. Kosugi, K. Murata, T. Nagatsuma, N. Kukutsu, and Y. Kado, "Transmission characteristics of 120-Ghz-band wireless link using radio-on-fiber technologies," *J. Lightw. Technol.*, vol. 26, no. 15, pp. 2338 –2344, 2008.

[7] F.-M. Kuo, C.-B. Huang, J.-W. Shi, N.-W. Chen, H.-P. Chuang, J. Bowers, and C.-L. Pan, "Remotely up-converted 20-Gbit/s error-free wireless OnOff-keying data transmission at W-band using an ultra-wideband photonic transmitter-mixer," *IEEE Photon. Journal*, vol. 3, no. 2, pp. 209 –219, 2011.

[8] I. Sarkas, S. Nicolson, A. Tomkins, E. Laskin, P. Chevalier, B. Sautreuil, and S. Voinigescu, "An 18-Gb/s, direct Qpsk modulation sige biCMOS transceiver for last mile links in the 70-80 Ghz band," *IEEE J. Solid-State Circuits*, vol. 45, no. 10, pp. 1968 –1980, 2010.

[9] J.-W. Shi, F.-M. Kuo, Y.-S. Wu, N.-W. Chen, P.-T. Shih, C.-T. Lin, W.-J. Jiang, E.-Z. Wong, J. Chen, and S. Chi, "A w-band photonic transmitter-mixer based on high-power near-ballistic uni-traveling-carrier photodiodes for bpsk and qpsk data transmission under bias modulation," *IEEE Photon. Technol. Lett.*, vol. 21, no. 15, pp. 1039 –1041, 2009.

[10] R. Ridgway, D. Nippa, and S. Yen, "Data transmission using differential phase-shift keying on a 92 Ghz carrier," *IEEE Trans. Microw. Theory Tech.*, vol. 58, no. 11, pp. 3117 –3126, 2010.

[11] H.-J. Song, K. Ajito, A. Hirata, A. Wakatsuki, T. Furuta, N. Kukutsu, and T. Nagatsuma, "Multi-gigabit wireless data transmission at over 200-Ghz," in *Infrared, Millimeter, and Terahertz Waves, 2009. IRMMW-THz 2009. 34th International Conference on*, sept. 2009, pp. 1 –2.

[12] R. Sambaraju, D. Zibar, A. Caballero, I. Tafur Monroy, R. Alemany, and J. Herrera, "100-Ghz wireless-over-fibre links with up to 16 Gb/s qpsk modulation using optical heterodyne generation and digital coherent detection," *IEEE Photon. Technol. Lett.*, vol. 22, no. 22, pp. 1650–1652, 2010.

[13] D. Zibar, R. Sambaraju, A. Caballero, J. Herrera, U. Westergren, A. Walber, J. B. Jensen, J. Marti, and I. T. Monroy, "High-capacity wireless signal generation and demodulation in 75 to 110 Ghz band employing all-optical ofdm," *IEEE Photon. Technol. Lett.*, vol. 23, no. 12, pp. 810 –812, 2011.

[14] S. Chandrasekhar and X. Liu, "Experimental investigation on the performance of closely spaced multi-carrier pdm-qpsk with digital coherent detection," *Opt. Express*, vol. 17, no. 24, pp. 21 350–21 361, 2009.

[15] Y. Ma, Q. Yang, Y. Tang, S. Chen, and W. Shieh, "1-Tb/s single-channel coherent optical ofdm transmission with orthogonal-band multiplexing and subwavelength bandwidth access," *J. Lightw. Technol.*, vol. 28, no. 4, pp. 308 –315, 2010.

[16] D. Zibar, R. Sambaraju, R. Alemany, A. Caballero, J. Herrera, and I. Tafur Monroy, "Radio-frequency transparent demodulation for broadband hybrid wireless-optical links," *IEEE Photon. Technol. Lett.*, vol. 22, no. 11, pp. 784–786, 2010.

[17] A. Caballero, D. Zibar, and I. Tafur Monroy, "Digital coherent detection of multi-gigabit 40 Ghz carrier frequency radio-over-fibre signals using photonic downconversion," *Electron. Lett.*, vol. 46, no. 1, pp. 58–58, 2010.

[18] D. Zibar, R. Sambaraju, A. Caballero, J. Herrera, and I. Tafur Monroy, "Carrier recovery and equalization for photonic-wireless links with capacities up to 40 Gb/s in 75-110 GHz band," in *Optical Fiber Communication Conference*. Optical Society of America, 2011, p. OThJ4.

[19] A. Caballero, D. Zibar, R. Sambaraju and I. Tafur Monroy, "Engineering rules for optical generation and detection of high speed wireless millimeter-wave band signals," in *37th European Conference and Exhibition on Optical Communication (ECOC), 2011*, p. We.10.P1.115.

[20] A. Beling and J. Campbell, "InP-based high-speed photodetectors," *J. Lightw. Technol.*, vol. 27, no. 3, pp. 343 –355, 2009.

[21] M. Chacinnandski, U. Westergren, B. Stoltz, R. Driad, R. Makon, V. Hurm, and A. Steffan, "100 Gb/s ETDM transmitter module," *IEEE J. Sel. Topics Quantum Electron.*, vol. 16, no. 5, pp. 1321 –1327, 2010.

[22] I. Charles H. Cox, *Analog Optical Links, Theory and Practice*. Cambridge University Press, 2004.

[23] D. Zibar, L. Johansson, H.-F. Chou, A. Ramaaswamy, M. Rodwell, and J. Bowers, "Phase-locked coherent demodulator with feedback and sampling for optically phase-modulated microwave links," *J. Lightw. Technol.*, vol. 26, no. 15, pp. 2460–2475, 2008.

PLACE PHOTO HERE

Antonio Caballero was born in 1985 in Zaragoza, Spain. He received the B.Sc. and M.Sc. degree in Telecommunications Engineering from Centro Politcnico Superior, Zaragoza, Spain, in 2008. He is currently pursuing a Ph.D. in optical communications engineering at DTU Fotonik, Technical University of Denmark. He was a Visiting Researcher at The Photonics and Networking Research Laboratory (PNRL) at Stanford University from February to June 2010, under supervision of Prof. Leonid G. Kazovsky. His research interests are in the area of coherent optical communications as well as radio-over-fiber links.

PLACE PHOTO HERE

Darko Zibar was born on December 9th, 1978, in Belgrade former Yugoslavia. He received the M.Sc. degree in Telecommunication in 2004 from the Technical University of Denmark and the Ph.D. degree in 2007 from the Department of Communications, Optics and Materials, COM•DTU within the field of optical communications. He was a Visiting Researcher with Optoelectronic Research Group led by Prof. John E. Bowers, at the University of California, Santa Barbara (UCSB) from January 2006 to August 2006, and January 2008 working on coherent receivers for phase-modulated analog optical links. From February 2009 until July 2009, he was Visiting Researcher with Nokia-Siemens Networks working on digital clock recovery for 112 Gb/s polarization multiplexed systems. Currently, he is employed at DTU Fotonik, Technical University of Denmark as the Assistant Professor. His research interests are in the area of coherent optical communication, with the emphasis on digital demodulation and compensation techniques. Darko Zibar is a recipient of the Best Student Paper Award at the IEEE Microwave Photonics Conference (MWP) 2006, for his work on novel optical phase demodulator based on a sampling phase-locked loop as well as Villum Kann Rasmussen postdoctoral research grant in 2007.

PLACE PHOTO HERE

Idelfonso Tafur Monroy received the M.Sc. degree in multichannel telecommunications from the Bonch-Bruevitch Institute of Communications, St. Petersburg, Russia, in 1992, the Technology Licenciate degree in telecommunications theory from the Royal Institute of Technology, Stockholm, Sweden, and the Ph.D. degree from the Electrical Engineering Department, Eindhoven University of Technology, The Netherlands, in 1999. He is currently Head of the metro-access and short range communications group of the Department of Photonics Engineering, Technical University of Denmark. He was an Assistant Professor until 2006 at the Eindhoven University of Technology. Currently, he is an Associate Professor at the Technical University of Denmark. He has participated in several European research projects, including the ACTS, FP6, and FP7 frameworks (APEX, STOLAS, LSAGNE, MUFINS). At the moment, he is in involved the ICT European projects Gi-GaWaM, ALPHA, BONE, and EURO-FOS. His research interests are in hybrid optical-wireless communication systems, coherent detection technologies and digital signal processing receivers for baseband and radio-over-fiber links, optical switching, nanophotonic technologies, and systems for integrated metro and access networks, short range optical links, and communication theory.

Paper 12: Engineering rules for optical generation and detection of high speed wireless millimeter-wave band signals

A. Caballero, D. Zibar, R. Sambaraju, N. Guerrero Gonzalez and I. Tafur Monroy, "Engineering rules for optical generation and detection of high speed wireless millimeter-wave band signals," in *Proc. 37th European Conference on Optical Communication, ECOC'11*, Geneva, Switzerland, 2011, paper We.10.P1.115.

Engineering Rules for Optical Generation and Detection of High Speed Wireless Millimeter-wave Band Signals

Antonio Caballero[1], Darko Zibar[1], Rakesh Sambaraju[2,*] Neil Guerrero Gonzalez[1] and Idelfonso Tafur Monroy[1]

1. DTU Fotonik, Department of Photonics Engineering, Technical University of Denmark, Ørsteds Plads, B. 343, DK 2800 Kgs. Lyngby
email:acaj@fotonik.dtu.dk
*2. Universidad Politecnica de Valencia, Camino de Vera S/N, Valencia 46022, Spain.*Currently at Corning Inc., Corning, N.Y, 14831 USA.*

Abstract: We analyze the design requirements for 40 Gbit/s wireless generation and detection in the millimeter-wave band, combining baseband optical I/Q modulation and coherent detection with wireless optical heterodyning generation and single-side band electro-optical modulation.
OCIS codes: (060.1660) Coherent communications; (120.5060) Phase modulation; (060.5625) Radio frequency photonics

1. Introduction

Photonics methods for the generation and detection of high speed wireless signals are gaining much attention due to the high capacity that optics can provide [1-3]. The use of high carrier frequencies, such as in the 75 GHz – 110 GHz band, could potentially provide very high capacity wireless links as there are several GHz of available bandwidth. Recently the use of the baseband optics for the generation and detection of high speed microwave signals in the 100 GHz band has been demonstrated to enable over 32 Gbit/s and high spectral efficient modulation formats [2]. The key technologies are, at the transmitter side, the use of advance modulation formats (QPSK, m-QAM) for the generation of high capacity and spectral efficient baseband optical signals. At the receiver side, the use of coherent detection assisted with digital signal processing (DSP) enables the compensation of link impairments, such as laser beating, filtering, etc. Based on the robustness of the receiver, the generation of the microwave signal can be realized by optical heterodyning the optical signal with a second laser source. In the reception, the microwave signal is re-modulated in the optical domain. By optical filtering the side-band generated, the signal is converted back to baseband, where standard coherent detection is applied for demodulation.

In this paper we evaluate the performance of the optical components for the generation and detection of microwave signals to establish the engineering rules for the link design. We have evaluated the performance for 10 Gbaud QPSK and 16QAM for a maximum bitrate of 40 Gbit/s at 100 GHz RF carrier frequency. We have studied the influence of the linewidth of the lasers, optical signal-to-noise ratio (OSNR), response of the transmitter photodiode, linearity of the optical modulator, as well as electrical amplifier non-linear distortion.

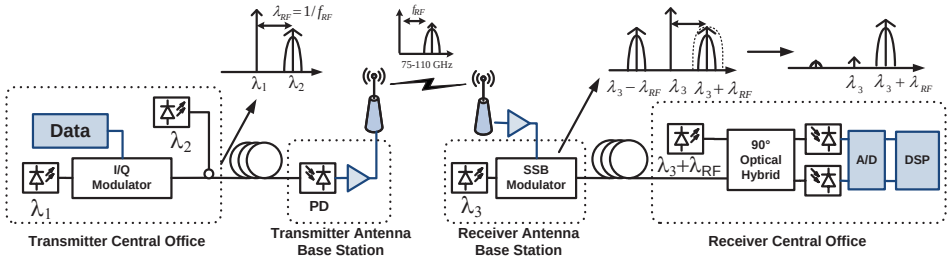

Fig. 1 Experimental set-up for generation and detection of optical generated wireless signal for millimeter frequency band.

2. Principle of optical transparent generation and detection of wireless signals

The block diagram of optical transparent generation and detection of wireless signal is shown in Fig. 1. At the transmitter central office (CO), an optical I/Q modulator is used to generate a high bitrate baseband signal centered at λ_1. This signal transported to the Antenna Base Station (BS) together with a second continuous wave laser source at a wavelength λ_2. The beating of the two optical signals at the photodiode in the BS creates an electrical signal at the frequency defined by the difference of the two wavelengths of the lasers. The received wireless signal is optically modulated using a high speed Electro-Absorption Modulator (EAM) or Mach-Zehnder Modulator (MZM). The optical side-band containing the information is narrow filtered, to create Single-Side Band (SSB) architecture. This signal is transmitted to the CO and detected using coherent detection and DSP.

The performance of the system in the generation and especially in the detection is degraded due to impairments in the optical and electrical domain. From the optical domain, the beating of the four lasers in the system results in

stringent requirements on the linewidth of the lasers, increasing also the complexity of the DSP carrier-phase recovery. Secondly, the photodiode at the transmitter antenna can induce distortion in the generation of the wireless signal, by the non flat response at high microwave frequencies. It should also be capable to support high optical power, so transmitter RF amplifier can be removed. Thirdly, single-side band modulation of the optical signal at high carrier frequency results in a low electro-optical efficiency, requiring high optical amplification and as a result low OSNR. The modulator design should be optimized to improve modulation index and have also a flat response in the microwave band. From the electrical domain, the wireless link losses can be tremendous, requiring a low-noise linear RF amplifier after the receiver antenna, which is very challenging with current technology.

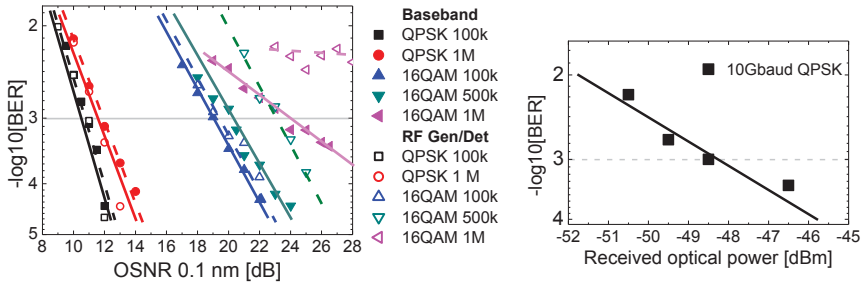

a) b)

Fig.2 a) BER performance as a function of OSNR for back-to-back baseband coherent detection and transparent generation and detection of RF signals in the 100 GHz band for different laser linewidths. b) Experimental results of receiver sensitivity prior amplification of a 10 Gbaud QPSK at 100 GHz RF frequency link with 100 kHz linewidth lasers.

3. Requirements for the detection of the optically generated wireless signal

The system described in the previous section has been simulated using Matlab and VPI transmission maker based on the experiments from [2,3]. A single carrier QPSK and 16QAM system has been simulated at 10 Gbaud for 100 GHz RF frequency generation and detection. The algorithms of the demodulation consist on Constant-Modulus Algorithm (CMA) blind equalization, decision-based carrier-phase recovery and symbol mapping [2,4]. In Fig. 2 are shown the BER results as a function of OSNR and linewidth for QPSK and 16QAM. OSNR of 11 dB is required to achieve BER below 10^{-3}, with only 1 dB penalty from 100 kHz to 1 MHz linewidth lasers and no penalty from Back-to-Back (B2B) baseband detection to RF generation and detection. For 16QAM modulation format, 100 kHz linewidth lasers requires an OSNR of 19 dB for both cases. For 500 kHz linewidth lasers 3 dB higher OSNR is required for RF generation and detection. For 1 MHz linewidth lasers the performance shows an error floor due to the failure of the carrier-phase recovery algorithm to track the fast phase drifts of the lasers. In the experimental validation demonstrated in [2], shown in Fig. 2b) for 10 Gbaud QPSK with 100 kHz linewidth lasers, the experimental BER results are plotted with respect to the optical power of the SSB received signal. The maximum experimental received power was -46.5 dBm with +10 dBm RF power to the modulator, meaning low modulation efficiency. To increase the received optical power, pass-band design of the modulator, matched for 100 GHz band, as well as a higher maximum optical power into modulator will be required.

4. Evaluation of the linearity of the Single-Side Band modulator

The performance of the system has been evaluated for two different modulators, EAM and MZM to perform the optical modulation of the detected microwave signal. The approach used in [2] is an EAM, which has high modulation bandwidth (>80 GHz). Both modulators have been simulated and the performance has been evaluated for different modulation indexes (MI). Fig. 3 shows their performance for QPSK and 16QAM at an OSNR of 11 dB and 20 dB respectively (BER ~10^{-3}) for the case of MZM 3a) and EAM Fig. 3b). A MZM shows a constant degradation for high MI, being more severe for 16QAM. For the EAM, an abrupt distortion is shown once the microwave signal enters in the saturation of the EAM. The use EAM is the only possible solution based on the current technology to achieve higher bandwidths. However, if the progression of MZM technology scales towards millimeter wave, it would be the preferred option due to higher linearity for low MI and higher maximum optical power capacity [6]. In Fig. 3 c) it is shown the influence of the photodiode filtering at the transmitter antenna station based on n-order Butterworth. The influence of high order filtering degrades the signal generation, when equivalent filtering order is over 3 (18 dB per octave). Thus, match design of the photodiode for millimeter wave frequencies is required for the generation of high capacity wireless signals.

To test the performance in terms of linearity of the RF amplifier prior the SSB modulation, we have simulated a 3rd order non-linear distortion amplifier model, quantified in terms of Interception Point of 3rd order (IP3). The

penalty of the amplifier for low IP3-to-RF signal power ratio is higher for 16QAM, with negligible difference for QPSK. This is due to the constant modulus of QPSK, which is less non-linear sensitive than 16QAM, and the CMA blind equalization capabilities. The distortion of the wireless 16QAM signal, due to this non-linearities results in non-squared constellation shape, especially significant in the outer symbols, which can be seen in fig. 3 f). To improve the performance in terms of BER, a modified decision algorithm based on k-means has been applied [5]. The algorithm consists on recursive adaptation of the 16QAM centroids from the statistics of the received symbols. In Fig. 3 e) is shown the advantage of k-means algorithm for the detection of high distorted RF signals, with an improvement of 1 dB for BER of 10^{-3} and 1.6 dB for $2{\cdot}10^{-3}$.

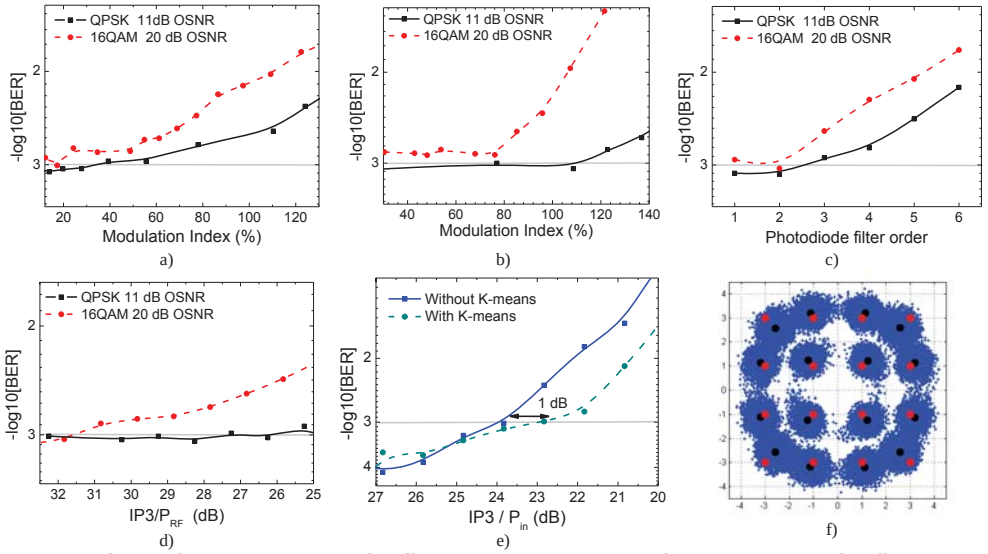

Fig.3 a) BER performance for MZM SSB modulation for different modulation indexes, b) EAM for SSB .c) BER penalty for different transmitted photodiode filter function, d) for different IP3 values of the pre-amplifier at the RX antenna station, e) k-means performance for 16QAM decision, f) constellation of 23 dB IP3/Pin including the original decision centroids (red) and after k-means (black).

5. Conclusions

We have analyzed the requirements for the generation and detection of high speed wireless signals using optics. We have studied the requirements for the design and implementation of a 100 GHz wireless system for the generation a detection of up to 40 Gbit/s high-order modulation format signals (QPSK and 16QAM) using optics. The results show the feasibility of the system for achieving high bitrates wireless transmission, but limitations of the electrical and optical components, such as photodiode, modulators and lasers, will decrease the performance of this type of systems, especially when wireless transmission would be implemented. Towards real-time implementation, this architecture could use the receivers developed for real-time coherent baseband, with minor adaptation, as standard baseband algorithms have been applied for the demodulation of the detected microwave signals.

Acknowledgment

This work has been supported by the European Commission FP7 under Network of Excellence project EUROFOS. The authors acknowledge Urban Westergren of the project ICT-HECTO.

References

[1] A. Stöhr, '10 Gbit/s Wireless Transmission Using Millimeter-Wave over Optical Fiber Systems' OFC'11, OTuO3, 2011

[2] R. Sambaraju et al., '100-GHz Wireless-Over-Fiber Links With Up to 16-Gb/s QPSK Modulation Using Optical Heterodyne Generation and Digital Coherent Detection' IEEE PTL, vol.22, no.22, pp.1650-1652, 2010

[3] R. Sambaraju et al., '16 Gb/s QPSK Wireless-over-Fiber Link in 75-110 GHz Band with Photonic Generation and Coherent Detection' MWP'10 PDP 1, 2010

[4] A. Caballero et al., 'Digital coherent detection of multi-gigabit 16-QAM signals at 40 GHz carrier frequency using photonic downconversion', ECOC'09, PDP 3.4, 2009

[5] N. Guerrero Gonzalez et al., 'Reconfigurable digital receiver for 8PSK subcarrier multiplexed and 16QAM single carrier phase-modulated radio over fiber links'. IEEE MOTL, vol. 22, issue. 5, pp. 335-337, 2010

[6] C. Cox, *Analog optical links, theory and practice*, (Cambridge University Press, 2004), Chap. 2

Bibliography

[1] L. Kazovsky, W.-T. Shaw, D. Gutierrez, N. Cheng, and S.-W. Wong, "Next-generation optical access networks," *J. Lightw. Technol.*, vol. 25, no. 11, pp. 3428–3442, Nov. 2007.

[2] R. Gaudino, D. Cardenas, M. Bellec, B. Charbonnier, N. Evanno, P. Guignard, S. Meyer, A. Pizzinat, I. Mollers, and D. Jager, "Perspective in next-generation home networks: Toward optical solutions?" *IEEE Commun. Mag.*, vol. 48, no. 2, pp. 39 –47, feb. 2010.

[3] J. Federici and L. Moeller, "Review of terahertz and subterahertz wireless communications," *J. Appl. Phys.*, vol. 107, no. 11, pp. 111101-1 – 111101-22, 2010.

[4] J. Wells, "Faster than fiber: The future of multi-G/s wireless," *IEEE Microw. Mag.*, vol. 10, no. 3, pp. 104 –112, may 2009.

[5] J. Capmany and D. Novak, "Microwave photonics combines two worlds," *Nature Photon.*, vol. 1, pp. 319–332, 2007.

[6] D. Wake, A. Nkansah, and N. Gomes, "Radio over fiber link design for next generation wireless systems," *J. Lightw. Technol.*, vol. 28, no. 16, pp. 2456 –2464, aug. 15, 2010.

[7] J. Yao, "Microwave photonics," *J. Lightw. Technol.*, vol. 27, no. 3, pp. 314–335, Feb. 1, 2009.

[8] A. Seeds, "Microwave photonics," *IEEE Trans. Microw. Theory Tech.*, vol. 50, no. 3, pp. 877–887, Mar. 2002.

[9] I. Charles H. Cox, *Analog Optical Links, Theory and Practice*. Cambridge University Press, 2004.

[10] H.-J. Song, K. Ajito, A. Hirata, A. Wakatsuki, T. Furuta, N. Kukutsu, and T. Nagatsuma, "Multi-gigabit wireless data transmission at over 200-Ghz," in *Proc. 34th International Conference on Infrared, Millimeter and Terahertz Waves, IRMMW-THz 2009*, sept. 2009, pp. 1 –2.

[11] A. Stohr, S. Babiel, P. Cannard, B. Charbonnier, F. van Dijk, S. Fedderwitz, D. Moodie, L. Pavlovic, L. Ponnampalam, C. Renaud, D. Rogers, V. Rymanov, A. Seeds, A. Steffan, A. Umbach, and M. Weiss, "Millimeter-wave photonic components for broadband wireless systems," *IEEE Trans. Microw. Theory Tech.*, vol. 58, no. 11, pp. 3071 –3082, nov. 2010.

[12] J. O'Reilly and P. Lane, "Remote delivery of video services using mm-waves and optics," *J. Lightw. Technol.*, vol. 12, no. 2, pp. 369 –375, feb. 1994.

[13] C. Lim, A. Nirmalathas, M. Bakaul, K.-L. Lee, D. Novak, and R. Waterhouse, "Mitigation strategy for transmission impairments in millimeter-wave radio-over-fiber networks," *J. Opt. Netw.*, vol. 8, no. 2, pp. 201–214, 2009.

[14] A. Hirata, H. Takahashi, R. Yamaguchi, T. Kosugi, K. Murata, T. Nagatsuma, N. Kukutsu, and Y. Kado, "Transmission characteristics of 120-Ghz-band wireless link using radio-on-fiber technologies," *J. Lightw. Technol.*, vol. 26, no. 15, pp. 2338 –2344, aug. 1, 2008.

[15] J.-W. Shi, F.-M. Kuo, Y.-S. Wu, N.-W. Chen, P.-T. Shih, C.-T. Lin, W.-J. Jiang, E.-Z. Wong, J. Chen, and S. Chi, "A W-band photonic transmitter-mixer based on high-power near-ballistic uni-traveling-carrier photodiodes for BPSK and QPSK data transmission under bias modulation," *IEEE Photon. Technol. Lett.*, vol. 21, no. 15, pp. 1039 –1041, aug. 1, 2009.

[16] R. Ridgway, D. Nippa, and S. Yen, "Data transmission using differential phase-shift keying on a 92 GHz carrier," *IEEE Trans. Microw. Theory Tech.*, vol. 58, no. 11, pp. 3117 –3126, nov. 2010.

[17] F.-M. Kuo, C.-B. Huang, J.-W. Shi, N.-W. Chen, H.-P. Chuang, J. Bowers, and C.-L. Pan, "Remotely up-converted 20-Gbit/s error-free wireless onoff-keying data transmission at W-band using an

ultra-wideband photonic transmitter-mixer," *IEEE Photonics Journal*, vol. 3, no. 2, pp. 209 –219, april 2011.

[18] U. Gliese, T. Nielsen, S. Norskov, and K. Stubkjaer, "Multifunctional fiber-optic microwave links based on remote heterodyne detection," *IEEE Trans. Microw. Theory Tech.*, vol. 46, no. 5, pp. 458 –468, may 1998.

[19] I. Insua and C. Schaffer, "Heterodyne radio over fiber system with 10 Gbps data rates," in *Proc. Conference on Optical Fiber Communication, OFC 2009,* San Diego, CA, 2009, p. JWA52.

[20] S. Chandrasekhar and X. Liu, "Experimental investigation on the performance of closely spaced multi-carrier PDM-QPSK with digital coherent detection," *Opt. Express*, vol. 17, no. 24, pp. 21 350–21 361, Nov. 2009.

[21] Y. Ma, Q. Yang, Y. Tang, S. Chen, and W. Shieh, "1-Tb/s single-channel coherent optical OFDM transmission with orthogonal-band multiplexing and subwavelength bandwidth access," *J. Lightw. Technol.*, vol. 28, no. 4, pp. 308 –315, feb. 15, 2010.

[22] I. Cox, C.H., E. Ackerman, G. Betts, and J. Prince, "Limits on the performance of rf-over-fiber links and their impact on device design," *IEEE Trans. Microw. Theory Tech.*, vol. 54, no. 2, pp. 906–920, Feb. 2006.

[23] R. Kalman, J. Fan, and L. Kazovsky, "Dynamic range of coherent analog fiber-optic links," *J. Lightw. Technol.*, vol. 12, no. 7, pp. 1263–1277, Jul. 1994.

[24] T. Kurniawan, A. Nirmalathas, C. Lim, D. Novak, and R. Waterhouse, "Performance analysis of optimized millimeter-wave fiber radio links," *IEEE Trans. Microw. Theory Tech.*, vol. 54, no. 2, pp. 921–928, 2006.

[25] Y.-C. Hung, B. Bortnik, and H. Fetterman, "Dynamic-range enhancement and linearization in electrooptically modulated coherent optical links," *J. Lightw. Technol.*, vol. 25, no. 11, pp. 3289 –3300, nov. 2007.

[26] C. Lim, A. Nirmalathas, M. Bakaul, P. Gamage, K.-L. Lee, Y. Yang, D. Novak, and R. Waterhouse, "Fiber-wireless networks and subsystem technologies," *J. Lightw. Technol.*, vol. 28, no. 4, pp. 390–405, 2010.

[27] V. Urick, F. Bucholtz, P. Devgan, J. McKinney, and K. Williams, "Phase modulation with interferometric detection as an alternative to intensity modulation with direct detection for analog-photonic links," *IEEE Trans. Microw. Theory Tech.*, vol. 55, no. 9, pp. 1978 –1985, sept. 2007.

[28] J. Zhang, H. Nicholas, and T. Darcie, "Phase-modulated microwave-photonic link with optical-phase-locked-loop enhanced interferometric phase detection," *J. Lightw. Technol.*, vol. 26, no. 15, pp. 2549 –2556, aug. 2008.

[29] B. Haas, V. Urick, J. McKinney, and T. Murphy, "Dual-wavelength linearization of optically phase-modulated analog microwave signals," *J. Lightw. Technol.*, vol. 26, no. 15, pp. 2748 –2753, aug. 2008.

[30] Y. Li and P. Herczfeld, "Coherent PM optical link employing ACP-PPLL," *J. Lightw. Technol.*, vol. 27, no. 9, pp. 1086–1094, May 2009.

[31] H. Chi, X. Zou, and J. Yao, "Analytical models for phase-modulation-based microwave photonic systems with phase modulation to intensity modulation conversion using a dispersive device," *J. Lightw. Technol.*, vol. 27, no. 5, pp. 511 –521, 2009.

[32] T. Clark, S. O'Connor, and M. Dennis, "A phase-modulation I/Q-demodulation microwave-to-digital photonic link," *IEEE Trans. Microw. Theory Tech.*, vol. 58, no. 11, pp. 3039–3058, 2010.

[33] D. Zibar, X. Yu, C. Peucheret, P. Jeppesen, and I. Monroy, "Digital coherent receiver for phase-modulated radio-over-fiber optical links," *IEEE Photon. Technol. Lett.*, vol. 21, no. 3, pp. 155–157, Feb. 2009.

[34] V. Urick, F. Bucholtz, J. McKinney, P. Devgan, A. Campillo, J. Dexter, and K. Williams, "Long-haul analog photonics," *J. Lightw. Technol.*, vol. 29, no. 8, pp. 1182 –1205, apr. 15, 2011.

[35] K.-I. Kitayana and R. Griffin, "Optical downconversion from millimeter-wave to IF-band over 50 km-long optical fiber link using an electroabsorption modulator," *IEEE Photon. Technol. Lett.*, vol. 11, no. 2, pp. 287–289, Feb. 1999.

[36] T. Kuri and K. Kitayama, "Novel photonic downconversion technique with optical frequency shift for millimeter-wave-band radio-on-fiber

systems," *IEEE Photon. Technol. Lett.*, vol. 14, no. 8, pp. 1163–1165, Aug. 2002.

[37] P. Juodawlkis, J. Hargreaves, R. Younger, G. Titi, and J. Twichell, "Optical down-sampling of wide-band microwave signals," *J. Lightw. Technol.*, vol. 21, no. 12, pp. 3116–3124, Dec. 2003.

[38] M. Bystrom, Y. Li, N. Vacirca, P. Herczfeld, and W. Jemison, "A coherent fiber-optic link with optical-domain down-conversion and digital demodulation," in *Proc. International Topical Meeting on Microwave Photonic, MWP'07*, Oct. 2007, pp. 164–167.

[39] A. Karim and J. Devenport, "High dynamic range microwave photonic links for RF signal transport and RF-IF conversion," *J. Lightw. Technol.*, vol. 26, no. 15, pp. 2718–2724, Aug. 1, 2008.

[40] S. R. O'Connor, M. C. Gross, M. L. Dennis, and T. R. Clark, "Experimental demonstration of RF photonic downconversion from 4–40 Ghz," in *Proc. International Topical Meeting on Microwave Photonics, MWP'09*, Oct. 2009, pp. 1–3.

[41] K. Sato, A. Hirano, N. Shimizu, and I. Kotaka, "High-frequency and low-jitter optical pulse generation using semiconductor mode-locked lasers," *IEEE Trans. Microw. Theory Tech.*, vol. 47, no. 7, pp. 1251 –1256, Jul. 1999.

[42] F. Derr, "Coherent optical QPSK intradyne system: concept and digital receiver realization," *J. Lightw. Technol.*, vol. 10, no. 9, pp. 1290 –1296, sept. 1992.

[43] T. Clark and M. Dennis, "Coherent optical phase-modulation link," *IEEE Photon. Technol. Lett.*, vol. 19, no. 16, pp. 1206–1208, Aug. 15, 2007.

[44] Z. Jia, J. Yu, G. Ellinas, and G.-K. Chang, "Key enabling technologies for optical–wireless networks: Optical millimeter-wave generation, wavelength reuse, and architecture," *J. Lightw. Technol.*, vol. 25, no. 11, pp. 3452–3471, Nov. 2007.

[45] J. Armstrong, "OFDM for optical communications," *J. Lightw. Technol.*, vol. 27, no. 3, pp. 189–204, Feb. 1, 2009.

[46] A. Gnauck, P. Winzer, S. Chandrasekhar, X. Liu, B. Zhu, and D. Peckham, "Spectrally efficient long-haul WDM transmission using 224-Gb/s polarization-multiplexed 16-QAM," *J. Lightw. Technol.*, vol. 29, no. 4, pp. 373 –377, feb. 15, 2011.

[47] T. Ismail, C.-P. Liu, J. Mitchell, and A. Seeds, "High-dynamic-range wireless-over-fiber link using feedforward linearization," *J. Lightw. Technol.*, vol. 25, no. 11, pp. 3274 –3282, nov. 2007.

[48] A. Ramaswamy, L. Johansson, U. Krishnamachari, S. Ristic, C. Chen, M. Piels, A. Bhardwaj, L. Coldren, M. Rodwell, J. Bowers, R. Yoshimitsu, D. Scott, and R. Davis, "Demonstration of a linear ultra-compact integrated coherent receiver," in *Proc. International Topical Meeting on Microwave Photonics, MWP 2010*, oct. 2010, pp. 31 –34.

[49] A. Stöhr, "10 Gbit/s wireless transmission using millimeter-wave over optical fiber systems," in *Proc. Optical Fiber Communication Conference and Exposition, OFC/NFOC 2011*, Los Angeles, CA, March 2011, p. OTuO3.

[50] W.-J. Jiang, C.-T. Lin, L.-Y. W. He, C.-C. Wei, C.-H. Ho, Y.-M. Yang, P.-T. Shih, J. Chen, and S. Chi, "32.65-Gbps OFDM ROF signal generation at 60Ghz employing an adaptive I/Q imbalance correction," in *Proc. 36th European Conference and Exhibition on Optical Communication, ECOC 2010*, p. Th.9.B, sept. 2010, pp. 1 –3.

[51] C.-T. Lin, A. Ng'oma, L.-Y. W. He, W.-J. Jiang, F. Annunziata, J. J. Chen, P.-T. Shih, and S. Chi, "31 Gbps RoF system employing adaptive bit-loading OFDM modulation at 60 GHz," in *Proc. Optical Fiber Communication Conference and Exposition, OFC/NFOC 2011*, Los Angeles, CA, March 2011, p. OWT7.

[52] I. Sarkas, S. Nicolson, A. Tomkins, E. Laskin, P. Chevalier, B. Sautreuil, and S. Voinigescu, "An 18-Gb/s, direct QPSK modulation sige BiCMOS transceiver for last mile links in the 70-80 Ghz band," *IEEE J. Solid-State Circuits*, vol. 45, no. 10, pp. 1968 –1980, oct. 2010.

[53] A. Kanno, K. Inagaki, I. Morohashi, T. Sakamoto, T. Kuri, I. Hosako, T. Kawanishi, Y. Yoshida, and K. ichi Kitayama, "20-Gb/s QPSK W-band (75-110Ghz) wireless link in free space using radio-over-fiber technique," *Electronics Express*, vol. 8, no. 8, pp. 612–617, 2011.

[54] G.-K. Chang, A. Chowdhury, Z. Jia, H.-C. Chien, M.-F. Huang, J. Yu, and G. Ellinas, "Key technologies of WDM-PON for future converged optical broadband access networks [invited]," *IEEE/OSA J. Opt. Commun. and Networking*, vol. 1, no. 4, pp. C35 –C50, sept. 2009.

[55] T. Kuri, H. Toda, J. Olmos, and K. Kitayama, "Reconfigurable dense wavelength-division-multiplexing millimeter-waveband radio-over-fiber access system technologies," *J. Lightw. Technol.*, vol. 28, no. 16, pp. 2247 –2257, aug. 15, 2010.

[56] S. Sarkar, S. Dixit, and B. Mukherjee, "Hybrid wireless-optical broadband-access network (WOBAN): A review of relevant challenges," *J. Lightw. Technol.*, vol. 25, no. 11, pp. 3329–3340, Nov. 2007.

[57] W.-T. Shaw, S.-W. Wong, N. Cheng, K. Balasubramanian, X. Zhu, M. Maier, and L. G. Kazovsky, "Hybrid architecture and integrated routing in a scalable optical-wireless access network," *J. Lightw. Technol.*, vol. 25, no. 11, pp. 3443–3451, Nov. 2007.

[58] Y.-Y. Won, H.-S. Kim, Y.-H. Son, and S.-K. Han, "Full colorless WDM-radio over fiber access network supporting simultaneous transmission of millimeter-wave band and baseband gigabit signals by sideband routing," *J. Lightw. Technol.*, vol. 28, no. 16, pp. 2213 –2218, aug. 15, 2010.

[59] D. Wake, A. Nkansah, N. Gomes, G. de Valicourt, R. Brenot, M. Violas, Z. Liu, F. Ferreira, and S. Pato, "A comparison of radio over fiber link types for the support of wideband radio channels," *J. Lightw. Technol.*, vol. 28, no. 16, pp. 2416 –2422, aug. 15, 2010.

[60] A. Chowdhury, H.-C. Chien, S.-H. Fan, J. Yu, and G.-K. Chang, "Multi-band transport technologies for in-building host-neutral wireless over fiber access systems," *J. Lightw. Technol.*, vol. 28, no. 16, pp. 2406 –2415, aug. 15, 2010.

[61] K. Prince, J. B. Jensen, A. Caballero, X. Yu, T. B. Gibbon, D. Zibar, N. Guerrero Gonzalez, A. V. Osadchiy, and I. Tafur Monroy, "Converged wireline and wireless access over a 78-km deployed fiber long-reach WDM PON," *IEEE Photon. Technol. Lett.*, vol. 21, no. 17, pp. 1274–1276, 2009.

[62] M. Chacinnandski, U. Westergren, B. Stoltz, R. Driad, R. Makon, V. Hurm, and A. Steffan, "100 Gb/s ETDM transmitter module," *IEEE J. Sel. Topics Quantum Electron.*, vol. 16, no. 5, pp. 1321 – 1327, sept.-oct. 2010.

[63] T. Habruseva, S. O'Donoghue, N. Rebrova, D. Reid, L. Barry, D. Rachinskii, G. Huyet, and S. Hegarty, "Quantum-dot mode-locked lasers with dual-mode optical injection," *IEEE Photon. Technol. Lett.*, vol. 22, no. 6, pp. 359 –361, march. 15, 2010.

[64] M. Birk, P. Gerard, R. Curto, L. Nelson, X. Zhou, P. Magill, T. Schmidt, C. Malouin, B. Zhang, E. Ibragimov, S. Khatana, M. Glavanovic, R. Lofland, R. Marcoccia, R. Saunders, G. Nicholl, M. Nowell, and F. Forghieri, "Real-time single-carrier coherent 100 Gb/s PM-QPSK field trial," *J. Lightw. Technol.*, vol. 29, no. 4, pp. 417 –425, feb. 15, 2011.

List of Acronyms

CW	Continuous Wave
DQPSK	differential quadrature phase shift keying
NRZ	non return-to-zero
OOK	On-Off Keying
PSK	Phase Shift Keying
QPSK	Quadrature Phase Shift Keying
SMF	Single Mode Fibre
WDM	Wavelength Division Multiplexing
RoF	Radio-over-Fiber
LTE	Long Term Evolution
IM-DD	Intensity Modulated with Direct Detection
EVM	Error Vector Magnitude
WDM	Wavelength Division Multiplexing
DAS	Distributed Antenna System
MIMO	Multi-Input Multi-Output
LO	Local Oscillator
RF	Radio Frequency
I	In-phase

Q Quadrature

IF Intermediate Frequency

PDC Photonic Downconversion

DSP Digital Signal Processing

BS Base Station

CS Central Station

QPSK Quadrature Phase Shift Keying

PSK Phase Shift Keying

QAM Quadrature Amplitude Modulation

OFDM Orthogonal Frequency-Division Multiplexing

O-OFDM all-Optical OFDM

MZM Mach-Zehnder Modulator

CW Continuous Wave

EAM Electro-Absorption Modulator

SSB Single Side-Band

CO Central Office

PD Photodiode

A/D Analogue-to-Digital Converter

PM-Coh Phase Modulated RoF link assisted with Coherent Detection

IM-Coh Intensity Modulated RoF link assisted with Coherent Detection

PON Passive Optical Network

PLL Phase-Locked Loop

SFDR Spurious-Free Dynamic Range

MWP Microwave Photonics

VCSEL Vertical-Cavity Surface-Emitting laser

SNR Signal-to-Noise Ratio

TDM Time Division Multiplexing

GSM Global System for Mobile Communications

UWB Ultra-Wide Band

RSOA Reflective Semiconductor Optical Amplifier

SSB Single-Side Band

DSB Double-Side Band

IR Impulse Radio